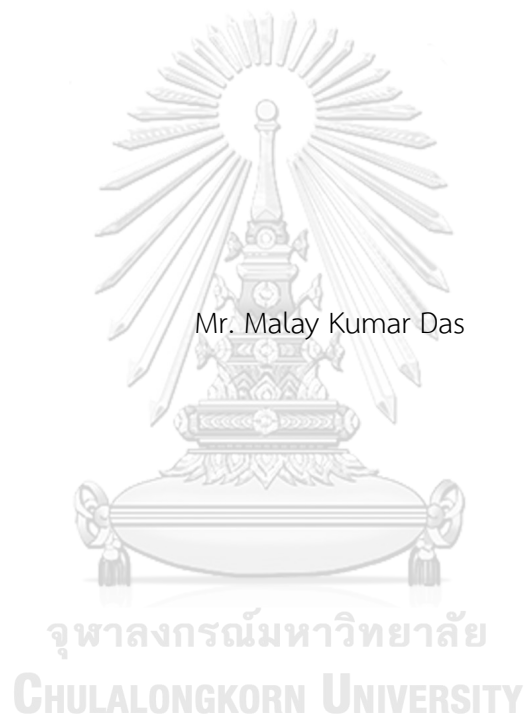


PREPARATION AND CHARACTERIZATION OF NICKEL BASED NANOCOMPOSITE
COATINGS WITH ENHANCED MECHANICAL AND SURFACE PROPERTIES



A Dissertation Submitted in Partial Fulfillment of the Requirements
for the Degree of Doctor of Philosophy in Nanoscience and Technology
Inter-Department of Nanoscience and Technology
Graduate School
Chulalongkorn University
Academic Year 2018
Copyright of Chulalongkorn University

การเตรียมและการตรวจสอบลักษณะเฉพาะผิวเคลือบนาโนคอมโพสิตเนื้อพ่นนิกเกิลเพื่อเพิ่ม
คุณสมบัติเชิงกลและสมบัติเชิงผิว



วิทยานิพนธ์นี้เป็นส่วนหนึ่งของการศึกษาตามหลักสูตรปริญญาวิทยาศาสตรดุษฎีบัณฑิต
สาขาวิชาวิทยาศาสตร์นาโนและเทคโนโลยี สหสาขาวิชาวิทยาศาสตร์นาโนและเทคโนโลยี

บัณฑิตวิทยาลัย จุฬาลงกรณ์มหาวิทยาลัย

ปีการศึกษา 2561

ลิขสิทธิ์ของจุฬาลงกรณ์มหาวิทยาลัย

Thesis Title PREPARATION AND CHARACTERIZATION OF NICKEL
BASED NANOCOMPOSITE COATINGS WITH ENHANCED
MECHANICAL AND SURFACE PROPERTIES

By Mr. Malay Kumar Das

Field of Study Nanoscience and Technology

Thesis Advisor Dr. Jiaqian Qin, Ph.D.

Thesis Co Advisor Associate Professor YUTTANANT BOONYONGMANEERAT,
Ph.D.

Accepted by the Graduate School, Chulalongkorn University in Partial
Fulfillment of the Requirement for the Doctor of Philosophy

..... Dean of the Graduate School
(Associate Professor Thumnoon Nhujak, Ph.D.)

DISSERTATION COMMITTEE

..... Chairman
(Associate Professor Vudhichai Parasuk, Ph.D.)

..... Thesis Advisor
(Dr. Jiaqian Qin, Ph.D.)

..... Thesis Co-Advisor
(Associate Professor YUTTANANT BOONYONGMANEERAT,
Ph.D.)

..... Examiner
(Assistant Professor Nutthita Chuankrerkkul, Ph.D.)

..... Examiner
(Assistant Professor Ratthapol Rangkupan, Ph.D.)

..... External Examiner
(Dr. Wannipha Amatyakul, Ph.D.)

มาเลย์ย์ कुमार ดาส : การเตรียมและการตรวจสอบลักษณะเฉพาะผิวเคลือบนาโนคอมโพสิตเนื้อพื้นนิเกิลเพื่อเพิ่มคุณสมบัติเชิงกลและสมบัติเชิงผิว. (PREPARATION AND CHARACTERIZATION OF NICKEL BASED NANOCOMPOSITE COATINGS WITH ENHANCED MECHANICAL AND SURFACE PROPERTIES) อ.ที่ปรึกษาหลัก : ดร. เจียเขียน ฉิน, อ.ที่ปรึกษาร่วม : ยุทธนันท์ บุญยงมณีรัตน์

การเตรียมโลหะผสม Ni-W และ Ni-W / Diamond และวัสดุผสมหลายชั้นได้ถูกเตรียมโดยการชุบด้วยไฟฟ้าจากการเคลือบผิว Ni-W ด้วยอนุภาคเพชรที่แขวนลอยลงในอ่างอาบน้ำเคลือบด้วยสารเคลือบผิว Ni-W / Diamond เตรียมด้วยสารเติมแต่งโคบอลต์ซัลไฟต์ในปริมาณที่แตกต่างกัน ลักษณะทางสัณฐานวิทยาและองค์ประกอบของเงินฝากได้รับการตรวจสอบโดย SEM และ EDS ตามลำดับ ศึกษาผลของสภาวะการทำงานและสารเติมแต่งของสารเคลือบผิว Ni-W ได้ ทำการศึกษาอิทธิพลของพารามิเตอร์การชุบ, ขนาดของอนุภาคคอมโพสิต, ของฝากหลายชั้นและสารเติมโคบอลต์ต่อโครงสร้างจุลภาคและสมบัติทางกลของวัสดุผสม Ni-W / Diamond Composite มีค่าความแข็งสูงสุดที่ 1207 ± 32 Hv ขณะที่ค่าความแข็งสูงสุดที่รายงานโดยโลหะผสม Ni-W มีค่าน้อยกว่า 750 Hv ซึ่งเป็นปัจจัยสำคัญที่ทำให้อนุภาคเพชรมีส่วนช่วยในการเพิ่มความแข็งของฐานเมทริกซ์ Ni-W การเพิ่มโคบอลต์ซัลไฟต์ในถังเคลือบในปริมาณน้อย ๆ มีแนวโน้มที่จะเพิ่มความแข็งและความต้านทานต่อการสึกหรอของวัสดุเคลือบผิว Ni-W / Diamond และแนวโน้มนี้กลับตรงกันข้ามเนื่องจากปริมาณซัลเฟตโคบอลต์ในบ่อชุบจะเพิ่มขึ้นเกิน 0.1 กรัม / ลิตร

จุฬาลงกรณ์มหาวิทยาลัย
CHULALONGKORN UNIVERSITY

สาขาวิชา วิทยาศาสตร์นาโนและ

เทคโนโลยี

ปีการศึกษา 2561

ลายมือชื่อนิสิต

ลายมือชื่อ อ.ที่ปรึกษาหลัก

ลายมือชื่อ อ.ที่ปรึกษาร่วม

5687870020 : MAJOR NANOSCIENCE AND TECHNOLOGY

KEYWORD: Ni-W/diamond; Hardness; Wear

Malay Kumar Das : PREPARATION AND CHARACTERIZATION OF NICKEL BASED NANOCOMPOSITE COATINGS WITH ENHANCED MECHANICAL AND SURFACE PROPERTIES. Advisor: Dr. Jiaqian Qin, Ph.D. Co-advisor: Assoc. Prof. YUTTANANT BOONYONGMANEERAT, Ph.D.

Ni-W alloy and Ni-W/diamond monolayer and multilayer composite coatings were prepared by electrodeposition from a Ni-W plating bath with diamond particles suspended into the bath. Ni-W/diamond composite coatings were also prepared with varying amounts of Cobalt sulphate additives. The morphology and the composition of the deposits was investigated by means of SEM and EDS, respectively. The effect of operating conditions and additives on the Ni-W coatings were analyzed. The effect of the plating parameters, composite particle size, multilayer deposits and cobalt additives on microstructure and mechanical properties of the Ni-W/diamond composite coatings was investigated. The electrodeposited Ni-W/diamond deposits reported a maximum hardness of $1207 \pm 32 H_v$ whereas, the maximum hardness reported by the Ni-W alloy coatings was recorded to be less than $750 H_v$ which underlines the significant impact the diamond particles have on enhancing the hardness of the base Ni-W matrix. The addition of Cobalt sulphate in the plating bath in smaller quantities tends to enhance the hardness and wear resistance of the Ni-W/diamond composite coatings and this trend is reversed as the amount of cobalt sulphate in the plating bath is increased beyond 0.1 g/L.

Field of Study: Nanoscience and
Technology

Student's Signature

Academic Year: 2018

Advisor's Signature

Co-advisor's Signature

ACKNOWLEDGEMENTS

I would like to express my gratitude to my thesis advisor Dr. Jiaqian Qin for his continued support and guidance throughout my stint as a PhD candidate under his supervision. Dr. Qin has continuously been inspiring me to try out newer ideas and come up with better results. There has been several occasions when I have been greatly inspired by Dr. Qin's motivation to keep working hard. I'm really proud to be the first PhD student of a very competent and inspiring advisor that Dr. Qin really is.

I would also like to take this opportunity to thank my co-advisor Associate Professor Dr. Yuttanant Boonyongmaneerat for the inspiration he really has been throughout my time at my lab. Dr. Boonyongmaneerat is one of the few persons I know to whom I can attribute my analytical skills and also my tendency to always think at a wider perspective. I fondly remember our inspiring group meetings where Dr. Yuttanant would help us to learn the subject by mutual discussion and critical reasoning.

I would like to thank all the lab support staff especially our metallographic support staff for having me taught the basics of samples polishing and grinding with much efforts. I have always felt very supported and inspired by the always ready to help attitude of our esteemed lab support staff.

The contribution of our program committee especially Assistant Professor Dr. Ratthapol Rangkupan needs a special mention because of his sincere efforts to offer me a place at our prestigious university and Nano-science program and also for Dr. Ratthapol for helping me so much during my initial days at university.

The help and support extended by my lab mates and my family back home also needs a special mention and a big thanks for their constant support and guidance.

Malay Kumar Das

TABLE OF CONTENTS

	Page
ABSTRACT (THAI).....	iii
ABSTRACT (ENGLISH).....	iv
ACKNOWLEDGEMENTS	v
TABLE OF CONTENTS	vi
List of Tables	x
List of Figures.....	xi
LIST OF ABBREVIATIONS AND SYMBOLS.....	17
CHAPTER I INTRODUCTION.....	19
1.1 Introduction.....	19
1.2 Research Objectives	21
1.3 Scope of Research.....	22
CHAPTER II THEORY	26
2.1 Ni-W alloy coatings	30
2.2 Ni-W/diamond composite coatings	32
CHAPTER III.....	37
ELECTRODEPOSITION OF NI-W ALLOYS AND THE COMPARISON OF THE EFFECT OF OPERATING CONDITIONS AND SURFACTANTS ON THE NI-W ALLOYS.....	37
3.1 Effect of operating conditions and saccharin sodium on electrodeposited Ni-W alloy.....	37
Abstract.....	38
3.1.1 Introduction.....	38
3.1.2 Experimental Details	39

3.1.3 Results and Discussions	40
3.1.3.1 Effect of current density	41
3.1.3.2 Effects of Saccharin Sodium on the coatings	1
3.1.4 Conclusions.....	4
3.2 Effect of SDS and sodium bromide additives on Ni-W nanocoatings	6
Abstract.....	6
3.2.1 Introduction.....	7
3.2.2 Experimental Details	9
3.2.3 Results and Discussions.....	12
3.2.3.1 Effect of current density	12
3.2.3.2 Effects of SDS on the coatings.....	18
3.2.3.3 Effect of sodium bromide.....	24
3.2.4 Conclusions.....	31
CHAPTER IV.....	33
FABRICATION OF NI-W/DIAMOND NANOCOMPOSITE COATINGS WITH ENHANCED STRUCTURE AND MECHANICAL PROPERTIES AND ANALYSIS OF THE EFFECT OF CO ₂ + ADDITIVES ON THE STRUCTURE AND MECHANICAL PROPERTIES OF THE NI-W/DIAMOND COMPOSITE COATINGS.....	33
4.1 Effect of electrodeposition conditions on structure and mechanical properties of Ni-W/diamond composite coatings.....	33
Abstract.....	34
4.1.1 Introduction.....	34
4.1.2 Experimental details.....	37
4.1.3 Results and discussion.....	39
4.1.4 Supplementary Information.....	59

4.1.5 Conclusion.....	66
4.2 Effect of diamond particles on the microstructure and composition of pulse plated multilayer Ni-W/diamond composite coatings.....	67
Abstract.....	68
4.2.1 Introduction.....	68
4.2.2 Experimental Details	70
4.2.2.1 Preparation of Steel.....	71
4.2.2.2 Pulse Parameters.....	71
4.2.2.3 Estimation of crystalline size by XRD	72
4.2.2.4 Scanning Electron microscope (SEM) and Energy Dispersive X-Ray Spectroscopy (EDS) Analysis	73
4.2.3 Results and Discussions.....	73
4.2.3.1 Effect of the Pulse plating on the Grain size.....	73
4.2.3.2 SEM and EDS Analysis.....	75
4.2.3.3 EDS analysis	78
4.2.3.4 Relationship between Grain Size and Tungsten content.....	79
4.2.4 Conclusion.....	81
4.3 Influence of Co ²⁺ ions on the microstructure and mechanical properties of Ni-W/diamond nano-composite coatings.....	83
Abstract.....	83
4.3.1 Introduction.....	84
4.3.2 Experiment details.....	88
4.3.3 Results and Discussion.....	90
4.3.3.1 Effect of the cobalt concentration on the NWD deposits	90
4.3.3.2 Wear results.....	96

4.3.3.3 Wear and Friction co-efficient correlation.....	99
4.4 Conclusion.....	104
CHAPTER V	106
CONCLUSIONS AND FUTURE PRESPECTIVE.....	106
5.1 Conclusions	106
5.2 Future Perspective	110
REFERENCES	112
VITA.....	126



List of Tables

	Page
Table 1 Elemental composition of the Ni-W coating prepared at temperature of 75 °C, pH value of 8.9, and different current density.....	15
Table 2 Elemental composition of the Ni-W coatings deposited at temperature of 75 °C, pH value of 8.9, and current density 0.1 A/cm ² , with different SDS concentration.	23
Table 3 Elemental composition of the Ni-W coatings fabricated at temperature of 75 °C, pH value of 8.9, and current density 0.1 A/cm ² , with different NaBr concentration.	29
Table 4 Pulse Parameters for the Experiments.....	71
Table 5 Grain size of the coatings.....	74
Table 6 Elemental composition of Ni and W in the deposits as reported by the EDS results.....	78
Table 7 Grain Size and Tungsten Content comparison for various conditions	80
Table 8 Plating bath composition and deposition conditions for the NWD composite coatings with varying amounts of CoSO ₄	88

List of Figures

	Page
Figure 1 SEM Image for current density (a) 0.05A/cm ² (b) 0.1A/cm ² (c) 0.15 A/cm ² (d) 0.2 A/cm ²	41
Figure 2 Composite graphs for the tungsten content and Faradic efficiency of the coatings.....	42
Figure 3 Composite Graph for Hardness and grain size obtained from XRD spectra for the coatings	43
Figure 4 SEM images of the coatings with various quantities of Saccharin Sodium (a) 0g/L (b) 0.5g/L (c) 1g/L (d) 2g/L.....	43
Figure 5 Composite graphs for the effect of Saccharin Sodium on tungsten content and Faradic efficiency of the coatings.....	3
Figure 6 Composite graphs for the effect of Saccharin Sodium on hardness and Grain Size of the coatings.....	4
Figure 7 XRD pattern with peak value for different current densities in Ni-W alloy coatings fabricated at temperature of 75 °C, and pH value of 8.9.....	13
Figure 8 Effect of current densities on the hardness, W content and crystalline size of the Ni-W alloy deposits fabricated at temperature of 75 °C, and pH value of 8.9.	14
Figure 9 SEM images for the Ni-W coatings prepared at temperature of 75 °C, and pH value of 8.9 for various current densities (a) 0.05 A/cm ² (b) 0.1 A/cm ² (c) 0.15 A/cm ² (d) 0.2 A/cm ²	15
Figure 10 Effect of current density on the faradaic efficiency of the coatings fabricated at temperature of 75 °C, and pH value of 8.9.....	17
Figure 11 XRD pattern for different quantities of SDS in the plating bath for Ni-W alloy coatings fabricated at current density of 0.1 A/cm ² , temperature of 75 °C, and pH value of 8.9.....	18

Figure 12 Effect of SDS on the hardness, W content and crystalline size of the Ni-W alloy deposits fabricated at current density of 0.1 A/cm ² , temperature of 75 °C, and pH value of 8.9.....	20
Figure 13 SEM images for the coatings deposited at current density of 0.1 A/cm ² , temperature of 75 °C, and pH value of 8.9 for various quantities of SDS in the plating bath (a) 0 g/L (b) 0.1 g/L (c) 0.5 g/L (d) 0.8 g/L.....	21
Figure 14 Effect of SDS on the faradaic efficiency of the coatings fabricated at current density of 0.1 A/cm ² , temperature of 75 °C, and pH value of 8.9.....	23
Figure 15 XRD pattern for different quantities of NaBr in the plating bath for Ni-W alloy coatings fabricated at current density of 0.1 A/cm ² , temperature of 75 °C, and pH value of 8.9.....	25
Figure 16 Effect of NaBr on the hardness, W content and crystalline size of the Ni-W alloy deposits fabricated at current density of 0.1 A/cm ² , temperature of 75 °C, and pH value of 8.9.....	26
Figure 17 SEM images for the coatings prepared at current density of 0.1 A/cm ² , temperature of 75 °C, and pH value of 8.9 for various quantities of NaBr in the bath (a) 0 g/L (b) 18 g/L (c) 25 g/L.....	28
Figure 18 Effect of NaBr on the faradiac efficiency of the coatings fabricated at current density of 0.1 A/cm ² , temperature of 75 °C, and pH value of 8.9.....	29
Figure 19 Effect of the W content and crystalline size on the hardness of the Ni-W coatings.....	31
Figure 20 Effect of diamond concentration in plating solution on morphology of Ni-W/diamond composite coatings prepared at temperature of 75°C, pH 8.9, and current density of 0.15 A/cm ² , SEM images, (a) 1 g/L, (b) 3 g/L, (c) 5 g/L, (d) 10 g/L, and cross section SEM images, (e) 1 g/L, (f) 3 g/L, (g) 5 g/L, (h) 10 g/L.....	41

Figure 21 EDS element mapping images of Ni-W/diamond composite films fabricated at current density of 0.15 A/cm^2 , temperature of 75°C , pH 8.9, and different diamond concentrations in the plating bath, (a) 1 g/L, (b) 3 g/L, (c) 5 g/L, (d) 10 g/L.	42
Figure 22 Effect of diamond concentrations and current density on diamond content of Ni-W/diamond composite deposits fabricated at temperature of 75°C and pH 8.9.	44
Figure 23 Effect of diamond concentration in the plating bath on the hardness, W content and grain size of the Ni-W/diamond composite deposits prepared at temperature of 75°C , pH 8.9 and current density of 0.15 A/cm^2	46
Figure 24 Effect of the current density on the hardness, W content and grain size of the Ni-W/diamond composite coatings prepared at temperature of 75°C , pH 8.9, and 10 g/L of diamond concentration in the plating bath.....	48
Figure 25 SEM images of Ni-W/diamond composite coatings fabricated at current density of 0.15 A/cm^2 , diamond concentration of 10 g/L, temperature of 75°C and pH 8.9, for different size of diamond particles, (a) $0.2 \mu\text{m}$, (b) $0.3 \mu\text{m}$, (c) $0.9 \mu\text{m}$, (d) $3 \mu\text{m}$, (e) $6 \mu\text{m}$. The inserted images are the SEM image at higher magnification for (a), (b), and (c), respectively.....	50
Figure 26 Diamond content of Ni-W/diamond composite deposits for various size of diamond particles fabricated at diamond concentration of 10 g/L, temperature of 75°C and pH 8.9.....	51
Figure 27 Effect of the diamond particle size on the hardness, W content and grain size of the Ni-W/diamond composite deposits fabricated at current density of 0.15 A/cm^2 , 10 g/L of diamond concentration, temperature of 75°C and pH 8.9.	53
Figure 28 The hardness of the Ni-W/diamond composite deposits presented as a function of diamond content in the coatings.	55
Figure 29 Effect of diamond concentration in the plating bath on the wear rate of Ni-W/diamond composite coatings fabricated at temperature of 75°C and pH 8.9.....	57

Figure 30 The friction coefficient of the Ni-W alloy and Ni-W/diamond (10 g/L) composite coatings fabricated at temperature of 75°C and pH 8.9.....	58
Figure 31 (a-c) SEM images of Ni-W/diamond composite coatings prepared at temperature of 75°C, pH 8.9, and diamond concentration in plating bath of 10 g/L, for various current densities, (a) 0.05 A/cm ² (b) 0.1 A/cm ² (c) 0.2 A/cm ²	60
Figure 32 EDS elemental mapping images of Ni-W/diamond composite coatings fabricated at diamond concentration of 10 g/L, temperature of 75°C, pH 8.9, and different current densities, (a) 0.05 A/cm ² (b) 0.1 A/cm ² (c) 0.15 A/cm ² (d) 0.2 A/cm ²	61
Figure 33 (a) Effect of diamond concentration in the plating bath on the deposition rate of the Ni-W/diamond composite deposits fabricated at current density of 0.15 A/cm ² , temperature of 75°C and pH 8.9 (b) Surface roughness for different diamond concentration in the plating bath at various current densities for Ni-W/diamond composite deposits fabricated at temperature of 75°C and pH 8.9.	62
Figure 34 SEM images for the surface and cross section of Ni-W/diamond composite coatings prepared at temperature of 75°C and pH 8.9, for various current densities at 5 g/L diamond concentration in the plating bath (a) surface SEM image for 0.05 A/cm ² , (b) surface SEM image for 0.1 A/cm ² and 5 g/L, (c) surface SEM image for 0.15 A/cm ² , (d) surface SEM image for 0.2 A/cm ² , (e) cross-section SEM image for 0.05 A/cm ² , (f) cross-section SEM image for 0.1 A/cm ² , (g) cross-section SEM image for 0.15 A/cm ² and (h) cross-section SEM image for 0.2 A/cm ²	63
Figure 35 (a) Effect of the current density on the deposition rate of the Ni-W/diamond composite deposits fabricated at diamond concentration of 10 g/L, temperature of 75°C and pH 8.9 (b) surface roughness of Ni-W/diamond composite deposits fabricated at temperature of 75°C and pH 8.9, for different diamond concentration in the plating bath and current density.	63
Figure 36 EDS elemental mapping images of Ni-W/diamond composite films fabricated at current density of 0.15 A/cm ² , diamond concentration of 10 g/L,	

temperature of 75°C, pH 8.9, and different size of diamond particles, (a) 0.2 μm , (b) 0.3 μm , (c) 0.9 μm , (d) 3 μm , (e) 6 μm	64
Figure 37 (a) Surface roughness values for Ni-W/diamond composite deposits at different size of diamond particles fabricated at 10g/L of diamond concentration, current density of 0.15 A/cm ² , temperature of 75°C and pH 8.9 (b) The effect of the tungsten content on the hardness of the Ni-W/diamond composite deposits fabricated at current densities ranging from 0.05-0.2 A/cm ² , diamond concentration ranging from 1-10 g/L, 75°C temperature and pH 8.9.....	65
Figure 38 The wear properties of Ni-W/diamond composite coatings fabricated at temperature of 75°C and pH 8.9 (a) The friction co-efficient of the Ni-W/diamond (10 g/L and 2 g/L) composite coatings (b) The friction co-efficient of the Ni-W/diamond (10 g/L and 20 g/L) composite coatings.....	65
Figure 39 SEM Images of (a) A monolayer layer (b) B monolayer (c) C monolayer (d) D monolayer.....	76
Figure 40 SEM Images for A layer without diamond (a) for 1000X (b) for 2000X (c) for 3000X (d) for 5000X	77
Figure 41 SEM Images for (a) AB_0.1 (b) AC_0.1 (c) AD_0.1.....	78
Figure 42 (a-d) SEM micrographs for the Ni-W/diamond composite coating samples fabricated with varying amounts of CoSO ₄ additive (a) 0 g/L (b) 0.1 g/L (c) 0.5 g/L (d) 1.5 g/L at 75° C (e-h) cross-sectional SEM micrographs for the Ni-W/diamond composite coating samples fabricated with varying amounts of CoSO ₄ additive (e) 0 g/L (f) 0.1 g/L (g) 0.5 g/L and (h) 1.5 g/L.....	90
Figure 43 Effect of CoSO ₄ on the deposition rate of the Ni-W/diamond samples.	92
Figure 44 Effect of CoSO ₄ on the hardness, Co content, W content and grain size of the Ni-W/diamond samples.....	93
Figure 45 Effect of CoSO ₄ on the surface roughness of the Ni-W/diamond samples..	95
Figure 46 Effect of CoSO ₄ on the wear rate of the Ni-W/diamond samples.....	96

Figure 47 Effect of CoSO_4 on wear friction co-efficient of the Ni-W/diamond samples.

..... 99

Figure 48 Section of the Wear track profile of NWD coatings fabricated with (a) 0 g/L CoSO_4 (b) 0.1 g/L CoSO_4 (c) 1.5 g/L CoSO_4 as reported by the surface profilometer.100

Figure 49 SEM (BSE mode) micrograph of worn surface of Ni-W/diamond composite coatings fabricated with (a) 0 g/L CoSO_4 (b) 0.1 g/L CoSO_4 and (c) 1.5 g/L CoSO_4 101



LIST OF ABBREVIATIONS AND SYMBOLS

SEM	Scanning electron microscope
XRD	X-ray diffraction
NWD	Ni-W/diamond
Co	Cobalt
H _v	Vicker's Hardness
Ni-W	Nickel-Tungsten
NaOH	Sodium Hydroxide
HCL	Hydrochloric Acid
SDS	Sodium dodecyl sulphate
NaBr	Sodium bromide
pH	pouvoir hydrogene
EDS	Energy dispersive spectroscopy
A/cm ²	Ampere/centimeters ²
g/L	gram/litre
λ	Lambda
Å	Angstorm number
β	Beta
θ	Theta

Kv	Kilo-volt
mA	Mili-ampere
°	Degree
N	Avogadro's number
c_i	weight fraction of the element (either nickel or tungsten) in the binary alloy deposit
N_i	is the number of electrons transferred in the reduction of 1 mol atoms of an element ($n_i=2$ for nickel and 6 for tungsten)
M_i	atomic weight of that element (g mol^{-1})
(g mol^{-1})	gram/mole
F	Faraday constant

CHAPTER I INTRODUCTION

1.1 Introduction

Hard protective coatings are used to improve the longevity of products, facilitate the enhancement of performance for cutting tools and other materials which are coated with hard materials such as diamond by various wet and dry processes. Ceramic particle reinforced metal or alloy matrix composite typically exhibit wide range of industrial and engineering applications owing to their high values of hardness, excellent wear resistance ability and an enhanced corrosion resistance as compared to the base metal or alloy. Contemporary researchers have used various ceramics to fabricate composite coatings. Diamond is one such materials that has of late been used to fabricate various metal and metal alloy based composite deposits[1-6].

Various equipment used in machining, tools, boiler, automobile and allied industries are exposed to damage by wear and corrosion. The materials used in the aforesaid industries should offer a high value of inherent and uniform hardness to avoid failures while in operation. Various techniques of surface finishing such as electroplating, electroless deposition, dip coating etc. have been used by researchers to render mechanical strength and toughness to the base materials (alloy or metals) by means of a sustainable coating with enhanced properties. Moreover, the hardness and other mechanical properties of various metals is quite limited in contrast to the diversified

demands of the flourishing machining/tools industries that need better performance coatings citing increase in production and consumer demands. Alloys and ceramic composite coatings fabricated from a wide range of electrolytes namely Ni-W, Ni-P, Ni-Co, Ni-Mo lend the deposits much needed enhancement in mechanical and surface properties as compared to metal deposits. Tool steel is known to exhibit hardness of around 450-500 H_v [2, 7-12]

The study and subsequent experimentation have dealt with the co-deposition of inert/ chemically stable particles (diamond) with a Ni-W alloy base matrix and study its effect on the hardness of the deposits which in turn has tremendous scope and application in the industries. The other aspect that has been investigated by means of various characterization techniques is the content and level of diamond particles incorporation into the coatings. Diamond being hard; the higher and uniform distribution and incorporation of diamond particles into the deposits are sure to yield better results in terms of morphology, crack reduction and hardness. The motivation of this study comes from the excellent properties of various composite coatings showcased by contemporary and former researchers in preparing Ni/diamond[5, 13], Ni-Co/diamond [6, 14], Ni-P/diamond[15-17] and Ni-B/diamond[18] composite coatings.

Electrodeposited Ni-W alloys and diamond composite coatings have in recent times emerged as a viable and effective alternative to hard chrome coatings owing to their ease of fabrication cost effectiveness and properties comparable to hard chrome

coatings. The former also gains preference over and above the latter because of its relative lack of hazards and toxicity as compared to the latter which is reportedly toxic and carcinogenic due to the presence of chromium.

Various operating conditions and other experimental and operating attributes are responsible for successful co-deposition of Ni-W/diamond composite coatings. Taking the aforesaid factors into account the studies conducted during the course of my research have encompassed operating parameters (such as effects of current density, diamond particle concentration), diamond particle size, introduction of Co additives to the Ni-W/diamond composite deposits, development of multilayer Ni-W/diamond composite coatings to modifying the molar ratio of Ni-W in the plating bath during the plating process. This thesis report includes the study of the effect of current density, diamond concentration in the plating bath, effect of micron and sub-micron size diamond particles in the plating bath, effect of Co additives to the Ni-W/diamond composite coatings, development of multilayer Ni-W/diamond composite coatings and also the effect of additives in the plating bath on the Ni-W alloys and Ni-W/diamond composite coatings.

1.2 Research Objectives

The major objectives of this dissertation are as follows:

- (a) Synthesis of Ni-W alloy deposits by electrodeposition method and investigation of the effect of current density, saccharine sodium on the Ni-W alloy coatings.
- (b) To analyze the effect of sodium dodecyl sulphate and sodium bromide additives/surfactants on the surface of the Ni-W alloy coatings.
- (c) Design and fabrication of Ni-W/diamond composite coatings and analysis of the effect of various operating conditions and diamond particle size on the morphology and mechanical properties of the coatings.
- (d) To investigate the effect of additives on the Ni-W/diamond nanocomposite coatings.
- (e) To analyze the effect of diamond particles on the pulse deposited multilayer Ni-W/diamond composite coatings.
- (f) To fabricate Ni-W/diamond composite coatings with varying amount of Cobalt sulphate in the plating bath and to study the effect of the variation of Co content on the Ni-W alloy and composite deposits.

1.3 Scope of Research

The research objectives were accomplished by designing a set-up for the electrodeposition of Ni-W alloy deposits and also for the fabrication of Ni-W/diamond composite coatings. In various industrial applications (for example boilers) it has been

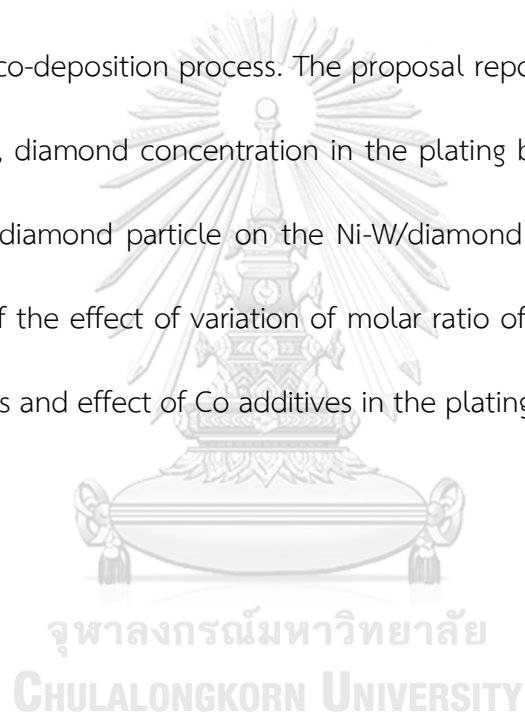
documented that the surface of the equipment and components involved in the running of the plant are highly prone to mechanical stress, corrosion and damage by wear. This in turn leads to plant closures and subsequent loss in revenue and operations in related industries like mining, mineral processing etc. Therefore, the need arises to develop non-toxic sustainable substitutes of hard chrome coatings that can offer an effective protection against corrosion, wear along with an enhanced value of hardness/toughness and an enhanced microstructure leading to certain enhanced surface properties. Citing the above examples of contemporary and previous researchers, the present study and subsequent experimentation has dealt with the co-deposition of diamond particles on a Ni-W alloy base matrix and study its effect on the hardness and microstructure of the deposits which in turn has tremendous scope and application in the industries. There are extensive applications of diamond composites in cutting tools and high precision cutting equipment. The diamond composite deposits exhibit a higher value of hardness than various composites with an enhanced wear resistance and a good fracture toughness. Moreover, the means of fabrication is simple and can be fabricated by low cost, commercially available equipment and materials as has been documented by various researchers[2, 5-7, 15, 18-24]. The properties exhibited by diamond composite coatings can be tailored to meet a wide range of performance requirements for example enhancement of the mechanical properties such as hardness, wear resistance and anti-corrosion

properties[1, 7, 13, 16, 17, 25, 26]. The diamond composite deposits can also be used to obtain protective coatings, sliding bearing, wear parts and high strength tools.

The coatings were subjected to various characterization techniques to analyze and report the variations in morphology and mechanical and surface properties including analysis using a Horiba scanning electron microscope, hardness measurement using a Vickers micro-indenter hardness measuring instrument, wear analysis using a ball-on-disc tribometer, surface analysis using a Taylor hobson surface profilometer, surface grinding and polishing using Buehler's automated and manual grinding and polishing system. The characterization and subsequent results analysis yielded several significant results which have been reported in the later sections of the dissertation.

The major aspect that has been investigated by means of various characterization techniques is the content and level of diamond particles incorporation into the coatings. Diamond being hard; the higher and uniform distribution and incorporation of diamond particles into the deposits are sure to yield better results in terms of morphology, crack reduction and hardness. Various operating conditions and other composite particle attributes are responsible for successful co-deposition of Ni-W/diamond composite coatings. Taking the aforesaid factors into account the studies conducted during the course of this research have covered operating parameters (such

as effects of current density, diamond particle concentration), diamond particle size, effect of additives into the Ni-W/diamond matrix and variation of molar ratio of Ni-W in the plating bath. The aforesaid properties and attributes of the diamond composite deposits acted as a motivation for our research in the field of enhancement of the mechanical and surface properties of diamond composite deposits by instituting various modifications in the alloy system, composite material and the operating conditions of the co-deposition process. The proposal reports the study of the effect of current density, diamond concentration in the plating bath and the effect of μm and sub μm size diamond particle on the Ni-W/diamond composite coatings along with an analysis of the effect of variation of molar ratio of Ni-W, multilayer diamond composite coatings and effect of Co additives in the plating bath.

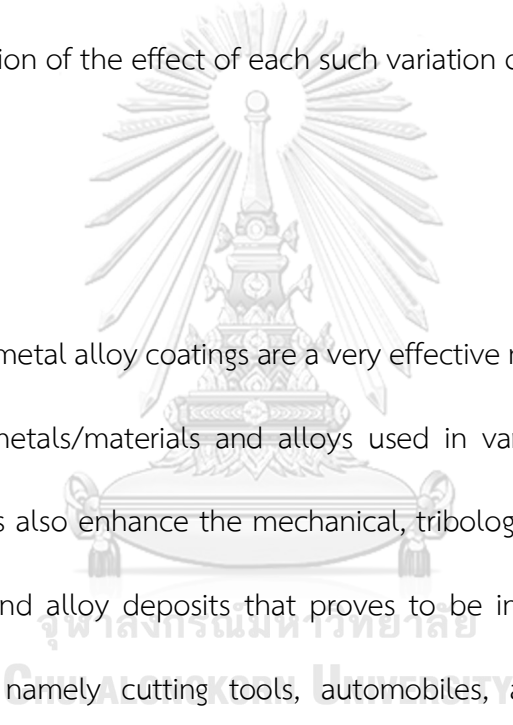


CHAPTER II THEORY

Composite electrodeposition is a reliable technique of co-depositing various particles of pure metals, ceramics and organic materials in a base matrix of metal/metal alloys to improve the deposits properties such as hardness, wear resistance, surface roughness and uniformity of distribution of co-deposited particles [5, 6, 13-18, 27]. Hardness, wear resistance and surface roughness are important surface properties which relates to the mechanical strength of the material. There are various advantages of wet process of fabrication of coatings over the dry process which involves the use of costly equipment, extreme reaction conditions and higher costs. Electrodeposition is a simple and very commonly used method of wet process deposition of films. It is extensively used to fabricate hard metal and alloy films on materials (for example Cr, Ni-W alloy) [9, 12, 23, 28-53] to name a few.

The composite particles co-deposition on the base matrix render mechanical strength to the base metal or alloy matrix. The enhancement in the properties contributed by co-deposition of ceramic particles on metal/ metal alloy matrix depends upon the extent of incorporation and distribution of the particles on the base matrix [2, 7, 21]. Various contemporary as well as past researchers have been trying to obtain the high concentration and uniform distribution of ceramic particles such as diamond, boron co-deposited on a metal/metal alloy matrix. They have in part

succeeded to a fair extent to obtain a high particle content and distribution of the aforesaid ceramic particles on the base matrix. However, there lies a vast span of scope of research and innovation towards obtaining further enhanced surface and mechanical properties of the composite deposits fabricated with ceramics such as diamond or boron by means of obtaining an optimal molar mixing ratio of composites. This could be achieved by instituting various modifications on the system and a thorough investigation of the effect of each such variation on the overall properties of the deposits.



Composite and metal alloy coatings are a very effective means to initiate protective layer for various metals/materials and alloys used in various industries. Moreover, composite deposits also enhance the mechanical, tribological and surface properties of various metal and alloy deposits that proves to be intermittently beneficial for various industries namely cutting tools, automobiles, aerospace and machining industries. Various ceramics with excellent mechanical properties have been used by researchers to fabricate composite coatings of a metal or a metal alloy. Diamond, boron, silicon nitride, tungsten carbide, silicon carbide, zirconia oxide and titanium nitride are certain examples of such composite materials that have been used of late by various contemporary researchers to fabricate deposits that exhibit enhanced properties as compared to the base metal or alloy deposits. However, there lies a

significant gap in the various surface and mechanical properties exhibited by the composite deposits and the individual properties of the ceramic particles that is used for the fabrication of such deposits. The ceramic particles tend to enhance the base properties of the alloy/metal matrix, but the level of enhancement doesn't stack up to the level of the excellent properties that the aforesaid ceramic particles individually are endowed with. There is a scope of further enhancement of the properties exhibited by various composites including diamond and boron composite deposits. Various new ideas and modifications can be instituted on the diamond, boron composite coatings system towards that end.

Electrodeposited metal alloy and composite coatings are widely used in the industry as a sustainable alternative to metal coatings. Composite coatings render the substrate with enhanced mechanical properties and also offer in situ protection to the base material from damages by various factors such as corrosion or wear. Typically, composites comprise of a base metal or alloy matrix reinforced by various ceramic materials which are co-deposited and incorporated into the base matrix. Ni-diamond composite deposits have been proven to exhibit fairly good surface and mechanical properties viz. hardness, wear resistance and durability by various contemporary researchers.

Electrodeposited Ni-W alloy coatings have been able to serve as a replacement to the hazardous hexavalent chromium coatings [1, 4, 29]. Various researchers report that the hardness of the Ni-W alloy is mainly determined by the W content and grain size of the electrodeposited Ni-W. The hardness of the as-deposited Ni-W alloy has been reported to vary between 460-670 H_v. [32, 36, 54]. However, the hardness of the Ni-W alloy is significantly lesser than that of chromium coatings which report high hardness of 1100 H_v [32, 55]. Moreover, various literatures have stated that addition of suitable particles (for example diamond, Al₂O₃, WC and SiC) to a hard alloy matrix can significantly enhance mechanical properties such as hardness, wear resistance and corrosion resistance of the deposits [3, 9, 56-58]. Xu et al. [25] has reported that the Ni-P/nano diamond composite coating returns a substantially high wear resistance and low friction coefficient in comparison with the Ni-P alloy coatings. Burkat et al. has demonstrated that the addition of pure detonation synthesis nano-diamonds in nickel and iron-based deposits results in a significant increase in micro-hardness and wear resistance of the coatings. Lee et al. [19] have exhibited the increase in micro-hardness of co-deposited surface upon increase in the concentration of the diamond powder in the plating bath. Hou et al. [20] prepared Ni-W/diamond composite coatings and investigated its wear properties. They reported that the highest level of incorporation of diamond was about 21.1 volume % as per their work. Wang et al. [21] studied the effect of heat treatment on the microstructure and mechanical properties of Ni-W/diamond composite monocrystalline coatings developed by means of

electrodeposition. They reported a maximum hardness of 1205 H_v after annealing the deposits at 600°C (caused due to the precipitation of Ni₄W phase). Zhang et al. [7] investigated the hardness of Ni-W/diamond composite coatings fabricated by pulse electrodeposition. They reported that the pulse current can affect the diamond incorporation and W content in the deposit. They also report that the diamond content in the deposits is the primary contributor towards improving the hardness of the deposits. The motivation of this study comes from the excellent surface and mechanical properties of various composite coatings showcased by contemporary and former researchers in preparing Ni-W/diamond [7, 20, 21], Ni- diamond [5, 13], Ni-Co/diamond [6, 14], Ni-P/diamond [15-17], Ni-B/diamond [18] composite coatings. This research aims to further investigate and examine the effect of electrodeposition conditions and particle size on microstructure and mechanical properties for the Ni-W/diamond composite coating.

2.1 Ni-W alloy coatings

Ni-W alloys can be prepared by using electrodeposition technique. There are a wide variety of applications of Nanocrystalline nickel tungsten (Ni-W) alloys that also tends to be environmentally safe substitute for hard chromium plating in the aerospace industry, etc. [59]. Various contemporary researchers have used Hard-chrome plating as a surface finishing technique and it has in turn been applied in various engineering industries because it has good advantages such as high hardness, corrosion resistance,

wear resistance, aesthetic qualities and durability. However, hard-chrome plating solutions are toxic, carcinogenic and hazardous to human health[60], so the need arises to develop a coating that can substitute hard-chrome plating and also be non-toxic. Hence it becomes imperative to work upon strategies to enhance the surface properties rather than bulk properties [61-63] in a wide scope of engineering materials and components used in industries. We synthesized Ni-W alloys with SDS and sodium bromide surfactants for a few perimammary samples and examined its impact on the hardness and microstructure of the deposits. It is revealed that the addition of SDS significantly alters the composition of the coatings, surface morphology and crack density microstructure[64]. However, the hardness value has been found to be maximum for the Ni-W coating prepared without SDS. The impact of NaBr has also been studied as a preliminary means to study and enhance the morphology and mechanical properties of the deposits. Upon increasing the amount of NaBr in the plating bath from 18 g/L to 25 g/L, sharp reduction in cracks and improvement in film quality was observed during the course of our which demonstrates that suitable amounts of NaBr has strong impact on the morphology of the deposits in terms of crack reduction and improvement/enhancement in the film quality. The hardness of the deposits decreases with increasing the concentration of NaBr in the plating bath. The highest hardness is observed at 0 g/L of NaBr. However, the decline in the value of hardness isn't as sharp whereas, there is a significant improvement in film quality

and enhancement of the microstructure in terms of crack reduction with the addition of NaBr surfactants in the plating bath of Ni-W electrodeposits.

2.2 Ni-W/diamond composite coatings

Composite electrodeposition is a suitable technique of co-depositing various particles of pure metals, ceramics and organic materials in a base matrix of metal/metal alloys to improve the deposits properties such as hardness, wear resistance, surface roughness and uniformity of distribution of co-deposited particles. Hardness is an important surface property which relates to the mechanical strength of the material. However, there are various advantages of wet process of fabrication of coatings over the dry process which involves the use of costly equipment, extreme reaction conditions and higher costs. Electrodeposition is a simple and very commonly used method of wet process deposition of films. It is extensively used to fabricate hard metal and alloy films on materials (for example Cr, Ni-W alloy) to name a few.

Electrodeposited Ni-W /diamond composite coatings have been able to serve as a replacement to the hazardous hexavalent chromium coatings. Various researchers report that the hardness of the Ni-W alloy is mainly determined by the W content and grain size of the electrodeposited Ni-W. The hardness of the as-deposited Ni-W alloy has been reported to vary between 460-670 H_v . However, the hardness of the Ni-W

alloy is significantly lesser than that of chromium coatings which report high hardness of 1100 H_v. Moreover, various literatures have stated that addition of suitable particles (for example diamond, Al₂O₃, WC and SiC) to a hard alloy matrix can significantly enhance mechanical properties such as hardness, wear resistance and corrosion resistance of the deposits. Xu et al. [25] has reported that the Ni-P/nano diamond composite coating returns a substantially high wear resistance and low friction coefficient in comparison with the Ni-P alloy coatings. Burkat et al. has demonstrated that the addition of pure detonation synthesis nano-diamonds in nickel and iron-based deposits results in a significant increase in micro-hardness and wear resistance of the coatings. Lee et al. [19] have exhibited the increase in micro-hardness of co-deposited surface upon increase in the concentration of the diamond powder in the plating bath. Hou et al. [20] prepared Ni-W/diamond composite coatings and investigated its wear properties. They reported that the highest level of incorporation of diamond was about 21.1 volume % as per their work. Wang et al. [21] studied the effect of heat treatment on the microstructure and mechanical properties of Ni-W/diamond composite monocrystalline coatings developed by means of electrodeposition. They reported a maximum hardness of 1205 H_v after annealing the deposits at 600°C (caused due to the precipitation of Ni₄W phase). Zhang et al. [7] investigated the hardness of Ni-W/diamond composite coatings fabricated by pulse electrodeposition. They reported that the pulse current can affect the diamond incorporation and W content in the deposit. They also report that the diamond content in the deposits is the primary

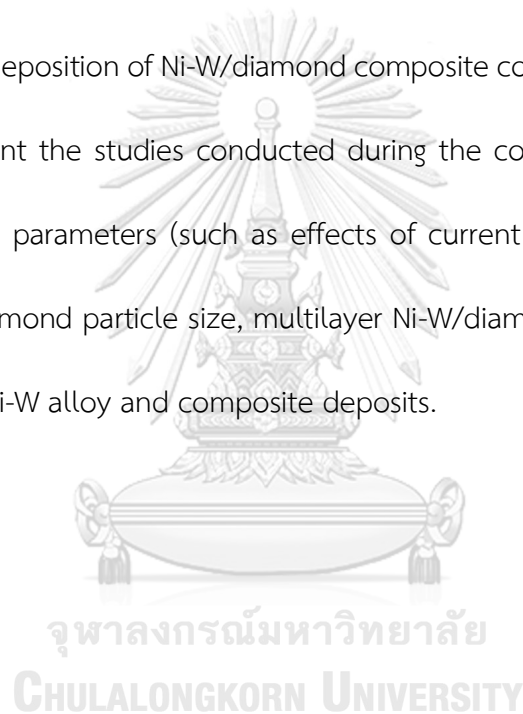
contributor towards improving the hardness of the deposits. The motivation of this study comes from the excellent surface and mechanical properties of various composite coatings showcased by contemporary and former researchers in preparing Ni-W/diamond [2, 20, 27], Ni/diamond [8, 13], Ni-Co/diamond [6, 14], Ni-P/diamond[15], Ni-B/diamond [18]. This dissertation aims to further investigate and examine the effect of electrodeposition conditions and particle size, additives, and the effect of pulse plated deposits on the microstructure and mechanical properties of the Ni-W/diamond composite coating.

Composite diamond coatings have been known to exhibit excellent mechanical, tribological and corrosion resistance properties[1, 2, 7, 8, 10, 20, 21, 23, 65]. Haung et al. prepared Ni-diamond composite deposits with a high particle content of diamond. The samples reported an increase in the value of hardness with an increase in the diamond content of the deposits. The wear resistance of the Ni-diamond composite deposits was significantly improved for the Ni-diamond composite samples fabricated with electrodeposition and electrophoretic co-deposition of diamond particles. Qin et. al also fabricated Ni-diamond composite deposits and reported an increase in diamond content in the deposits as the diamond concentration in the plating bath was increased at various current densities [8]. They further reported an enhanced anti-wear performance for the Ni-diamond samples fabricated with a high diamond content. Ogihara et al. fabricated Ni-B/diamond composite deposits and investigated the effect of the deposition conditions on the deposits[1]. They reported high diamond content

and hardness values in the deposits as the diamond concentration in the plating bath was increased to ~20 g/L. The hardness also increased significantly by about 1000 units on the vicker's scale upon heat treatment at 573 K. Zhang et al. fabricated Ni-W/diamond composite deposits and reported an increase in the micro hardness and the tribological properties of the deposits upon an increase in the diamond content of the deposits. The hardness was reported to be ~2250 H_v for the samples with 64% at% diamond content. The hardness of the deposits also increased significantly upon heat treatment at 873 K for 60 minutes to ~2650 H_v. In addition to the industrious work of the aforesaid researchers' various contemporary researchers working on the diamond composite system have exhibited a direct dependence of the surface, mechanical, tribological and corrosion resistant properties of the deposits on the diamond content of the deposits. They have employed various modifications and innovation onto the diamond composite plating techniques and conditions to obtain the desired high diamond content in the diamond composite deposits. Therefore, it appears evident the increase in diamond content of diamond composite deposits tends to enhance the surface, mechanical and tribological properties of the deposits.

The present study and subsequent experimentation have dealt with the co-deposition of diamond particles on a Ni-W alloy base matrix and study its effect on the hardness, wear resistance and microstructure of the deposits which in turn has

tremendous scope and application in the industries. The other aspect that has been investigated by means of various characterization techniques is the content and level of diamond particles incorporation into the coatings. Diamond being hard; the higher and uniform distribution and incorporation of diamond particles into the deposits are sure to yield better results in terms of morphology, crack reduction and hardness. Various operating conditions and other composite particle attributes are responsible for successful co-deposition of Ni-W/diamond composite coatings. Taking the aforesaid factors into account the studies conducted during the course of this research have covered operating parameters (such as effects of current density, diamond particle concentration) diamond particle size, multilayer Ni-W/diamond coatings and effect of additives on the Ni-W alloy and composite deposits.



CHAPTER III

ELECTRODEPOSITION OF NI-W ALLOYS AND THE COMPARISON
OF THE EFFECT OF OPERATING CONDITIONS AND SURFACTANTS
ON THE NI-W ALLOYS

3.1 Effect of operating conditions and saccharin sodium on electrodeposited Ni-W alloy
Malay Kumar Das ^{a,b}, Jiaqian Qin^{b*}, E. Srikaen^c, Y. Xue^d, X. Zhang^d, A. Thueploy^b, S.

Limpanart^b, Yuttanat Boonyongmaneerat^b

^aInternational Graduate Program of Nanoscience & Technology, Chulalongkorn
University, Thailand

^bMetallurgy and Materials Science Research Institute, Chulalongkorn University,
Bangkok, Thailand

^cDepartment of Physics, King Mongkut's University of Technology Thonburi, Bangkok,
Thailand

^dState Key Laboratory of Metastable Materials Science and Technology, Yanshan
University, Qinhuangdao, P.R. China

Email: jiaqianqin@gmail.com

Keywords: Electrodeposition, Additives

Key Engineering Materials, 659 (2015) 535-539

Abstract

Nickel-tungsten alloy deposits were fabricated by means of electrodeposition on carbon steel substrate. The effect of current density on the coatings were analyzed, which quite evidently suggested a constant increase in faradic efficiency along with increasing current density whereas the tungsten content and hardness tend to attain a maximum critical value beyond which they progressively tend to attain lower values. The Addition of saccharine as an organic additive also has a profound impact on the morphology of the coatings as suggested by the Scanning Electron Microscope (SEM). Moreover, the addition of Saccharin also tends to enhance the tungsten content in the coatings along with hardness and the grain size of the deposits.

3.1.1 Introduction

Nowadays, with the progress of the world in general and mankind in particular the subsequent consumption of metal and related alloys has also increased manifold. Metals and alloys are perhaps the greatest and the most significant discoveries by mankind. Electrodeposition as a means of alloy fabrication has by far has been reported to be a substantial tool for preparing novel nanocrystalline alloys[66] which could in turn lead us to various important and useful applications rendering such fabrication of nanocrystal alloys profitable and sustainable in practice. Metal and its various alloys have many advantages such as good strength, enhanced hardness and resistivity to heat, fairly economical and the inherent ability to form into various alloys

and combination coatings which further enhance their properties. On the other hand, metals have certain disadvantages also. Metals are typically easy to corrode[67] and exhibit low wear resistance. There are many methods to improve the properties of metals such as hardening, tempering and coating. From many researches, fabrication of metal alloys by means of adding suitable constituents under appropriate experimental conditions significantly results in high enhanced hardness and mechanical properties[62, 68-73]. It would be an interesting prospect to obtain a strengthened and enhanced Nickel-Tungsten electrodeposited coating matrix compared to the coatings as fabricated by previous researchers. Citing the aforesaid excellent physical and mechanical properties of such coatings it would be an interesting prospect if we could delve deeper into the realm of Ni-W alloy coatings and the effect of organic additives like saccharin sodium on the aforesaid mechanical properties namely hardness, tungsten content, grain size and effect on the SEM morphology in our case as well as the effect of certain operating conditions.

3.1.2 Experimental Details

Ni-W alloy was electrodeposited from an ammonia-citrate bath. The bath composition was Nickel Sulphate 18g/L, Sodium tungstate 53g/L, Tri Sodium Citrate 168 g/L, Ammonium Chloride 31g/L, Sodium Bromide 18g/L, Saccharine Sodium 0.5,1 and 2g/L respectively. The operating temperature was 75 °C The pH, RPM and the Deposition time was kept constant at 8.9, 200 and 2 hours respectively. The current

density was varied between $0.05\text{A}/\text{cm}^2$ - $0.2\text{A}/\text{cm}^2$. The substrate was subjected to pre-treatment before deposition by means of washing it with soap solution, keeping it immersed in 10% NaOH solution for 20 minutes and 14% HCL for 10 minutes. Subsequently the substrate was washed with Distilled water and subjected to sonication while being immersed in ethanol for 5 minutes before being dried and weighed. Prior to insertion of the electrodes in the plating bath containing the electrolytic solution the deposition area of the substrate was again activated by pouring few drops of 14% HCL over it and later it was again washed with distilled water to remove any traces of acid on the surface so as to maintain a uniform pH throughout the experiment. The electrodeposition was carried out by a Direct current power source. Structural analysis and grain size of the alloys were obtained by X-ray diffraction (XRD) technique and using Scherrer's equation for calculation of the grain size. The surface morphologies and the compositions were investigated by scanning electron microscopy (SEM) and energy -dispersive X-ray spectroscopy (EDS). Vickers hardness was measured by Mitutoyo Hardness Tester.

3.1.3 Results and Discussions

3.1.3.1 Effect of current density

During the course of the experiment the applied current density was varied from $0.05\text{A}/\text{cm}^2$ to $0.2\text{A}/\text{cm}^2$. The samples were further characterized by means of SEM, X-ray diffraction spectra patterns, hardness Testing by Mitutoyo Hardness tester and Elemental constituents by EDS.

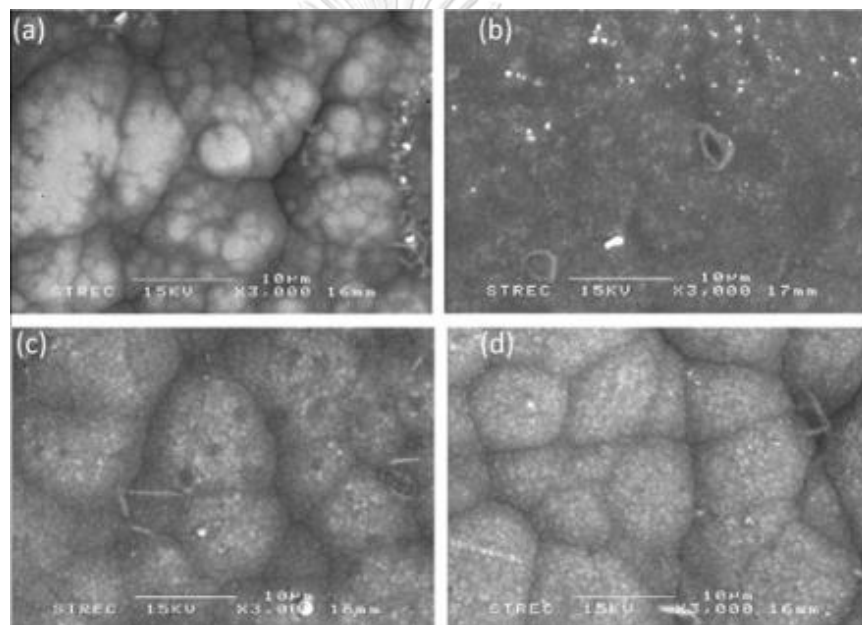


Figure 1 SEM Image for current density (a) $0.05\text{A}/\text{cm}^2$ (b) $0.1\text{A}/\text{cm}^2$ (c) $0.15\text{A}/\text{cm}^2$ (d) $0.2\text{A}/\text{cm}^2$

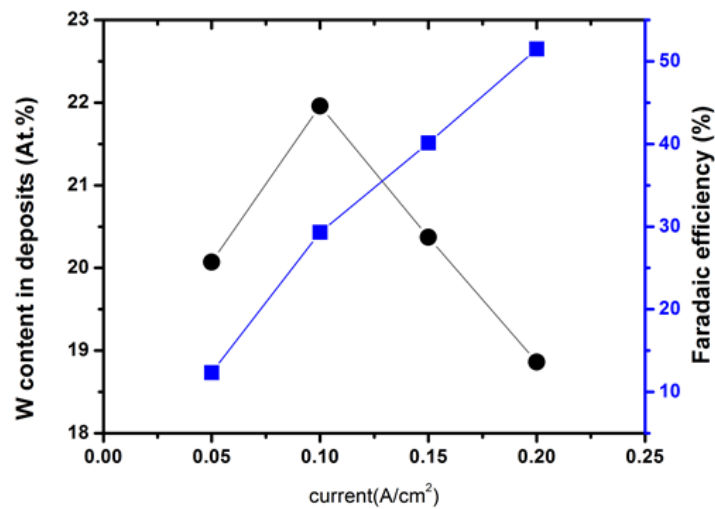


Figure 2 Composite graphs for the tungsten content and Faradic efficiency of the coatings.

The coatings exhibited maximum hardness at $0.15\text{A}/\text{cm}^2$ with slightly lower value of hardness at $0.1\text{A}/\text{cm}^2$ current density. The tungsten content was also found to be maximum at $0.1\text{A}/\text{cm}^2$. The grain size attains a critical minimum at $0.1\text{A}/\text{cm}^2$ beyond which successive enhancement is observed in the grain size. However, at high current densities the Faradic Efficiency tends to exhibit an increasing trend which in turn causes the hydrogen evolution become more prominent[59] leading to additional agitation in the solution.

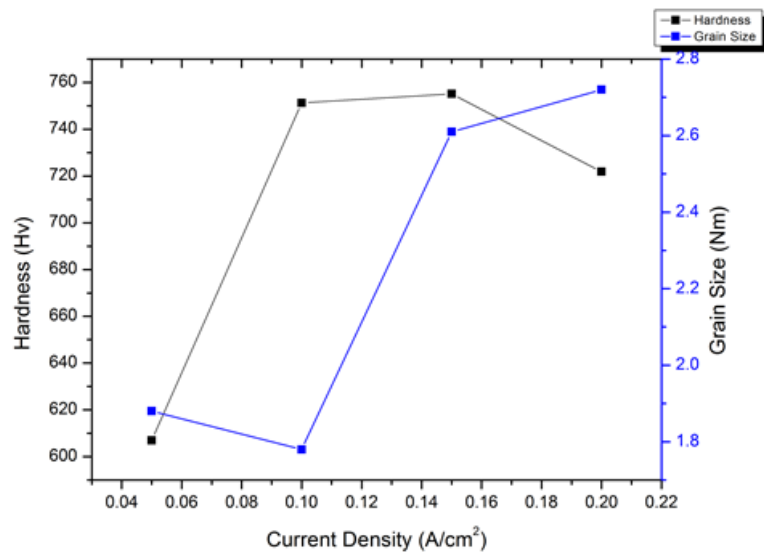


Figure 3 Composite Graph for Hardness and grain size obtained from XRD spectra for the coatings

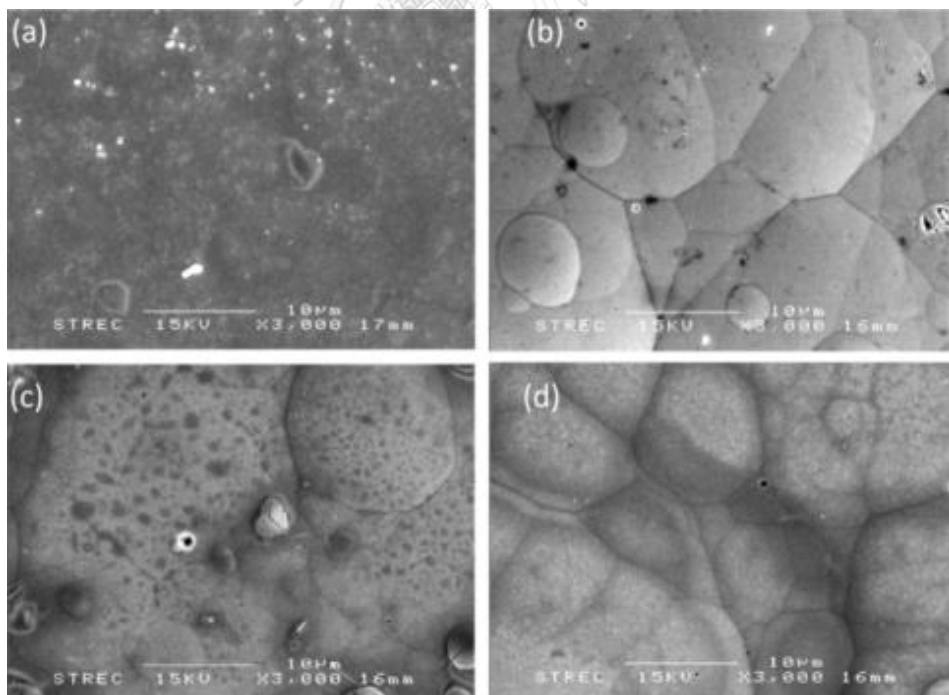


Figure 4 SEM images of the coatings with various quantities of Saccharin Sodium (a) 0g/L (b) 0.5g/L (c) 1g/L (d) 2g/L.

Contemporary researchers have also suggested that with the gradual increase in current density there is a relative decrease in Ni ion concentration in the deposits[74]. Since Nickel is deposited easily as compared to tungsten[59] owing to the fact that it's a lighter than tungsten and comparatively easier to undergo electrodeposition directly, a higher value of Faradic efficiency results in higher concentration and distribution of Nickel on the coatings which is undesirable as per our research goals. Therefore, we need an optimum pair of current density and suitable faradic efficiency which would lead to optimized and relatively higher tungsten content in our deposits. Various contemporary researchers in the metal alloys electrodeposition field have reported an increase in residual stress with an increase in current density[23]. While analyzing the SEM images the deposits were found to be amorphous for lower current densities. However, at $0.1\text{A}/\text{cm}^2$ current density a remarkable refinement of the surface quality with reduced cracks and in turn possibly reduced internal stress as compared to various other current densities is observed. Also, at the aforesaid current density the grain boundaries are finer and continuous and relatively less conspicuous and pronounced in appearance. Owing to an optimized tungsten content, a suitable grain size as per XRD results and a fairly better SEM morphology of the image $0.1\text{A}/\text{cm}^2$ was fixed as the optimal operating current for the subsequent studies on the effects of various additives on our coatings as already mentioned.

3.1.3.2 Effects of Saccharin Sodium on the coatings

The amounts of Saccharin sodium added were 0.5, 1 and 2 g/L respectively. Saccharin sodium acts as a grain refiner with further offers enhanced film quality and reduction in the diffusion of contaminates in the coatings[75]. According to Figure 5 and Figure 6 the tungsten content of the coating shoots up to a maximum value at 2g/L of saccharin sodium concentration. Moreover, there is successive and continuous increase in the tungsten content of the deposits as the concentration of saccharin sodium is increased in our coatings. The faradic efficiency on the other hand shows a similar downward trend which could perhaps be due to the fact that Saccharin sodium atoms tends to block the active sites in the deposits by means of a reversible process of diffusion on the coated surface thereby reducing further crystal growth[75] and subsequently lowering the efficiency of the current to cause further deposition and dissociation of ions including deposition of contaminates and also evolution of hydrogen as contaminate. The addition of saccharine also tends to have an effect in terms of reduction of the internal stress of the coatings[75, 76] and also the quality of deposits[75] in terms of reduction of irregularities in the morphologies which occasionally manifest themselves in the forms of cracks or irregular distribution or thickness of the alloy deposits. Moreover, along with the addition of saccharin we see a progressive increase in grain size as shown in Figure 6. This above mentioned

phenomena could most possibly be attributed to the reduction in the concentration of Ni ions at the boundary separating the coating with the electrolyte[77].

There is possibly also an obvious modification of the boundary/interface of crystal growth by hydrogen evolved during the course of reaction. Hydrogen is known to decrease the surface energy of vertical planes (100) which in turn leads to crystal growth thereby facilitating the presence of larger grains as is evident from Figure 6. We can also see that addition of saccharin sodium progressively doesn't seem to alter the mechanical properties of hardness to great extent. The hardness and ductility typically has been reported to be grossly unaffected by the addition of organic additives/size refiners like saccharine[78]. The phenomena of grain refining in terms of transition to Nano crystalline coatings could also possibly enhance the corrosion resistance of the deposits by means of a formation of a highly increased passive resistance[79] of the film . Now as the purview is shifted towards analyzing the various SEM images for the deposits it is evident that there is a marked difference in the morphologies on increasing the amount of saccharin sodium in the constituents on the reaction. The coating exhibits an almost amorphous structure in the absence of saccharin whereas at the least level of saccharin as in Figure 4 (a) well defined boundaries and somewhat crystalline structures are observed. The globular formations with circular or almost quasi circular formations in Figure 4 (b, c, d) also suggests that real grain boundaries

probably exist between the individual grains pointing towards the prevalence of somewhat crystalline structure. Also, there is a marked increase in grain size along with subsequent refinement of the grain boundaries and morphology/film quality with the addition of SS.

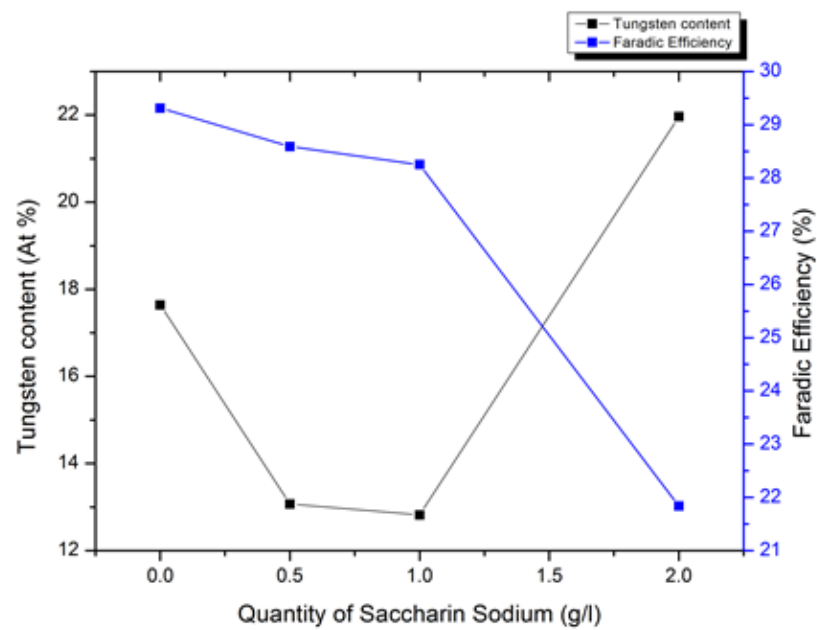


Figure 5 Composite graphs for the effect of Saccharin Sodium on tungsten content and Faradic efficiency of the coatings

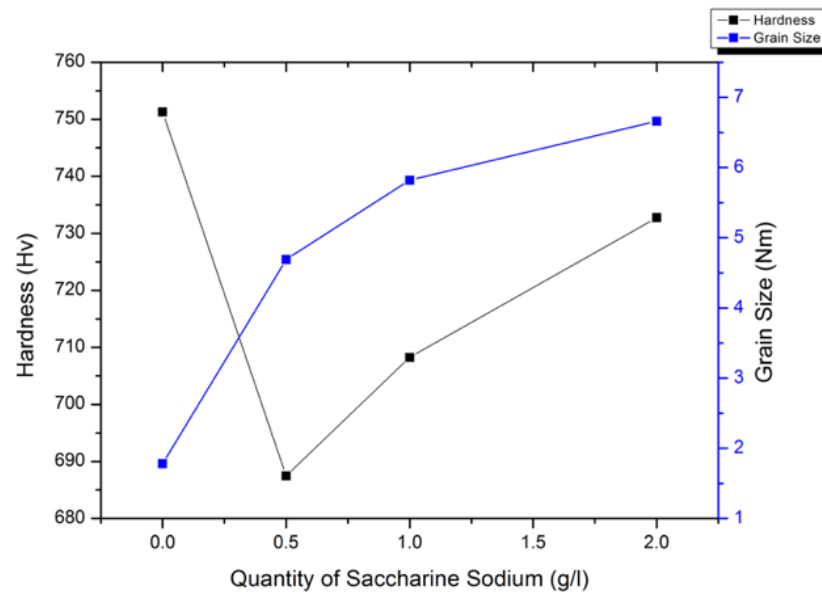


Figure 6 Composite graphs for the effect of Saccharin Sodium on hardness and Grain Size of the coatings

3.1.4 Conclusions

During the course of our research it is observed that there is a profound and marked difference in the effect of saccharin sodium on the coatings as compared to coatings without saccharin sodium additives. The pivotal role of the applied current density in the nature and attributes of the deposits has also been established by means of the significant changes in properties upon successive variations of the current density. The above mentioned results have established that almost all of the parameters under investigation for the coatings tend to attain an optimal/critical value of current density

at $0.1A/cm^2$ beyond which they exhibit sharp variations. The effect of saccharine sodium tends to be quite beneficial towards obtaining enhanced tungsten content in the deposits along with enhancement of the morphology of the coatings in terms of crack reduction and reduction of amorphous or coarse nature of the deposits. In context of the above mentioned observation and experimental results it can be inferred that addition of saccharine sodium tends to optimize the various desirable components of the coatings to a comparatively greater extent.



3.2 Effect of SDS and sodium bromide additives on Ni-W nanocoatings

Malay Kumar Das^{a,b}, Jiaqian Qin^{b*}, Xinyu Zhang^{c*}, Rongxia Li^c, Adisak Thueploy^b, Sarintorn Limpanart^b, Yuttanat Boonyongmaneerat^b, Mingzhen Ma^c, Riping Liu^c

^aInternational Graduate Program of Nanoscience &Technology, Chulalongkorn University, Bangkok 10330, Thailand

^bMetallurgy and Materials Science Research Institute, Chulalongkorn University, Bangkok 10330, Thailand,

^cState Key Laboratory of Metastable Materials Science and Technology, Yanshan University, Qinhuangdao 066004, P.R. China

Journal of Nanoscience and NanoTechnology 17(2017) 1217-1224

จุฬาลงกรณ์มหาวิทยาลัย
CHULALONGKORN UNIVERSITY

Abstract

Nickel-tungsten (Ni-W) coatings were fabricated by electrodeposition method with varying quantities of sodium dodecyl sulphate and sodium bromide to examine the effects of the aforesaid additives on the coatings. The obtained nanocoatings were studied by X-ray diffraction, scanning electron microscopy, energy dispersive x-ray spectroscopy, and hardness tester. The hardness, tungsten content and grain size attained a maximum value at current density of 0.15 A/cm², 0.1 A/cm² and 0.1 A/cm²,

respectively. There was a pronounced impact of both the additives on the microstructure and morphology of the coatings. According to results, there are considerable difference in terms of the impact caused by the additives to the tungsten content, hardness and grain size of the coatings. The obtained results suggest that hardness of coatings is mainly contributed by W content in the deposits.

Keywords: Ni-W nanocoating, Electrodeposition, SDS, Sodium bromide

*Corresponding author. Tel: +66 2218 4243; fax: +66 2611 7586.

Email addresses: jiaqianqin@gmail.com (J. Qin), xyzhang@ysu.edu.cn (X. Zhang)

3.2.1 Introduction

Nanocrystalline nickel tungsten (Ni-W) alloys have a wide array of applications such as fabricating the alloys in some sort of barrier/capping layers for ultra large scale integration applications in copper metallization, potential applications in microelectromechanical systems, various allied applications in mold inserts, magnetic heads and relays, bearings, resistors, electrodes accelerating hydrogen evolution from alkaline solutions, environmentally safe substitute for hard chromium plating in the aerospace industry, etc.[59]. Hard-chrome plating has been used as a surface finishing technique in various engineering industries because it has good advantages such as high hardness, corrosion resistance, wear resistance, aesthetic qualities and durability. However, hard-chrome plating solutions are toxic, carcinogenic and hazardous to

human health[60], so to substitute chromium; the new alternate surface finishing method must maintain hard-chrome's advantages. One very important and sustainable prospect is to substitute hard-chrome plating with metal alloy plating. In various industrial applications (for example boilers) it has been documented that the surface of the equipment and components involved in the running of the plant are highly prone to mechanical stress, corrosion and damage by wear. This in turn leads to plant closures and subsequent loss in revenue and operations in related industries like mining, mineral processing etc. Hence it becomes imperative to work upon strategies to enhance the surface properties rather than bulk properties [62, 63, 80] in a wide scope of engineering materials and components used in industries.

There has been fairly substantial amount of study on the effect of surfactants on various metal alloys and composites. Wu et al.[81] investigated the effect of boric acid on electrodeposition processes and structure of Ni-W alloy coatings and reported that the boric acid acts as a surfactant in the solution causing an increase in both the current efficiency and W content. The boric acid impeded the proton reduction, resulting in the formation of a certain complex with tungstate which in turn aided the co-deposition of tungsten leading to an increase in the tungsten content in the deposits. Hamid et al.[82] investigated the effect of various surfactants on the electroless deposition of Ni-W-P alloys. The surfactants influenced the tungsten content of the deposits along with enhancing hardness, corrosion resistance and crystalline refinement[82]. Le et al.[83] synthesized Ni-W sulfide hydro-treating catalysts under

various methodologies of preparation with the influence of organic surfactants as one of the preparation methods. They subsequently studied the effects of the variations in the fabrication methods on the Ni-W hydro-treating catalysts[83]. It is evident by the study of past as well as contemporary researchers that incorporation of suitable surfactants (cationic or anionic) into a metal alloy or alloy composites coatings tends to have an impact on the surface properties of the deposits. The study of the effect of surfactants on various other metal alloys has also been a field of significant interest for various researchers [64, 81-91]. However, there have been almost negligible studies on the effects of sodium dodecyl sulphate (SDS) and sodium bromide (NaBr) on Ni-W alloy in terms of microstructure, hardness, crystalline size, tungsten content and faradaic efficiency. The aforesaid fact along with the quest for further investigation and enhancement of the surface properties of electrodeposited Ni-W alloy was the prime motivation behind this work. In this paper the effect of additives and current density of Ni-W alloys has been discussed. The results that were reported threw up certain useful facts which could be used to develop optimal use of additional additives on the Ni-W alloy.

3.2.2 Experimental Details

Ni-W coating was fabricated on a stainless-steel substrate by means of electrodeposition from an ammonia-citrate bath. The bath composition was nickel sulphate 18 g/L, sodium tungstate 53 g/L, tri-sodium citrate 168 g/L, ammonium

chloride 31 g/L, sodium bromide 18 g/L and 25 g/L, SDS 0.1 g/L, 0.5 g/L and 0.8g/L respectively. The operating temperature was 75 °C, the pH value, stirring speed and the deposition time was kept constant at 8.9, 200 RPM and 2 hours, respectively. The current density was varied between 0.05-0.2 A/cm².

The substrate was subjected to pre-treatment before deposition by means of washing it with soap solution, keeping it immersed in 10% NaOH solution and 14% HCL. Prior to insertion of the electrodes in the plating bath, the substrate was activated by 14% HCL. Except the deposition area the other undesirable parts of the substrate were covered with polymer tape.

X-Ray diffraction (XRD) technique was employed to analyze the phases of the deposits along identification and analysis of the grain size of the coatings. Brooker D8 advance X-ray diffractometer operated at Cu K α radiation at a rating of 40 kV, 20 mA was used. The scan rate was 0.02° per step and the measuring time 0.5 second/step. Scherer's equation was employed for the calculation of the grain size of the coatings:

$$D = \frac{0.9 \lambda}{\beta \cos \theta} \quad (1)$$

where, D is the grain size, λ is the incident radiation (1.5418 Å), β is the corrected peak width at half maximum intensity and θ is the angular position.

The samples were characterized in terms of morphology and microstructure by JEOL JSM-6400 scanning electron microscope (SEM) with energy dispersive X-ray

spectroscopy (EDS) capability embedded into it. The coating hardness was measured on the surface using Mitutoyo hardness tester with a Vickers's diamond indenter under a load of 100 g (0.98 N). The dwell time for each indentation was 15 seconds and the values reported represent the average and standard deviation of a minimum of seven measurements. The Vickers hardness can be calculated in accordance with the formula:

$$H_v = 1854 \frac{L}{d^2} \quad (2)$$

where, H_v is the hardness in Vickers's and L is the applied load and d is the diagonal of the indentation.

The Faradaic efficiency (FE) was calculated from the charge passed, the weight gained, and the chemical composition of the deposit as determined by EDS, using the following equation mentioned below. Each sample was weighed before and after deposition and the coating weight was found by calculating the difference in weight. The faradaic efficiency was determined for each specimen using the difference in weights before and after plating. The faradaic efficiency of the alloy is calculated as equation below:

$$FE = \frac{w}{It} \sum \frac{c_i n_i F}{BM_i} \times 100 \quad (3)$$

where, FE is the faradaic efficiency, w is the measured weight of the deposit (g), I is the current passed (A), t is the deposition time (h), c_i is the weight fraction of the element

(either nickel or tungsten) in the binary alloy deposit, n_i is the number of electrons transferred in the reduction of 1 mol atoms of that element ($n_i=2$ for nickel and 6 for tungsten), M_i is the atomic weight of that element (g mol^{-1}), F is the Faraday constant ($96,485.3 \text{ C mol}^{-1}$) and B is a unit conversion factor ($3600 \text{ C A}^{-1}\text{h}^{-1}$)[92].

3.2.3 Results and Discussions

3.2.3.1 Effect of current density

The samples were fabricated at temperature of 75°C , pH value of 8.9, and current densities ranging from 0.05 A/cm^2 to 0.2 A/cm^2 . X-ray diffraction patterns for the Ni-W alloy deposits for different current densities are shown in Figure 7. The analysis of the peaks revealed a face centered cubic (FCC) structure of deposits. No W peaks were found. The grain size of the deposits as obtained from the Scherer's equation is 1.9 nm, 1.8 nm, 2.6 nm and 2.7 nm for current density of 0.05 A/cm^2 , 0.1 A/cm^2 , 0.15 A/cm^2 and 0.2 A/cm^2 , respectively (Figure 8). The XRD results are consistent with the findings of Yamasaki et al.[93] for Ni-W alloys fabricated by electrodeposition. For all the samples, the appearance of Ni peak was related to (111) plane as the major and significant peak in the deposits. The development of this texture was associated with the preferred growth along (111) orientation because of the lower strain associated[94]. The grain size of the deposits prepared at current density of 0.1 A/cm^2 is smaller than those of Ni-W coatings fabricated at other current densities.

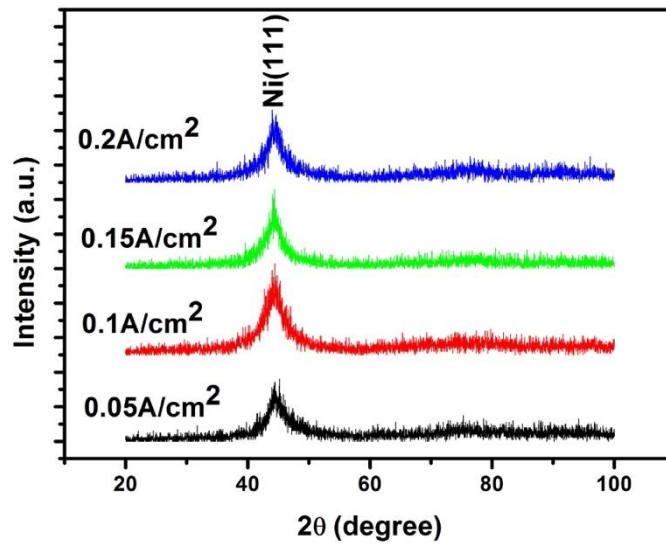


Figure 7 XRD pattern with peak value for different current densities in Ni-W alloy coatings fabricated at temperature of 75 °C, and pH value of 8.9.

The hardness as reported on the Vickers's scale by the Mitutoyo hardness tester is 607, 751, 755 and 722 for the coatings prepared at current density of 0.05 A/cm², 0.1 A/cm², 0.15 A/cm² and 0.2 A/cm², respectively (Figure 8).

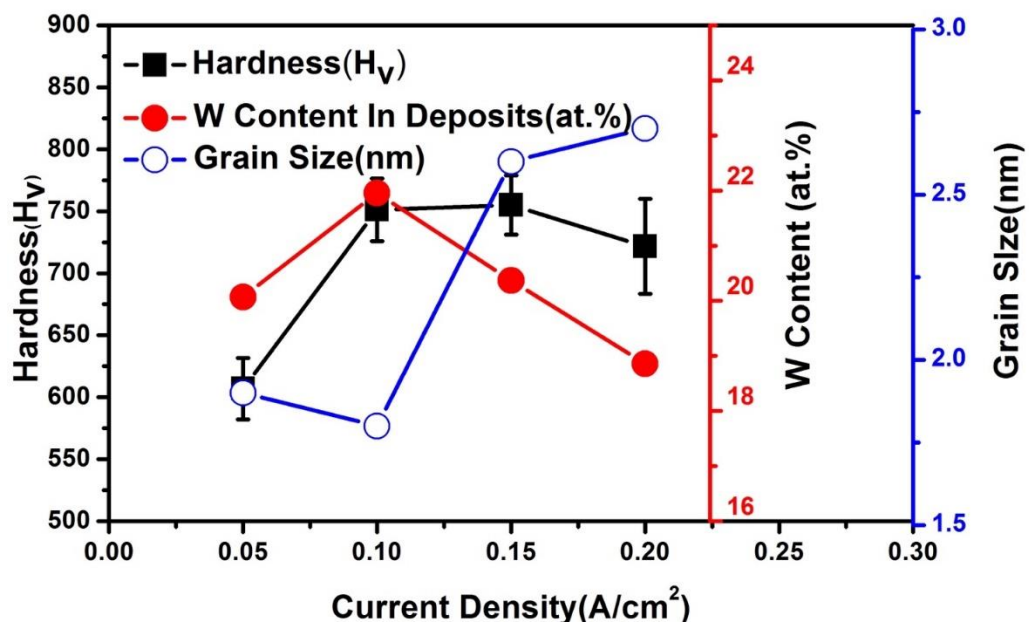


Figure 8 Effect of current densities on the hardness, W content and crystalline size of the Ni-W alloy deposits fabricated at temperature of 75 °C, and pH value of 8.9.

Upon analysis of the SEM images in Figure 9, the deposits are inconsistent for lower current densities. The W content of Ni-W coatings prepared at current density of 0.05 A/cm², 0.1 A/cm², 0.15 A/cm², 0.2 A/cm² is reported to be 20.07 at. %, 21.96 at. %, 20.37 at. %, and 18.86 at. %, respectively (Table 1). At current density of 0.1 A/cm², a remarkable refinement of the surface quality with reduced cracks is observed. It might be due to reduced internal stress (in the deposits) as compared to higher current densities[23]. Also, at current density of 0.1 A/cm², the grain boundaries appear finer and relatively less conspicuous or pronounced in appearance. The tungsten content is found to be maximum at current density of 0.1 A/cm². Owing to optimized tungsten content, high hardness, a relatively smaller grain size and a fairly better morphology as per SEM results; current density of 0.1 A/cm² has been chosen as the operating current density for the subsequent studies on the effects of various additives on our coatings.

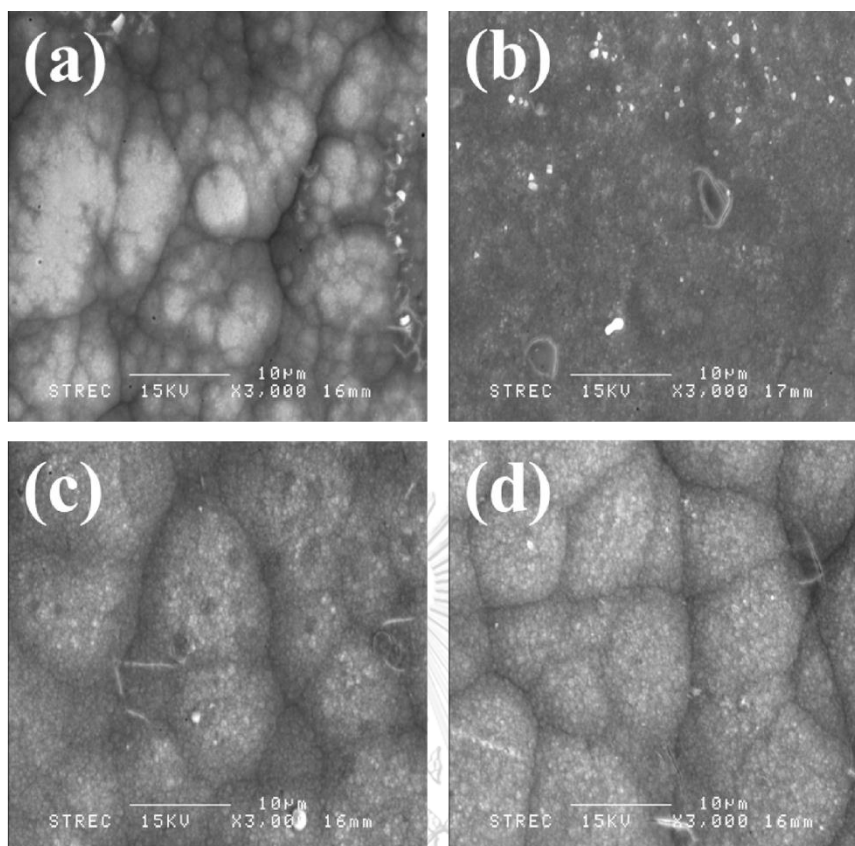


Figure 9 SEM images for the Ni-W coatings prepared at temperature of 75 °C, and pH value of 8.9 for various current densities (a) 0.05 A/cm² (b) 0.1 A/cm² (c) 0.15 A/cm² (d) 0.2 A/cm².

จุฬาลงกรณ์มหาวิทยาลัย
CHULALONGKORN UNIVERSITY

Table 1 Elemental composition of the Ni-W coating prepared at temperature of 75 °C, pH value of 8.9, and different current density.

Current density (A/cm ²)	Nickel (at. %)	Tungsten (at. %)
0.05	79.93	20.07
0.1	78.04	21.96

0.15	79.63	20.37
0.2	81.14	18.86

The faradaic efficiency is 12.32%, 29.31%, 40.12% and 51.48% for current density of 0.05 A/cm², 0.1 A/cm², 0.15 A/cm², 0.2 A/cm², respectively. The faradaic efficiency is continuously increasing with increasing in current density as reported in Figure 10. At lower current densities, the faradaic efficiency tends to exhibit an decreasing trend which in turn causes the hydrogen evolution become more prominent[59]. The increased hydrogen evolution leads to additional agitation in the solution. It is imperative to maintain an optimal current density during electrodeposition process to minimize hydrogen evolution and agitation in the plating bath. Contemporary researchers have also suggested that with the gradual increase in current density there is a relative increase in Ni ion concentration in the deposits[74]. Since, Ni is deposited easily as compared to tungsten[59], a higher value of faradaic efficiency results in higher concentration and distribution of Ni on the coatings which is undesirable as per the research goals. Various contemporary researchers in the metal alloys electrodeposition field have also reported an increase in residual stress with an increase in current density and faradaic efficiency [23]. Therefore, an optimum pair of current density and faradaic efficiency would lead to reduced residual stress and relatively higher tungsten content in the deposits.

The effect of current density on the grain size, tungsten content, and hardness is plotted in Figure 8. Considerably high value of the hardness coincides with high tungsten content and a reduced grain size. This suggests that the increase in tungsten content and the successive reduction in grain size tend to affect the hardness of the samples in a positive manner[44]. Therefore, a strong dependency of hardness values on both the grain size and W content of the coatings for variations in current density is established.

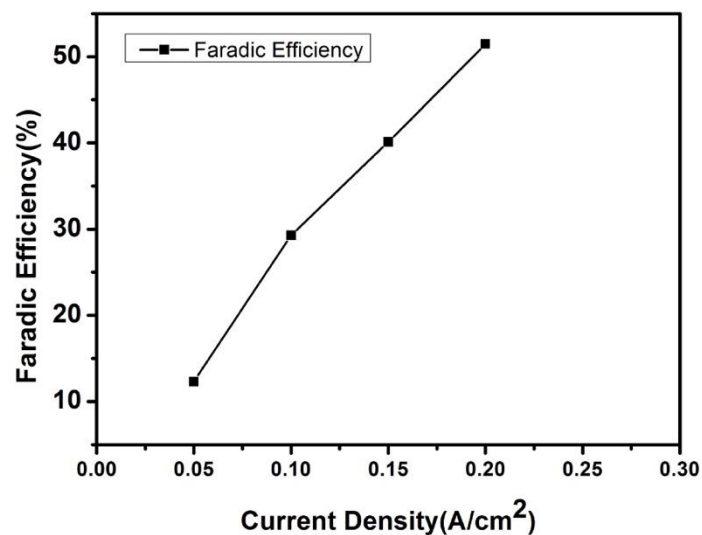


Figure 10 Effect of current density on the faradaic efficiency of the coatings fabricated at temperature of 75 °C, and pH value of 8.9.

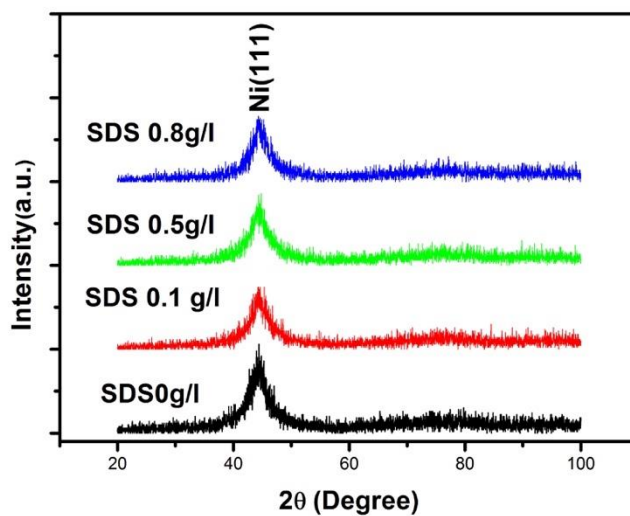


Figure 11 XRD pattern for different quantities of SDS in the plating bath for Ni-W alloy coatings fabricated at current density of 0.1 A/cm^2 , temperature of 75°C , and pH value of 8.9.

3.2.3.2 Effects of SDS on the coatings

Various quantities of SDS were added to the plating bath during the course of fabrication of the coatings to study its effects on the Ni-W coatings. The amounts of SDS added were 0.1, 0.5 and 0.8 g/L, respectively. XRD patterns of Ni-W coatings for different quantities of SDS are shown in Figure 11. The diffraction pattern revealed an FCC structure of Ni deposits. Similar to the case of XRD peaks for different current densities no W peaks were found. The grain size is 1.8, 1.8, 2 and 2.1 nm for 0, 0.1, 0.5 and 0.8 g/L of SDS, respectively (Figure 12). For all the samples a single high intensity

Ni peak was reported at (111) plane. The development of the texture was associated with the preferred growth along (111) orientation because of the lower strain associated. The grain size increases with increasing in the amount of SDS in the plating bath beyond 0.1 g/L.

The calculated hardness for various quantity of SDS is 751, 655, 667, and 716 for 0, 0.1, 0.5 and 0.8 g/L of SDS, respectively (Figure 12). The hardness value has been found to be maximum for the Ni-W coating prepared without SDS. However, the effect of SDS has been further studied in terms of SEM and EDS analysis to compare the microstructure and elemental composition in the coatings respectively. The microhardness of the coatings increases upon successive increase in the content of SDS up to a typical value of micelle concentration[64] beyond which it would be rather stabilized or not shows any such profound effects.

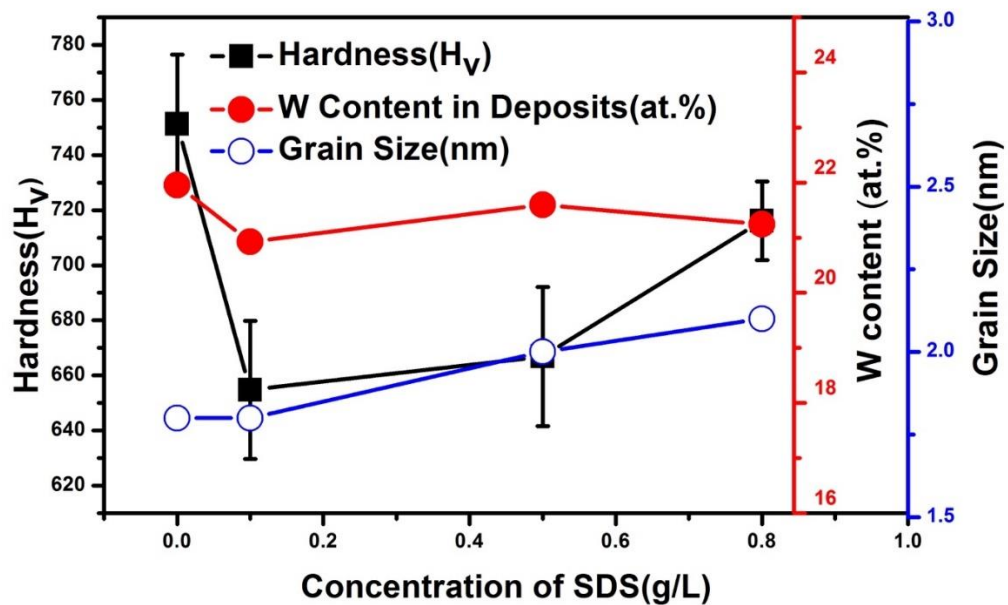


Figure 12 Effect of SDS on the hardness, W content and crystalline size of the Ni-W alloy deposits fabricated at current density of 0.1 A/cm^2 , temperature of $75 \text{ }^\circ\text{C}$, and pH value of 8.9.

The samples were also analyzed by SEM (Figure 13); it is revealed that the addition of SDS significantly alters the composition of the coatings, surface morphology and crack density of the microstructure [64]. The EDS results for the variation in the quantity of SDS in the plating bath are shown in Table 2. There seems to be an impact of SDS additions on the tungsten content, marginal impact on hardness, grain size and also the faradaic efficiency of the coatings. Moreover, the SEM images (Figure 13) suggest wide variations in the surface morphology, crack density and film quality and structure on the coatings with SDS as compared to samples without SDS.

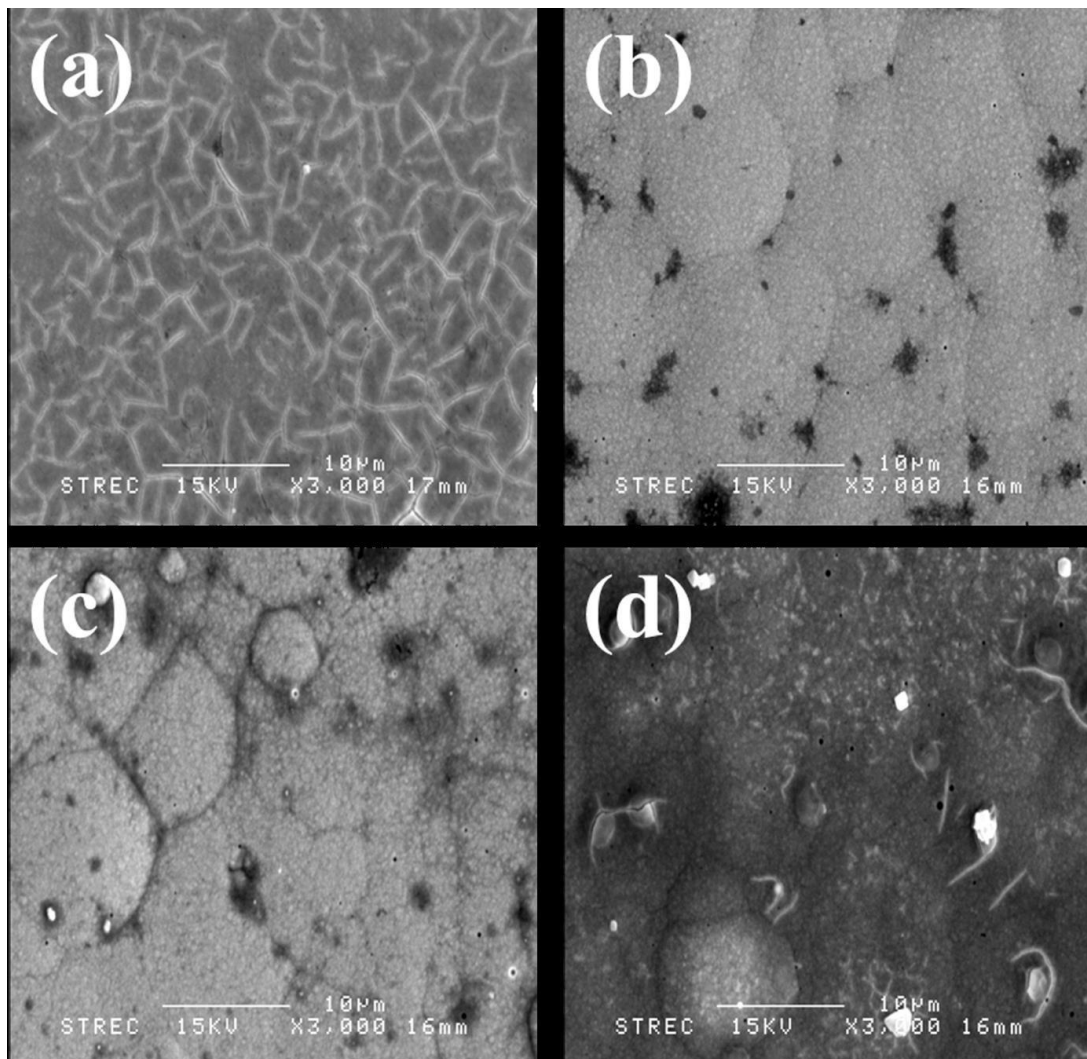


Figure 13 SEM images for the coatings deposited at current density of 0.1 A/cm^2 , temperature of $75 \text{ }^\circ\text{C}$, and pH value of 8.9 for various quantities of SDS in the plating bath (a) 0 g/L (b) 0.1 g/L (c) 0.5 g/L (d) 0.8 g/L.

The SEM image of Ni-W coatings prepared without SDS clearly shows numerous cracks on the surface in Figure 13 (a), whereas smoother boundaries and reduction of cracks is observed as SDS is added in small quantity in Figure 13 (b). This is because of reduction of internal strain and increase in ultimate tensile strength upon addition of SDS which acts as a surfactant [64, 84-90]. The increase in the ultimate tensile strength due to the addition of SDS surfactant is primarily responsible for the reduced crack

density and smoother boundaries in the deposits. The tungsten content of Ni-W coatings prepared at different SDS concentration keeps almost constant, and the hardness of the obtained coatings decreases quickly from 751 Hv to 655 Hv with addition of 0.1 g/L of SDS. From 0.1 g/L to 0.8 g/L SDS, the hardness slightly increases from 655 Hv to 716 Hv. The grain size as reported is increased with increasing in SDS concentration. The above results especially in respect of the change in morphology as per SEM data and EDS results for tungsten content establishes that the effects of the surfactant tends to attain a maximum critical point of influence which is due to attaining a critical micelle concentration [64] beyond which it tends not to have a considerable effect on the aforesaid parameters. The tungsten content and a suitable microstructure are quite important in order to attain good hardness and film quality. Surfactants are important contributors towards reducing the surface tension forces in the coatings which subsequently results in a better and uniform surface with considerably reduced cracks and as in an almost pit free microstructure as observed in Figure 13 (b and c) [64]. However, the Figure 13 (c) depicts sharper boundaries as compared to Figure 13 (b).

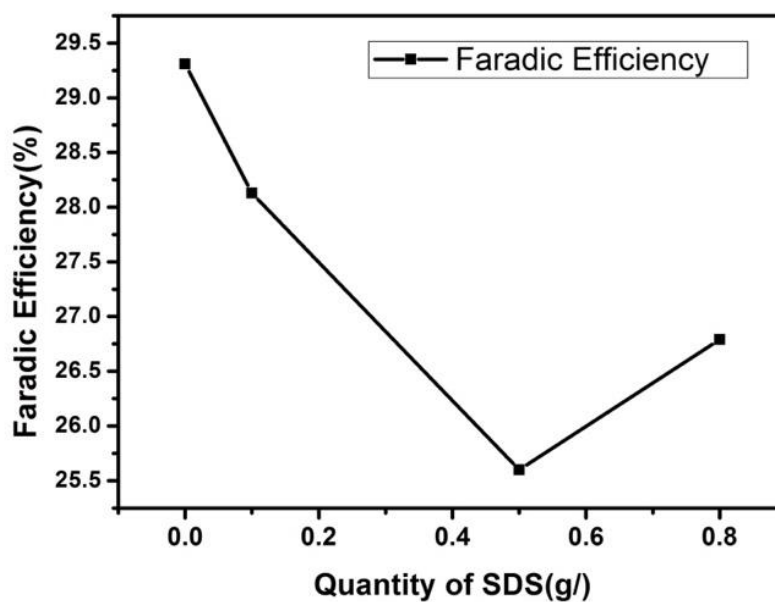


Figure 14 Effect of SDS on the faradaic efficiency of the coatings fabricated at current density of 0.1 A/cm^2 , temperature of $75 \text{ }^\circ\text{C}$, and pH value of 8.9.

Table 2 Elemental composition of the Ni-W coatings deposited at temperature of $75 \text{ }^\circ\text{C}$, pH value of 8.9, and current density 0.1 A/cm^2 , with different SDS concentration.

Amount of SDS (g/L)	Nickel (at. %)	Tungsten (at. %)
0	78.04	21.96
0.1	79.07	20.93
0.5	78.40	21.60
0.8	78.75	21.25

The variation of the faradaic efficiency with varying amounts of SDS is shown in Figure 14. There is a marked decrease in the values of faradaic efficiency up to a critical minimum value. Beyond 0.5 g/L of SDS the faradaic efficiency shows an increasing trend at 0.8 g/L. This is due to the fact that beyond a critical micelle concentration[64] the effect of SDS ceases to be more conspicuous in terms of decreasing the efficiency of the current to cause electrodeposition.

The effect of the grain size and tungsten content on the micro hardness has been shown in Figure 12. For different amounts of SDS the hardness is maximum at a point where both the crystalline size and tungsten content are relatively higher. As the grain size and tungsten content drop relatively, their effect on hardness is observed in terms of decreasing hardness. For the Ni-W coating prepared without SDS, the hardness is comparatively higher despite a lower value crystalline size suggesting a more pronounced impact of the tungsten content on the hardness than that of the grain size when the amount of SDS is varied in the plating bath.

3.2.3.3 Effect of sodium bromide

XRD patterns of Ni-W alloy deposits with different amounts of sodium bromide in the plating bath are shown in Figure 15. The XRD patterns show only nickel in the

coatings. No W peaks are found. For all the samples the appearance of Ni-peak as suggested by the various values in the diffractograms was related to (111) plane as the only major and significant peak. The development of this texture was associated with the preferred growth along the (111) orientation because of the lower strain associated with that plane [94]. The grain size is 1.6, 1.8 and 2.9 nm for obtained coatings prepared at sodium bromide concentration of 0, 18 and 25 g/L, respectively (Figure 16). The analysis of the grain size reveals continuous increase upon increasing the quantity of the sodium bromide in the bath.

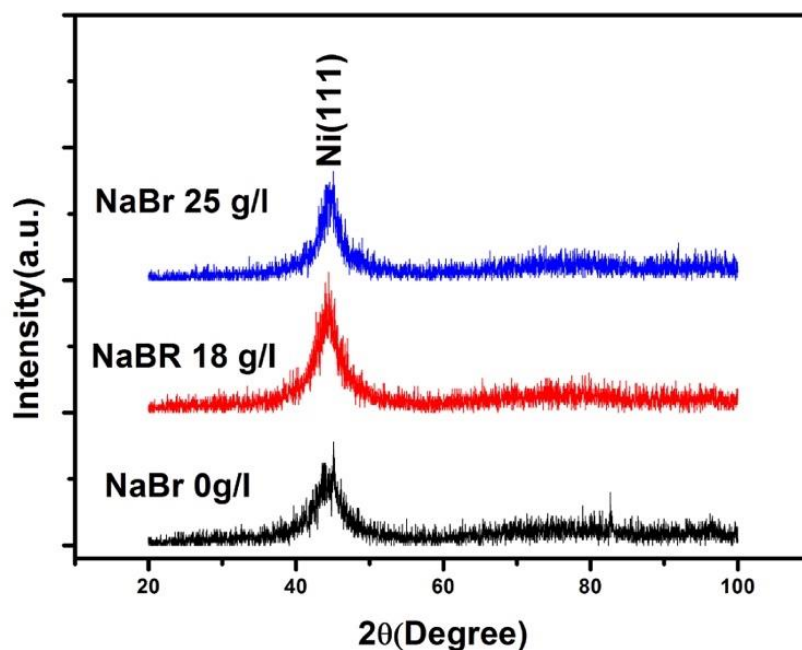


Figure 15 XRD pattern for different quantities of NaBr in the plating bath for Ni-W alloy coatings fabricated at current density of 0.1 A/cm^2 , temperature of $75 \text{ }^\circ\text{C}$, and pH value of 8.9

The hardness is 784, 751 and 718 for 0, 18 and 25g/L of sodium bromide, respectively (Figure 16). Moreover, with the decrease in the grain size a corresponding increase in the hardness of the alloy deposits is observed. The hardness data as reported corroborates with the Hall-petch analogy [44, 95-98] suggesting increase in surface toughness/hardness upon decrease in the grain size. The reduced hardness for 25 g/L of NaBr is due to substantially reduced internal stress and crack density in the deposits.

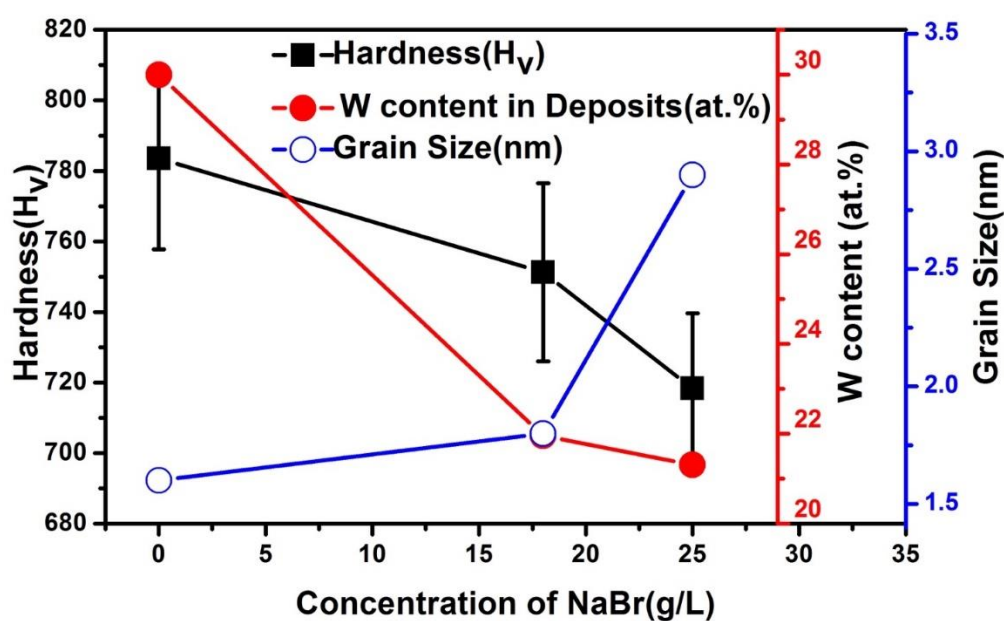
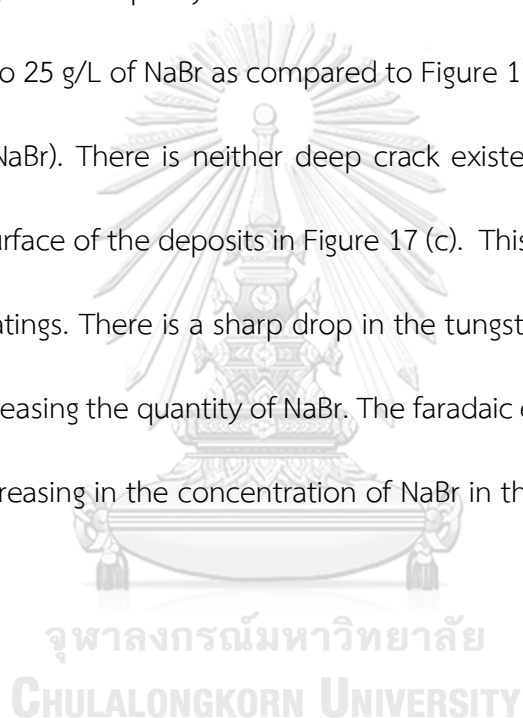


Figure 16 Effect of NaBr on the hardness, W content and crystalline size of the Ni-W alloy deposits fabricated at current density of 0.1 A/cm^2 , temperature of $75 \text{ }^\circ\text{C}$, and pH value of 8.9.

SEM analysis was carried out for deposits with NaBr concentration of 0 g/L, 18 g/L and 25 g/L, respectively (Figure 17). The sharp difference in cracks and film quality

could be seen in Figure 17 (b and c), which demonstrates that suitable amounts of NaBr has strong impact on the morphology of the deposits in terms of crack reduction and improvement/refinement of the film quality. Figure 17 (c) as compared with the Figure 17 (a and b) in terms of cracks and film quality exhibits a profound effect of NaBr on the coatings. The effect of NaBr has thus been proven to be detrimental towards enhancing the film quality. There seems to exist almost no cracks in Figure 17 (c) corresponding to 25 g/L of NaBr as compared to Figure 17 (b) (18g/L NaBr) and even Figure 17 (a) (no NaBr). There is neither deep crack existent nor any fissures or pits formation in the surface of the deposits in Figure 17 (c). This suggests a positive impact of NaBr on the coatings. There is a sharp drop in the tungsten content in the deposits (Table 3) upon increasing the quantity of NaBr. The faradaic efficiency of the deposition decreases with increasing in the concentration of NaBr in the plating bath. (Figure 18).



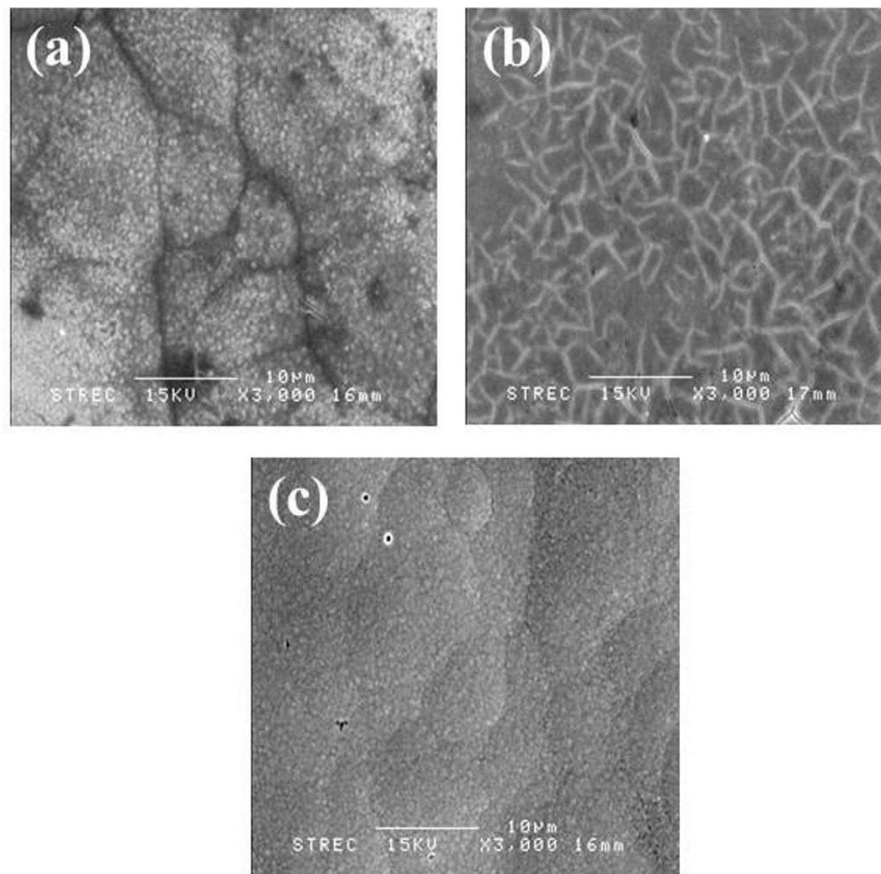


Figure 17 SEM images for the coatings prepared at current density of 0.1 A/cm^2 , temperature of $75 \text{ }^\circ\text{C}$, and pH value of 8.9 for various quantities of NaBr in the bath (a) 0 g/L (b) 18 g/L (c) 25 g/L.

The hardness as presented in Figure 16 shows that the hardness of the deposits decreases with increasing in the concentration of NaBr. The highest hardness is observed at 0 g/L of NaBr concentration when the grain size is the minimum and the tungsten content maximum. The lower grain size returns a high hardness in the deposits whereas, upon successive increase in the grain size, the hardness tends to

decrease as per the hall-petch analogy[44]. The hardness also decreases with the relative decrease in the tungsten content which suggests that the tungsten content in the deposits is also a major factor contributing to the hardness of the deposits. Hence, for the NaBr additive the hardness depends both on the tungsten content and the crystalline size of the deposits.

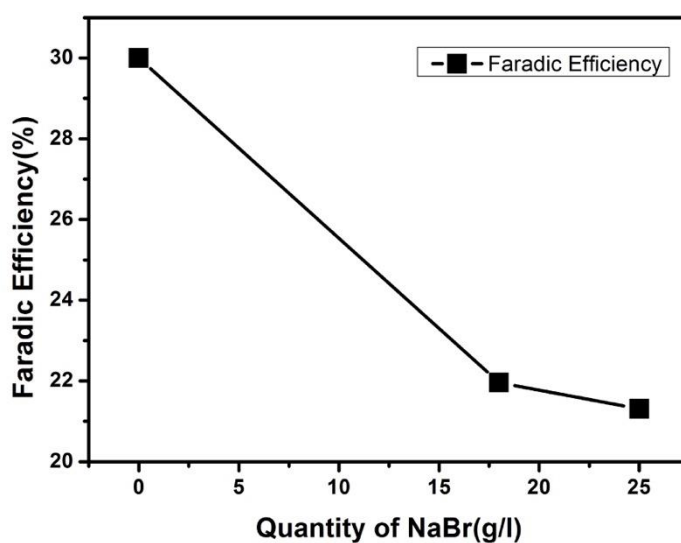


Figure 18 Effect of NaBr on the faradiac efficiency of the coatings fabricated at current density of 0.1 A/cm^2 , temperature of $75 \text{ }^\circ\text{C}$, and pH value of 8.9.

Table 3 Elemental composition of the Ni-W coatings fabricated at temperature of $75 \text{ }^\circ\text{C}$, pH value of 8.9, and current density 0.1 A/cm^2 , with different NaBr concentration.

Sodium Bromide (g/L)	Nickel (at. %)	Tungsten (at. %)
0	70.00	30.00

18	78.69	21.31
25	78.04	21.96

The effect of W content and the grain size on the hardness of the Ni-W coatings is analyzed for various quantities of SDS and NaBr in the plating bath as shown in Figure 19. It is observed that the hardness is maximum for the highest value of tungsten content in the deposits whereas, the corresponding value for the grain size was reported to be minimum. The increase in hardness and a corresponding increase in W content therefore, establish the enhanced effect of the W content on the hardness as compared to the grain size of the deposits. Most of the values of grain size follow inverse hall-petch relationship [44, 95-98] by means of an increasing value of hardness upon the successive increase in grain size except for the lower values of grain size enclosed in the rectangular box in the graph which report a corresponding high value of W content and hardness. The obtained results further suggest that hardness of coatings is mainly contributed by W content in the deposits.

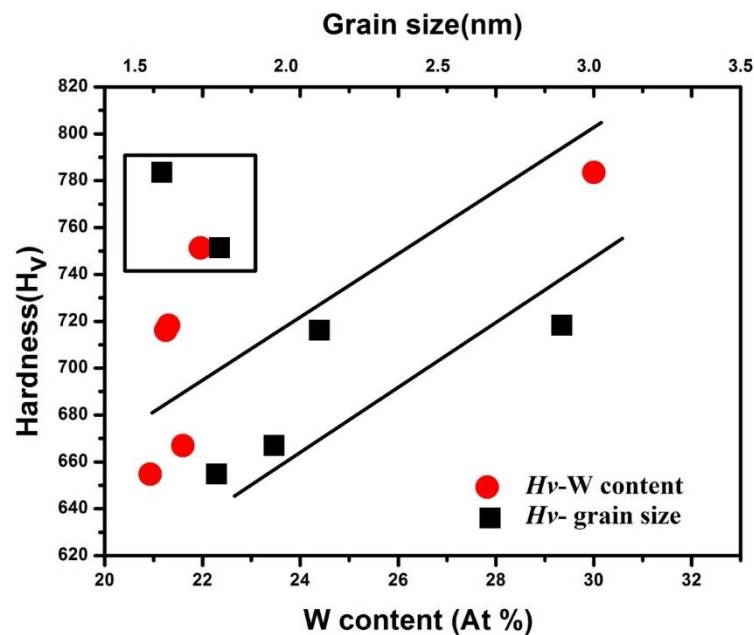


Figure 19 Effect of the W content and crystalline size on the hardness of the Ni-W coatings.

3.2.4 Conclusions

The investigations for the Ni-W alloy revealed profound and marked differences in the effect of various additives on the coatings as well as established the pivotal role of the applied current density in the nature and attributes of the deposits. SDS and NaBr both have a significant impact on the coatings in terms of the hardness, tungsten content, faradaic efficiency and grain size of the coatings. However, proper NaBr concentration (25g/L) in the plating bath offers better film quality enhancement and reduction of internal cracks with higher hardness(718 H_V), high tungsten content(21.31 at.%), moderate grain size (2.9 nm) and optimal value of faradaic efficiency (29.31%) as compared to SDS where for 0.1 g/L of SDS though the SEM results is quite better as

compared to other samples with different quantities of SDS but the other vital parameters namely hardness ($655 H_v$), tungsten content (20.93 at.%), grain size (1.8 nm) and faradaic efficiency (28.13%) are not as desirable as per the research objectives of obtaining a high hardness, high tungsten content deposits with relatively refined microstructure, enhanced film quality and lower crack density. The effect of NaBr tends to be the more pronounced towards obtaining an enhanced microhardness and suitable SEM results with low crack density and a refined film structure.



CHAPTER IV

FABRICATION OF NI-W/DIAMOND NANOCOMPOSITE COATINGS
WITH ENHANCED STRUCTURE AND MECHANICAL PROPERTIES
AND ANALYSIS OF THE EFFECT OF CO₂ + ADDITIVES ON THE
STRUCTURE AND MECHANICAL PROPERTIES OF THE NI-
W/DIAMOND COMPOSITE COATINGS4.1 Effect of electrodeposition conditions on structure and mechanical properties of Ni-
W/diamond composite coatings

Malay Kumar Das^{a,b}, Rongxia Li^c, Jiaqian Qin^{b*}, Xinyu Zhang^{c*}, Kumkumlata Das^d, Adisak Thueploy^b, Sarintorn Limpanart^b, Yuttanat Boonyongmaneerat^b, Mingzhen Ma^c, Riping Liu^c,

^aInternational Graduate Program of Nanoscience & Technology, Chulalongkorn University, Thailand

^bMetallurgy and Materials Science Research Institute, Chulalongkorn University, Bangkok, Thailand

^cState Key Laboratory of Metastable Materials Science and Technology, Yanshan University, Qinhuangdao, P.R. China

^dCollege of Allied and Medical Sciences, Purbanchal University, Nepal

Abstract

Ni-W/diamond composite coatings were prepared by electrodeposition from a Ni-W plating bath with diamond particles suspended into the bath. The effect of the plating parameters on microstructure and mechanical properties was investigated. The deposits reported a maximum hardness of $1207 \pm 32 H_v$. The film hardness is depended on the concentration of diamond particles in the plating bath and also on the size of the co-deposited diamond particles. The sample with diamond concentration of 10 g/L in the bath and co-deposited at current density of $0.15 A/cm^2$ reported the optimized wear resistance and diamond content in the deposit. In this paper the effect of the incorporation of diamond particles into the Ni-W matrix has been discussed in terms of the aforesaid operating conditions and particle size.

Keywords: Composite coatings; Electrodeposition; Diamond; Hardness; Wear resistance

*Corresponding author: e-mail address: jiaqian.q@chula.ac.th (J.Q), xyzhang@ysu.edu.cn (X.Z)

4.1.1 Introduction

Composite electrodeposition is a suitable technique of co-depositing various particles of pure metals, ceramics and organic materials in a base matrix of metal/metal alloys to improve the deposits properties such as hardness, wear

resistance, surface roughness and uniformity of distribution of co-deposited particles [5-7, 13-16, 99, 100]. Hardness is an important surface property which relates to the wear resistance and mechanical strength of the material. Hard coatings are used to improve the longevity of products, facilitate the enhancement of performance for cutting tools and other materials which are coated with hard materials such as diamond by various wet and dry processes. However, there are various advantages of wet process of fabrication of coatings over the dry process which involves the use of costly equipment, extreme reaction conditions and higher costs. Electrodeposition is a simple and very commonly used method of wet process deposition of films. It is extensively used to fabricate hard metal and alloy films on materials (for example Cr, Ni-W alloy) [29, 101-103] to name a few.

Electrodeposited Ni-W alloy coatings have been able to serve as a replacement to the hazardous hexavalent chromium coatings [3, 4, 104]. Various researchers report that the hardness of the Ni-W alloy is mainly determined by the W content and grain size of the electrodeposited Ni-W [54, 105-107]. The hardness of the as-deposited Ni-W alloy has been reported to vary between 460-670 H_v [54, 105-107]. However, the hardness of the Ni-W alloy is significantly lesser than that of chromium coatings which report high hardness of 1100 H_v [55, 106]. Moreover, various literatures have stated that addition of suitable particles (for example diamond, Al_2O_3 , WC and SiC) to a hard alloy matrix can significantly enhance mechanical properties such as hardness, wear resistance and corrosion resistance of the deposits [1, 3, 57, 108, 109]. However, for

composite coatings of nanostructured Ni-W matrix reinforced by diamond particles there are only a few publications. Hou et al. [110] prepared Ni-W/diamond composite coatings and investigated its mechanical properties. They reported that the highest level of incorporation of diamond was about 21.1 vol. % at diamond concentration in bath of 1 g/L. In our previous study, Ni-W/diamond composite coatings were also deposited by pulse electrodeposition[7] and sediment co-electrodeposition method[2]. The results demonstrated that the pulse current can affect the diamond incorporation and W content in the deposit. Further, the sediment co-electrodeposition method could significantly improve the diamond content in deposits, resulting high hardness of Ni-W/diamond composite coating. Combined with previous research on Ni-W/diamond[2, 7, 21, 110], Ni/diamond [5, 13], Ni-Co/diamond[6, 14], Ni-P/diamond[15-17], Ni-B/diamond[99] composite coatings, the electrodeposition parameters and size of diamond particles can strongly affect the properties of composite coating. Therefore, this paper aims to further investigate and examine the effect of electrodeposition conditions on microstructure and mechanical properties for the Ni-W/diamond composite coating.

In the present study, co-deposition of Ni-W/diamond composite coating was prepared from Ni-W plating bath containing diamond particles in suspension. The effect of electrodeposition parameters on the hardness, wear resistance and microstructure of the deposits were investigated. Microstructural and mechanical properties of the

obtained Ni-W/diamond composite coatings that were directly related to the electrodeposition conditions were also determined.

4.1.2 Experimental details

Ni-W/diamond composites were fabricated by means of electrodeposition from an ammonia-citrate bath. The bath composition was nickel sulphate 18 g/L, sodium tungstate 53 g/L, tri-sodium citrate 168 g/L, ammonium chloride 31 g/L, sodium bromide 18 g/L. The diamond concentration was varied in the bath (1 g/L, 2g/L, 3 g/L, 5 g/L, 10 g/L and 20 g/L) and the particle size of diamond used were 0.2, 0.3, 0.9, 3 and 6 μ m, respectively. The operating temperature was 75 °C. The pH, stirring speed and the deposition time was kept constant at 8.9, 200 RPM and 2 hours, respectively. The current density was varied between 0.05-0.2 A/cm².

The substrate was pre-treated before deposition by soap, 10% NaOH and 14% HCl solution. Prior to insertion of the electrodes in the plating bath, the substrate was activated by 14% HCl. Except the deposition area the other undesirable parts of the substrate was covered with polymer tape.

X-Ray diffraction (XRD) technique was employed to analyze the phases of the deposits along identification and analysis of the crystalline structure of the coatings. Brooker D8 advance X-ray diffractometer operated at Cu K α radiation at a rating of 40

kV, 20 mA. The scan rate was 0.02° per step and the measuring time 0.5 second/step. Scherer's equation[110] was employed for the calculation of the grain size of the electrodeposited coatings.

$$D = \frac{0.9\lambda}{\beta \cos \theta} \quad (1)$$

Where, D is the grain size, λ is the X-ray wavelength (1.5418 Å), β is the corrected peak width at half maximum intensity (FWHM) and θ is Bragg angle.

The samples were characterized in terms of morphology and microstructure by JEOL JSM-6400 scanning electron microscope (SEM) with energy dispersive X-ray spectroscopy (EDS) capability embedded into it. The volume percentages of the incorporated diamond particles in the obtained Ni-W/diamond composite coatings were determined from the cross-sectional SEM images by the image analysis software (ImageJ) to estimate the portion of diamond content in the coatings.

The coating hardness was measured on the surface using Mitutoyo hardness tester with a Vickers's diamond indenter under a load of 100 g (0.98N) at seven different locations of the coating. The dwell time for each indentation was 15 seconds. The Vickers hardness can be calculated in accordance with the formula:

$$H_V = 1854 \frac{L}{d^2} \quad (2)$$

Here, H_V is the hardness in Vickers's and L is the applied load and d is the diagonal of the indentation. The average value of the five measurements (except the maximum

and minimum values) is quoted here as the hardness of the obtained composite coating.

The tribological property of the deposits was analyzed by wear test. The wear test was carried out at an air humidity of 45 ± 10 RH% and a temperature of 24 ± 1 °C using a ball-on-disc tribometer with the sample placed horizontally on a turntable. The tests were performed by applying a load of 20 N to a zirconium dioxide ball of diameter 6 mm, a linear speed of 9.42 cm/s for a total sliding distance of 500m and for the total wear duration of 53 minutes. Before each test, both the sample and the ball counter face were ultrasonically cleaned in acetone for 10 min and dried by hot air. The anti-wear performance of the films was estimated from the weight loss of the specimens.



4.1.3 Results and discussion

จุฬาลงกรณ์มหาวิทยาลัย
CHULALONGKORN UNIVERSITY

Figure 20 (a-d) shows the SEM image of Ni-W/diamond (NWD) composite deposits fabricated at 1 g/L, 3 g/L, 5 g/L and 10 g/L diamond concentration in plating bath at current density of 0.15 A/cm^2 , respectively. Fewer diamond particles appear to be co-deposited on the surface for samples fabricated at 1 g/L (Figure 20 (a)) and 3 g/L (Figure 20 (b)) diamond concentration in the plating bath. Upon increasing the plating bath diamond concentration to 5 g/L (Figure 20 (c)) and 10 g/L (Figure 20 (d)) the number

of diamond particles co-deposited along with the uniformity of distribution of diamond particles appears drastically enhanced.

The increase in the diamond concentration of the deposits also enhances the morphology of the Ni-W matrix in terms of crack reduction and uniform incorporation of diamond particles. The sample fabricated with 10 g/L diamond concentration in the plating bath (Figure 20 (d)) exhibits the highest level of incorporation and uniformity in distribution of diamond particles throughout the matrix as compared to the samples fabricated with lower values of diamond concentration in the plating bath.

Figure 20 (e-h) shows the cross-sectional SEM images for the samples with variation in the diamond concentration in the plating bath. The cross-sectional SEM images also suggest an increase in the diamond incorporation and relatively more uniform distribution into the deposits upon increasing the diamond concentration in the plating bath from 1 g/L to 10 g/L (Figure 20 (e-h)). The cross-sectional SEM images also demonstrate clear enhancement in the number of diamond particles co-deposited into the surface of the deposits as the concentration of diamond particles in the bath is increased. The increase in the diamond concentration of the bath therefore enhances the co-deposition of the diamond particles in the deposits significantly.

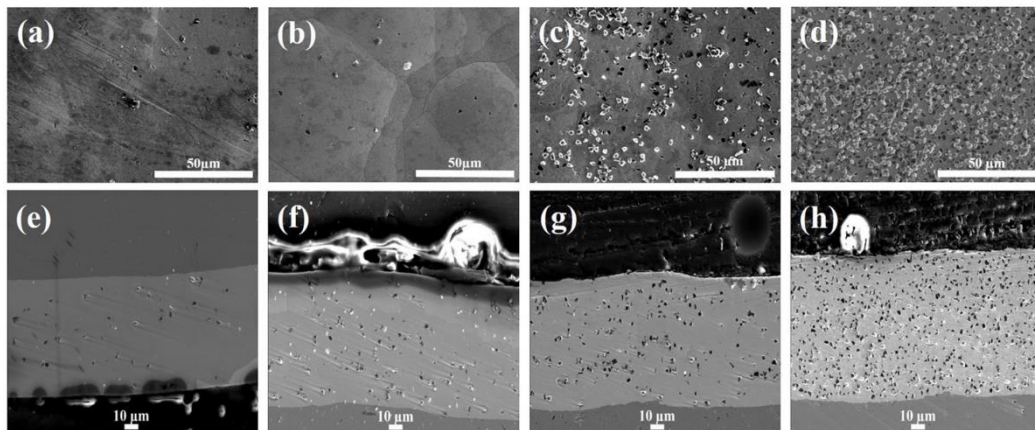


Figure 20 Effect of diamond concentration in plating solution on morphology of Ni-W/diamond composite coatings prepared at temperature of 75°C, pH 8.9, and current density of 0.15 A/cm², SEM images, (a) 1 g/L, (b) 3 g/L, (c) 5 g/L, (d) 10 g/L, and cross section SEM images, (e) 1 g/L, (f) 3 g/L, (g) 5 g/L, (h) 10 g/L.

Figure 21 indicates the element map distribution of diamond particles co-deposited into the Ni-W matrix. The diamond incorporation and carbon content in the deposits increases significantly upon increasing the diamond concentration in bath from 5 g/L to 10 g/L. The diamond distribution also seems more uniform for the sample containing 10 g/L diamond concentration in bath as compared to other concentrations.

The diamond content in the deposits increases upon increasing the diamond concentration in bath from 1 g/L to 10 g/L (Figure 22). The samples with 10 g/L diamond concentration in the plating bath and fabricated at current density 0.15 A/cm² reports the highest value of diamond content in the deposits at 32 vol. %. Similar results for increase in composite particle concentration in the deposits upon increasing the particles concentration in bath have been reported by Ogihara et al.[1] for Ni-B/diamond composite films and Guglielmi et al. [111] for Ni/Silicon carbide composite

films. The composite co-deposition process has been explained by Guglielmi et al. [111] wherein the composite particles are adsorbed onto the alloy surface and then incorporated into the electrodeposited alloy matrix[111]. Upon an increase in the diamond concentration in bath there is a corresponding increase in the number of diamond particles that collide onto the surface of the electrode which in turn results in the increase in the diamond content of the electrodeposited coatings[99, 111].

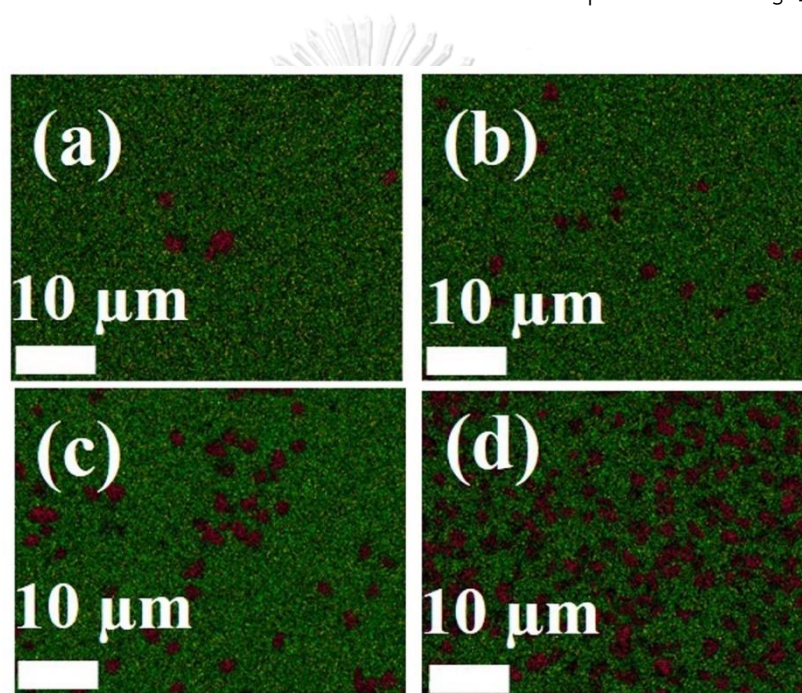


Figure 21 EDS element mapping images of Ni-W/diamond composite films fabricated at current density of 0.15 A/cm^2 , temperature of 75°C , pH 8.9, and different diamond concentrations in the plating bath, (a) 1 g/L, (b) 3 g/L, (c) 5 g/L, (d) 10 g/L.

The NWD samples exhibit slight increase in the deposition rate upon increasing the diamond concentration in the plating bath (Figure 33 (a)). The thickness of the deposits varied in the range of $\sim 56\text{-}66 \mu\text{m}$. The thickness of the deposits increases slightly upon an increase in the diamond concentration in the plating bath. The deposition rate was

reported to be 28 μm , 30 μm , 30 μm and 33 μm for the samples fabricated with 1 g/L, 3 g/L, 5 g/L and 10 g/L diamond concentration in the plating bath, respectively. It reveals that diamond incorporation doesn't strongly affect the deposition rate. The surface roughness of the NWD samples fabricated with different diamond concentration in the plating bath exhibits minor variation in the values upon increasing the diamond concentration in the plating bath (Figure 33 (b)). The roughness varies between 0.8 to 2.1 microns for all the samples fabricated with different diamond concentration. The sample fabricated with 1 g/L diamond concentration at current density 0.05 A/cm² reports the lowest value of surface roughness at 0.8 μm , whereas the sample fabricated with the same diamond concentration at current density 0.2 A/cm² reports the highest value of surface roughness at 2.1 μm . However, the samples with 10 g/L diamond concentration in bath have relatively lower values of surface roughness. This suggests that an increase in the diamond concentration in bath and incorporation in the deposits tends to reduce the roughness of the deposits[112].

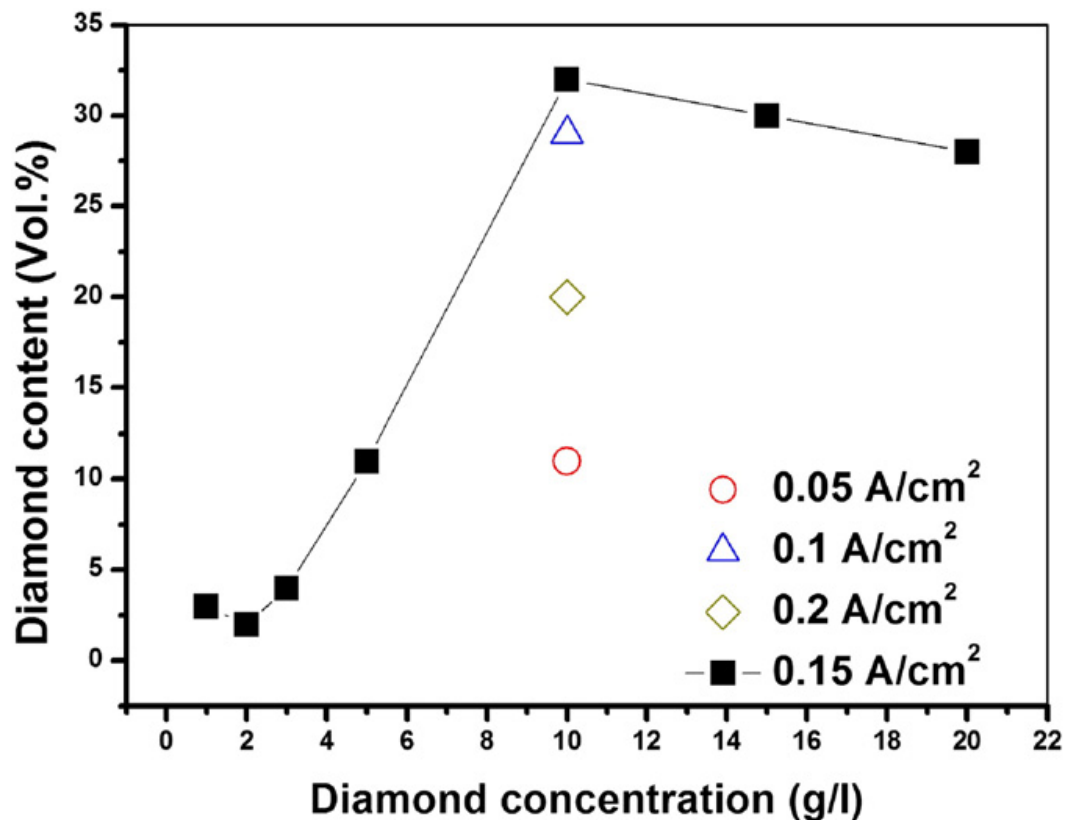


Figure 22 Effect of diamond concentrations and current density on diamond content of Ni-W/diamond composite deposits fabricated at temperature of 75°C and pH 8.9.

Figure 23 compares the effect of diamond concentration in bath on W content, grain size, and hardness of the deposits at 0.15 A/cm² current density. The samples report hardness values of 734 ± 15, 810 ± 36, 756 ± 27, 757 ± 31, 933 ± 53 and 1207 ± 32 for the samples fabricated at current density 0.15 A/cm² with 0 g/L, 1 g/L, 2 g/L, 3 g/L, 5 g/L and 10 g/L diamond concentration in the plating bath, respectively. As per Figure 23 it is quite evident that the hardness increases sharply upon an increase in the diamond concentration in the plating bath from 3 g/L to 5 g/L and 10 g/L, respectively. The W content of the NWD deposits varies between ~17.7 -19 at. % for the samples fabricated with different diamond concentration in the plating bath. The

grain size of the deposits varies between 2-2.5 nm. The samples exhibit high hardness even for the lower values of the W content in the deposits. However, an increase in the diamond concentration in the plating bath amounts to an increase in the diamond content of the deposits (Fig 3). The relatively uniform co-deposition of diamond particles at 10 g/L diamond concentration (as shown in Figure 20 (d)) also has a role in increasing the overall strength of the Ni-W alloy matrix as the hardness increases upon an increase in the diamond content of the deposits. This suggests to the enhanced role of the reinforced and co-deposited composite diamond particles towards enhancing the hardness of the deposits. The maximum hardness reported was $1207 \pm 32 H_v$ for the sample fabricated at 0.15 A/cm^2 current density and 10 g/L diamond concentration (Figure 23)).

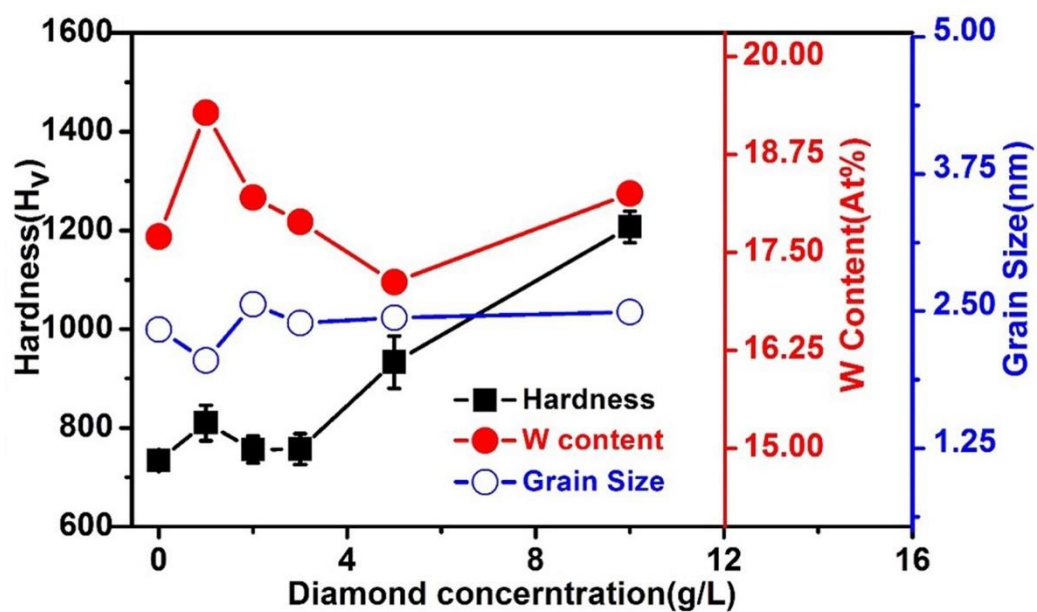


Figure 23 Effect of diamond concentration in the plating bath on the hardness, W content and grain size of the Ni-W/diamond composite deposits prepared at temperature of 75°C, pH 8.9 and current density of 0.15 A/cm².

The SEM images of the NWD coatings with 10 g/L diamond concentration in the plating bath and fabricated at various current densities (0.05 A/cm², 0.1 A/cm², 0.15 A/cm² and 0.2 A/cm²) reveals a relatively high incorporation of diamond particles and the co-deposited diamond particles also appear to be uniformly distributed throughout the base Ni-W matrix (Figure 31 (a, b)), Figure 20 (d) and Figure 31 (c)). Furthermore, the sample with current density of 0.15 A/cm² (Figure 20 (d)) exhibits a higher degree of co-deposition of diamond particles as compared to the samples fabricated at current densities 0.05 A/cm², 0.1 A/cm² and 0.2 A/cm² (Figure 31 (a-c)) for 10 g/L diamond concentration in the plating bath.

The cross-sectional SEM images for the NWD samples fabricated with 5 g/L diamond concentration and with different current densities (0.05 A/cm², 0.1 A/cm², 0.15 A/cm² and 0.2 A/cm²) exhibit noticeable diamond incorporation in the Ni-W matrix for all current densities (Figure 32 (e-h)). The cross-sectional images for various current densities also reveal an increase in uniformity of distribution and incorporation of diamond particles in the Ni-W matrix upon an increase in current density from 0.05 A/cm² to 0.2 A/cm². The cross-sectional SEM results indicate that the thickness of coating is strongly affected by the applied current density. Consequently, the deposition rate increases with increase in current density (Figure 34 (a) and Figure 32

(e-h)). The thickness of the deposits varied from ~32 to 93 μm . The deposition rate for the NWD samples was 16 μm , 24 μm , 29 μm and 46 μm for the samples fabricated with 5 g/L plating bath diamond concentration at current density 0.05 A/cm^2 , 0.1 A/cm^2 , 0.15 A/cm^2 and 0.2 A/cm^2 , respectively.

The comparison of element mapping images (Figure 35) along with the surface SEM images for samples fabricated at various current densities (Figure 31 (a-c) and Figure 20 (d)) confirms the uniform distribution of diamond particles into the base Ni-W matrix at 0.15 A/cm^2 current density and 10 g/L diamond concentration. Figure 22 shows the comparison of diamond content (vol. %) in the deposits for various current densities at 10 g/L diamond concentration. The samples fabricated at various current densities with 10 g/L diamond concentration invariably reports a higher diamond content at almost all current densities. The diamond content is reported to be quiet high at 29 vol. % and 32 vol. % for the sample fabricated at current density of 0.05 A/cm^2 and 0.15 A/cm^2 , respectively (Figure 22). The EDS element mapping results further confirm the SEM observation in respect of uniform distribution and incorporation of diamond particles at the aforesaid current densities.

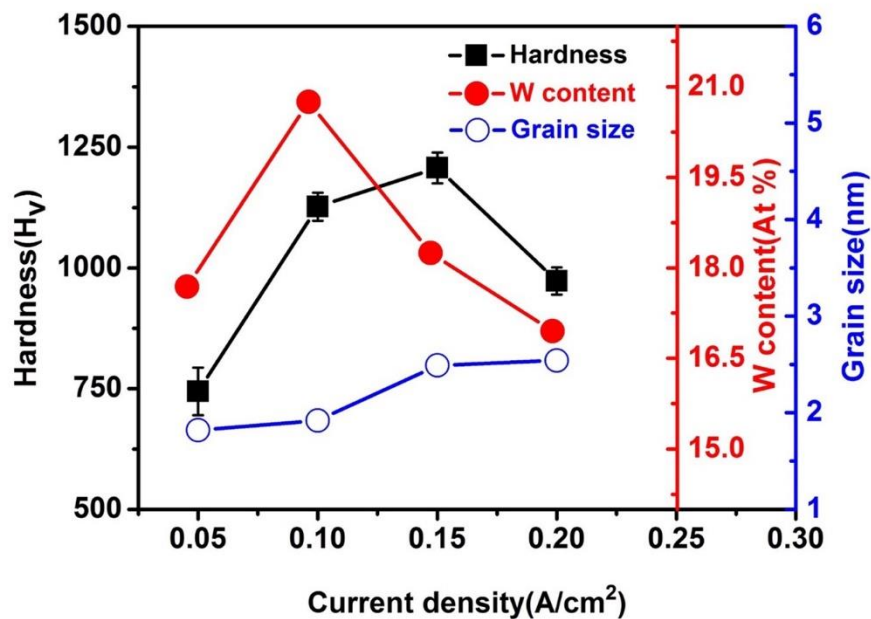


Figure 24 Effect of the current density on the hardness, W content and grain size of the Ni-W/diamond composite coatings prepared at temperature of 75°C, pH 8.9, and 10 g/L of diamond concentration in the plating bath.

Figure 24 shows the effect of current density on the hardness, grain size and W content of coatings prepared at 10 g/L diamond concentration in bath. The hardness tends to increase upon increase in the current density from 0.05 to 0.15 A/cm², and at current density >0.15 A/cm², the hardness decreases with current density. The values of hardness are 744 ± 49, 1127 ± 29, 1207 ± 32 and 973 ± 28 for the samples fabricated at 0.05 A/cm², 0.1 A/cm², 0.15 A/cm² and 0.2 A/cm², respectively. The grain size of all deposits was reported to be in the range of ~2-2.5 nm, which doesn't have very big difference (Figure 24). The W content varies between ~18 at. % - 21 at. %. There is a marked decrease in the W content of the deposits at current density > 0.1 A/cm² (Figure 24). The adsorption of diamond particles into the matrix tends to inhibit the

deposition of Ni^{2+} and W^{6+} ions [110, 113]. Various researchers report that absorption of hydrogen ions by the diamond particles near the cathode prevents the hydrogen ions from being reduced to nascent hydrogen. The hydrogen ions that are, thus absorbed by the diamond particles results in a decrease of the W content in the composite deposits [114, 115]. This is in agreement with the low W content values for samples having high diamond incorporation (Figure 35 (a, c)).

The surface roughness of the NWD composite coatings as a function of the applied current density was found to vary within a range of 0.8-2.1 μm (Figure 34 (b)). The sample fabricated with 10 g/L diamond concentration reports the least variation in the values of the surface roughness (1.2-1.4 μm) as the current density is increased from 0.05 A/cm^2 to 0.2 A/cm^2 . Though, the deposits are relatively smooth, the sample with 10 g/L plating bath diamond concentration exhibits lower values of surface roughness for various current densities than most other samples. The current density has little impact on the surface roughness of the deposits as compared to the diamond concentration in the plating bath and the diamond content of the deposits [112]. It is also observed that the value of surface roughness is lower (Figure 34 (b)) for samples which have a high diamond content (Figure 35 (c) and Figure 22). The high level of incorporation of diamond particles therefore, makes the co-deposited surface smoother as compared to samples having lower diamond content and incorporation in the deposits. This behavior has been confirmed by various previous researchers for other composite particles co-deposition [112, 116].

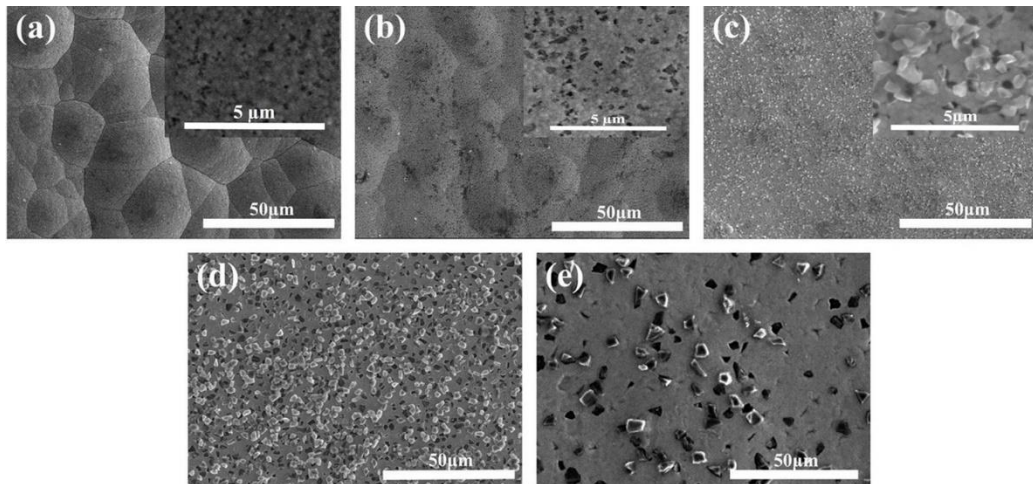


Figure 25 SEM images of Ni-W/diamond composite coatings fabricated at current density of 0.15 A/cm^2 , diamond concentration of 10 g/L , temperature of 75°C and pH 8.9, for different size of diamond particles, (a) $0.2 \mu\text{m}$, (b) $0.3 \mu\text{m}$, (c) $0.9 \mu\text{m}$, (d) $3 \mu\text{m}$, (e) $6 \mu\text{m}$. The inserted images are the SEM image at higher magnification for (a), (b), and (c), respectively.

Figure 25 (a-e) shows the SEM images of the NWD composite coatings fabricated with diamond particles of various sizes. The inserted images depict the higher magnification SEM observation of the corresponded sample. The diamond incorporation and distribution appear to increase with the increasing particle size of diamond up to $3 \mu\text{m}$ at which the diamond particles are uniformly distributed and co-deposited into the alloy matrix. However, upon further increasing the diamond size to $6 \mu\text{m}$ the distribution ceases to be as uniform as in case of $3 \mu\text{m}$.

The element mapping results for the samples fabricated with diamond particles of different size (fabricated at 10 g/L diamond concentration and current density 0.15 A/cm^2) exhibits an increase in the carbon content of the deposits as the size of the diamond particles is increased from $0.2 \mu\text{m}$ to $3 \mu\text{m}$ (Figure 37). However, as the

diamond particle size is increased from 3 μm to 6 μm the carbon content and in turn the incorporation of diamond particles appears to be diminished to a large extent.

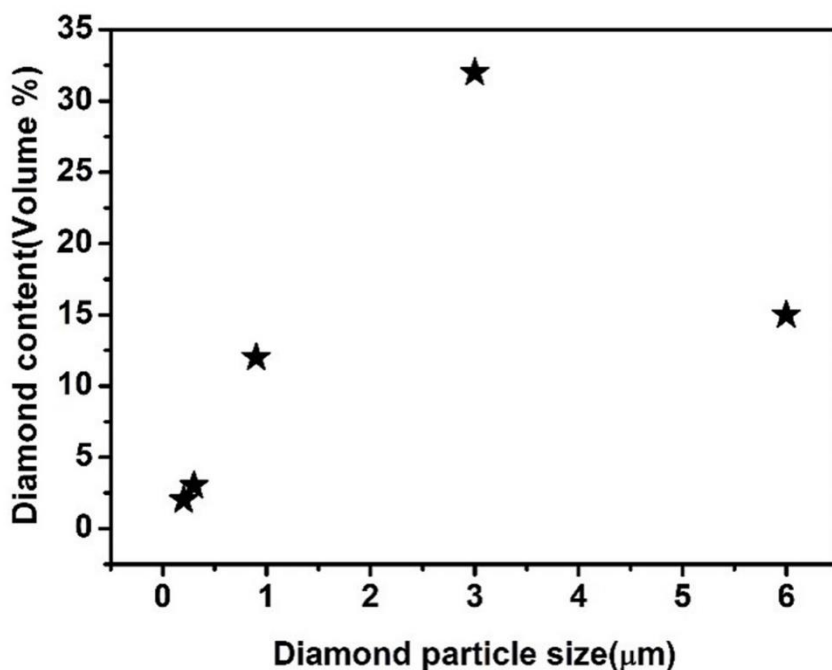


Figure 26 Diamond content of Ni-W/diamond composite deposits for various size of diamond particles fabricated at diamond concentration of 10 g/L, temperature of 75°C and pH 8.9.

The diamond content (vol. %) for the NWD samples fabricated with diamond particles of different size (fabricated at 10 g/L diamond concentration and current density 0.15 A/cm²) is reported in Figure 26. The diamond content of the deposits increases from 2 vol. % to 32 vol. % as the diamond particle size is increased from 0.2 μm to 3 μm , respectively. Upon further increasing the size of diamond particles from 3 μm to 6 μm the diamond particles content in the deposits exhibits a sharp decline.

The sample fabricated with 3 μm size diamond particles (Figure 26) reports a maximum diamond content of 32 vol. %. Ogihara et al. [1] reported that the diamond content in the deposits increases upon increasing the particle size of diamond because the weight change caused by the diamond co-deposition increases and is proportional to the mean particle radius(r^3) of the diamond particles. Therefore, the diamond content decreases as the size of diamond particles increases beyond 3 μm in this study because of the sedimentation of larger diamond particles before being properly incorporated into the matrix.

The surface roughness of the NWD samples fabricated (at 10 g/L diamond concentration and current density 0.15 A/cm²) with different size diamond particles was reported to be $0.3 \pm 0.02 \mu\text{m}$, $0.4 \pm 0.04 \mu\text{m}$, $1.5 \pm 0.27 \mu\text{m}$, $1.1 \pm 0.11 \mu\text{m}$, $1.2 \pm 0.12 \mu\text{m}$ for the samples fabricated with 0.2 μm , 0.3 μm , 0.9 μm , 3 μm and 6 μm diamond particle size, respectively (Figure 36 (a)). It can be seen that the NWD surface gets rougher upon increasing the diamond particle size from 0.2 μm to 0.9 μm . Beyond 0.9 μm as the diamond particle size is increased to 3 μm and 6 μm there is a slight reduction in the value of surface roughness. The SEM image for different size of diamond particles (Figure 25) also indicate the larger size diamond particles protruding out of the Ni-W matrix as compared to the sub-micron size diamond particles which are barely noticeable on the base Ni-W matrix. Therefore, it is natural to infer that the deposits fabricated with sub-microns size diamond particles would result in smoother surfaces as compared to samples with larger size diamond particles. Similar

dependence of the surface roughness on the composite particle size has also been reported by Ogihara et al. [1].

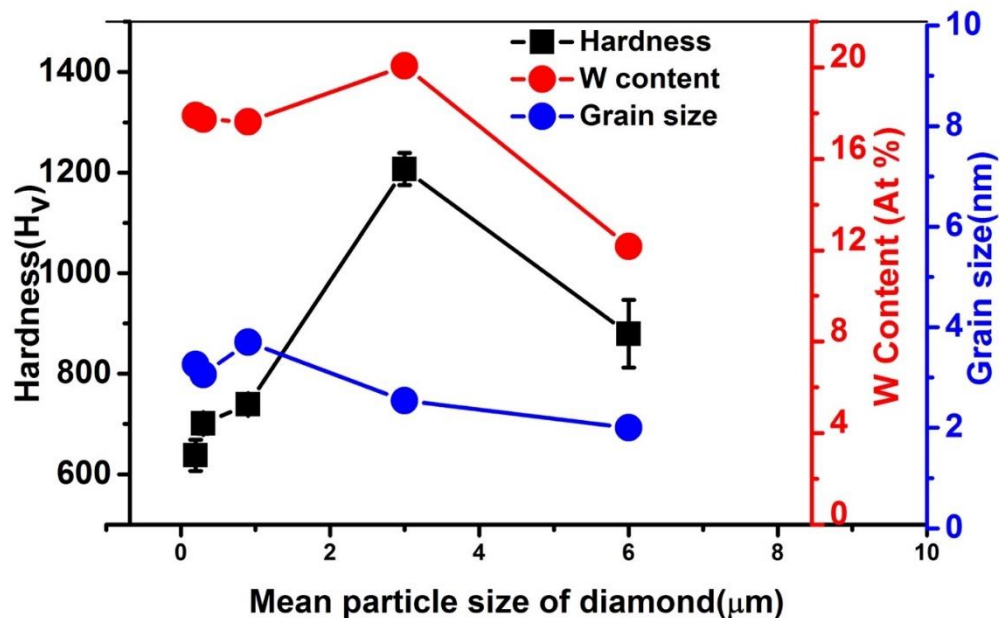


Figure 27 Effect of the diamond particle size on the hardness, W content and grain size of the Ni-W/diamond composite deposits fabricated at current density of 0.15 A/cm², 10 g/L of diamond concentration, temperature of 75°C and pH 8.9.

The hardness was reported to be 638 ± 31 , 701 ± 20 , 739 ± 14 , 1207 ± 32 , 879 ± 68 for the samples fabricated 0.2 μm, 0.3 μm, 0.9 μm, 3 μm and 6 μm size of diamond particles, respectively. The hardness of the deposits increased as the size of the diamond particles was increased from 0.2 μm to 3 μm. However, for samples fabricated with 6 μm size diamond particles the hardness of the deposits reported a sharp decline of more than 300 points on the Vicker's scale. The maximum hardness ($1207 \pm 32 H_v$) was reported for the sample fabricated with 3 μm diamond particles. The W content of the deposits varied between ~11-16 at. %. The W content of the deposits was also

reported to be high for the sample fabricated with 3 μm size diamond particles, whereas the grain size was in the range of 2-3 nm for different sizes of diamond particles. The high diamond content of the deposits for the samples fabricated with 3 μm size diamond particles (Figure 26) coincides with the high value of hardness for the same sample (Figure 27). This suggests that the diamond content in the coating is a major contributor towards enhancing the hardness of the deposits for the samples fabricated with different size of diamond particles. The high value of hardness also coincides with a higher value of W content in Figure 27. This indicates that the W content is also a factor in determining the hardness of the deposits for variation in the size of diamond particles. The hardness value is relatively low for samples fabricated with sub microns size diamond particles as compared to the samples fabricated with 3 μm diamond particles. Moreover, the hardness decreases even as the diamond particle size is increased beyond 3 μm to 6 μm .

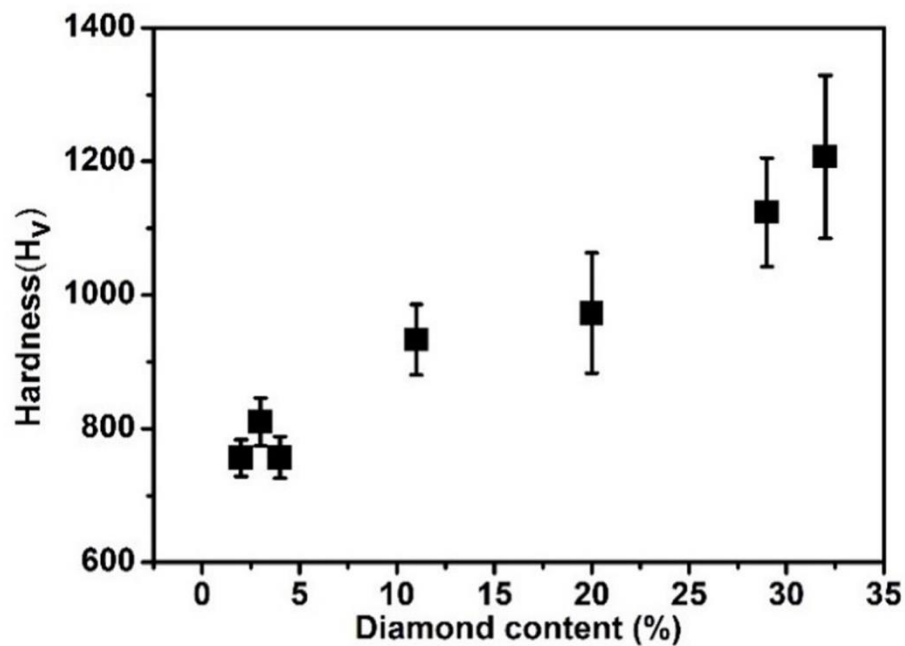


Figure 28 The hardness of the Ni-W/diamond composite deposits presented as a function of diamond content in the coatings.

The electrodeposition parameters and the diamond particle size could affect the composition of the base alloys and the incorporated diamond content in the deposits from this study, and this can influence the hardness of the obtained composite coatings. To further understand the mechanism of hardness enhancement, the hardness of the obtained deposits as a function of the diamond contents in the composite coatings is shown in Figure 28. The hardness increases with the increase in the diamond content of the deposits. The W content of the NWD deposits does not tend to enhance the hardness of the deposits (Figure 36 (a)) as compared to the diamond content in the deposits which tends to have a direct impact on the hardness

of the deposits (Figure 22 and Figure 23). The samples with high values of W content report a lower value of hardness (Figure 36 (a)), whereas the hardness of the deposits increases significantly as the plating bath diamond concentration and in turn the diamond content in the deposits increases (Figure 23 and Figure 22). The maximum value of hardness ($1207 \pm 32 H_v$) corresponds with the highest value of diamond content in the deposits (32 vol. %), whereas the corresponding W content (18.25 at. %) reported for the same isn't the highest value among all samples. Moreover, the hardness is quite high even for samples reporting a lower value of W content (Figure 36 (b)). The hardness reported for samples having lower diamond content is lower and there is a near linear relationship between the diamond content of the deposits and the film hardness (Figure 28). This indicates that the hardness depends more on the diamond content in the deposits as compared to the W content for the Ni-W/diamond composite coatings.

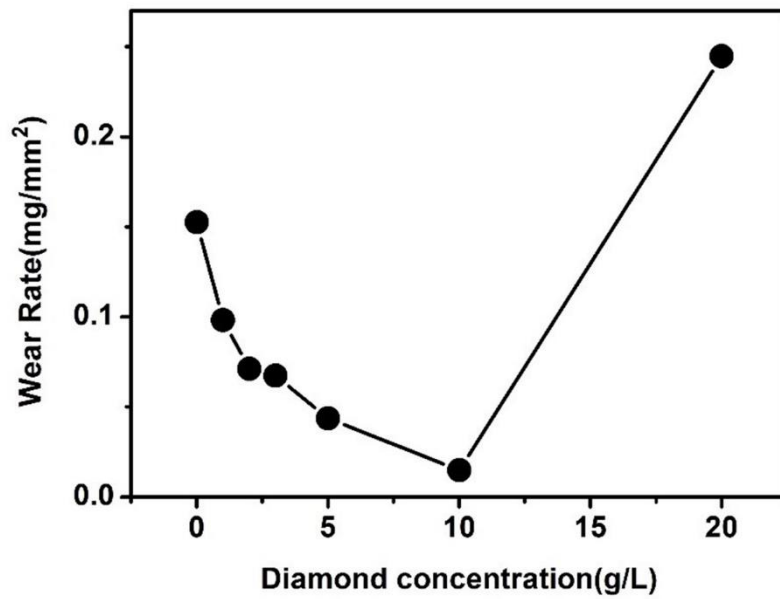


Figure 29 Effect of diamond concentration in the plating bath on the wear rate of Ni-W/diamond composite coatings fabricated at temperature of 75°C and pH 8.9.

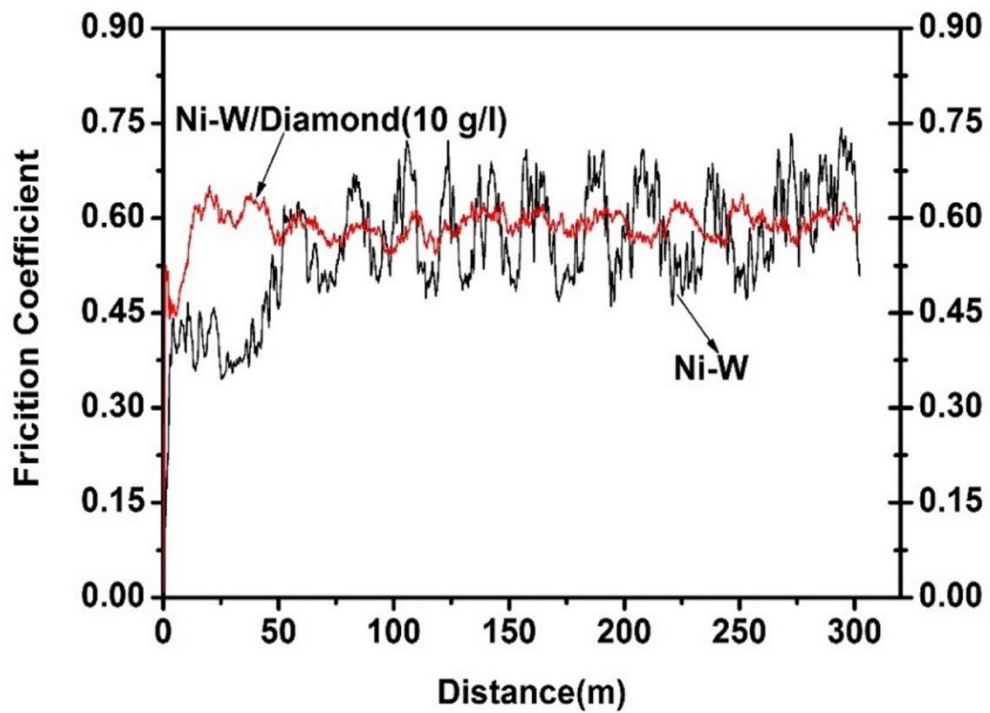


Figure 30 The friction coefficient of the Ni-W alloy and Ni-W/diamond (10 g/L) composite coatings fabricated at temperature of 75°C and pH 8.9.

The wear performance of Ni-W/diamond composite coatings was also performed by using a ball-on-disc tribometer. Figure 29 shows the wear rate for various diamond concentrations in the plating bath. The wear rate was reported to be 0.15 mg/mm², 0.098 mg/mm², 0.071 mg/mm², 0.067 mg/mm², 0.044 mg/mm², 0.014 mg/mm² and 0.24 mg/mm² for the NWD samples fabricated at current density 0.15 A/cm² and plating bath diamond concentration of 0 g/L, 1 g/L, 2 g/L, 3 g/L, 5 g/L, 10 g/L and 20 g/L, respectively. Moreover, additional comparisons for the friction co-efficient data of the samples with 10 g/L and 2 g/L diamond concentration and the samples with 10 g/L and 20 g/L diamond concentration has been shown in Figure 38 (a) and (b), respectively. The samples with the high plating bath concentration and content of diamond particles exhibit lower wear rate as compared to samples fabricated from plating baths having lower diamond concentrations and content (Figure 29). It is evident in Figure 29 that the wear rate decreases continuously upon increasing the plating bath diamond concentration and reaches a minimum value at 10 g/L beyond which it rises sharply at 20 g/L. This is because at higher plating bath concentration of diamond particles the co-deposition rate is considerably reduced due to aggregation of diamond particles at the electrode[1]. The diamond content values for the different diamond concentration in the element mapping images also co-relates to the wear rate data. The samples with the high diamond content (Figure 21, Figure 22) also report

a low wear rate (Figure 29) compared to samples having lower diamond content. The effect of diamond particles towards enhancing the wear resistance of the NWD deposits is clear by the wear rate results in Figure 29. The samples having a low wear rate (Figure 29) also report a lower value of surface roughness (Figure 33 (b)) and lower values of friction co-efficient (Figure 30) [117]. The variation in the friction co-efficient also is relatively lower for the samples having low wear rate as in case of sample having 10 g/L diamond concentration in the plating bath compared to pure Ni-W alloy (0 g/L diamond concentration in the bath) (Figure 30). The friction co-efficient of the Ni-W alloy varied from 0.37 to almost 0.75, whereas the variation was within the range of 0.5 to 0.65 for the NWD sample fabricated with 10 g/L diamond concentration in the plating bath. The variation in friction co-efficient was also higher for the 2 g/L (Figure 38 (a)) and 20 g/L (Figure 38 (b)) NWD samples as compared to the 10 g/L samples.

4.1.4 Supplementary Information

This supplementary information consists of the SEM images of Ni-W/diamond composite coatings prepared at temperature of 75°C and pH 8.9 at various current densities and diamond concentration as an additional illustration to the SEM images reported in the manuscript for 10 g/L diamond concentration and 0.15 A/cm² current density. The surface roughness, wear test friction co-efficient for various concentrations, effect of the W content on the deposits and deposition rates of the

Ni-W/diamond composite deposits have also been reported as additional information to further explain the effect of the operating conditions on the mechanical properties and deposition parameters of the deposits. Various surface and mechanical properties and results have been reported in the paper whereas, this additional file serves as an extension to further demonstrate the effect of the variation of the operating parameters on the Ni-W/diamond composite deposits.

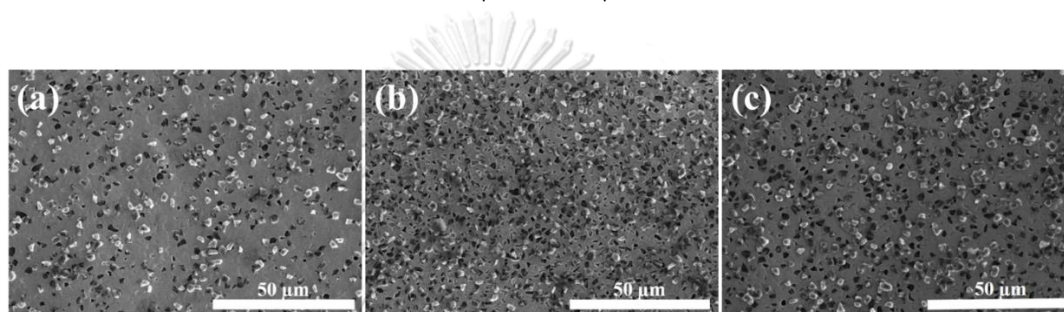


Figure 31 (a-c) SEM images of Ni-W/diamond composite coatings prepared at temperature of 75°C, pH 8.9, and diamond concentration in plating bath of 10 g/L, for various current densities, (a) 0.05 A/cm² (b) 0.1 A/cm² (c) 0.2 A/cm².

Figure 31 (a-c) show the effect of variation of the current density for the NWD samples fabricated with 10 g/L diamond concentration in the plating bath. The diamond is distributed throughout the base Ni-W matrix. The sample fabricated at current density of 0.05 A/cm² (Figure 31 (a)) appears to have a higher level of diamond incorporation into the base matrix.

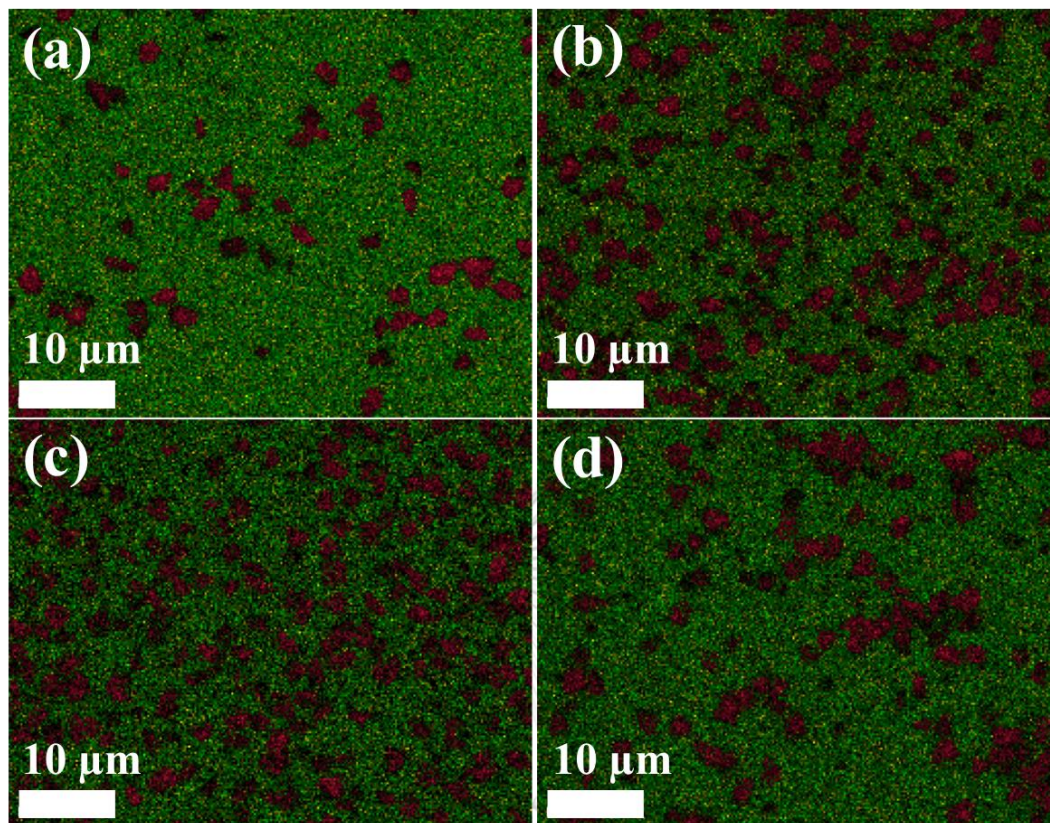


Figure 32 EDS elemental mapping images of Ni-W/diamond composite coatings fabricated at diamond concentration of 10 g/L, temperature of 75°C, pH 8.9, and different current densities, (a) 0.05 A/cm² (b) 0.1 A/cm² (c) 0.15 A/cm² (d) 0.2 A/cm².

The sample fabricated at current density of 0.15 A/cm² exhibits the highest value of diamond content at 32 vol. % and relatively higher level of incorporation of co-deposited diamond particles into the base Ni-W matrix.

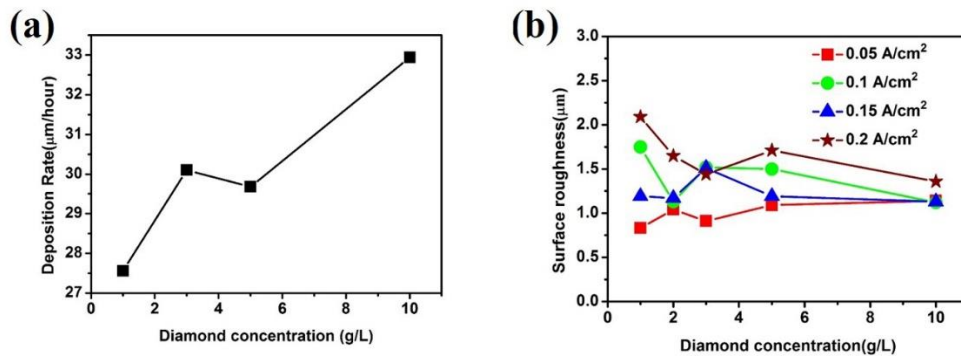


Figure 33 (a) Effect of diamond concentration in the plating bath on the deposition rate of the Ni-W/diamond composite deposits fabricated at current density of 0.15 A/cm², temperature of 75°C and pH 8.9 (b) Surface roughness for different diamond concentration in the plating bath at various current densities for Ni-W/diamond composite deposits fabricated at temperature of 75°C and pH 8.9.

The deposition rate slightly increases with an increase in the diamond concentration except for 5 g/L where it reduces slightly as shown in Figure 33 (a). There is a very small variation in surface roughness (Figure 33 (b)) of the samples for different values of current density at any diamond concentration in the bath.

จุฬาลงกรณ์มหาวิทยาลัย
CHULALONGKORN UNIVERSITY

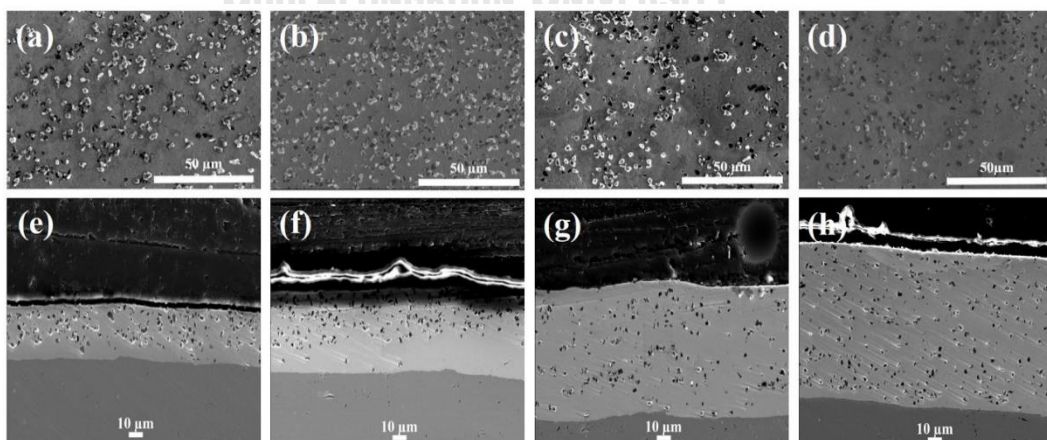


Figure 34 SEM images for the surface and cross section of Ni-W/diamond composite coatings prepared at temperature of 75°C and pH 8.9, for various current densities at 5 g/L diamond concentration in the plating bath (a) surface SEM image for 0.05 A/cm², (b) surface SEM image for 0.1 A/cm² and 5 g/L, (c) surface SEM image for 0.15 A/cm², (d) surface SEM image for 0.2 A/cm², (e) cross-section SEM image for 0.05 A/cm², (f) cross-section SEM image for 0.1 A/cm², (g) cross-section SEM image for 0.15 A/cm² and (h) cross-section SEM image for 0.2 A/cm².

In Figure 34 the diamond particles appear to be uniformly distributed and embedded in to the Ni-W base alloy matrix. The cross-sectional SEM images (Figure 32 (e-h)) exhibit enhancement in the uniformity of the deposits upon increasing the current density from 0.05 A/cm² to 0.2 A/cm².

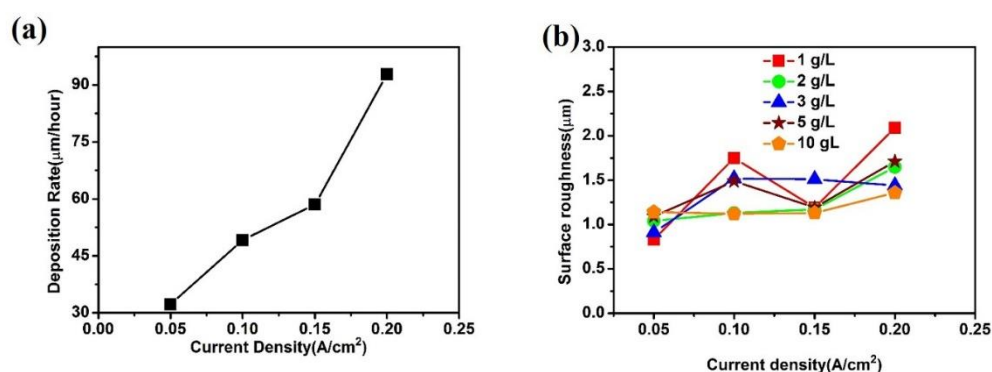


Figure 35 (a) Effect of the current density on the deposition rate of the Ni-W/diamond composite deposits fabricated at diamond concentration of 10 g/L, temperature of 75°C and pH 8.9 (b) surface roughness of Ni-W/diamond composite deposits fabricated at temperature of 75°C and pH 8.9, for different diamond concentration in the plating bath and current density.

The deposition rate as shown in Figure 35 (a) increases upon an increase in the current density. The surface roughness of the deposits shows a slight variation in the range of 1

micron for most values of current densities. However, the samples fabricated with 10 g/L diamond concentration exhibit the least variation in values of surface roughness with an increase in the applied current density.

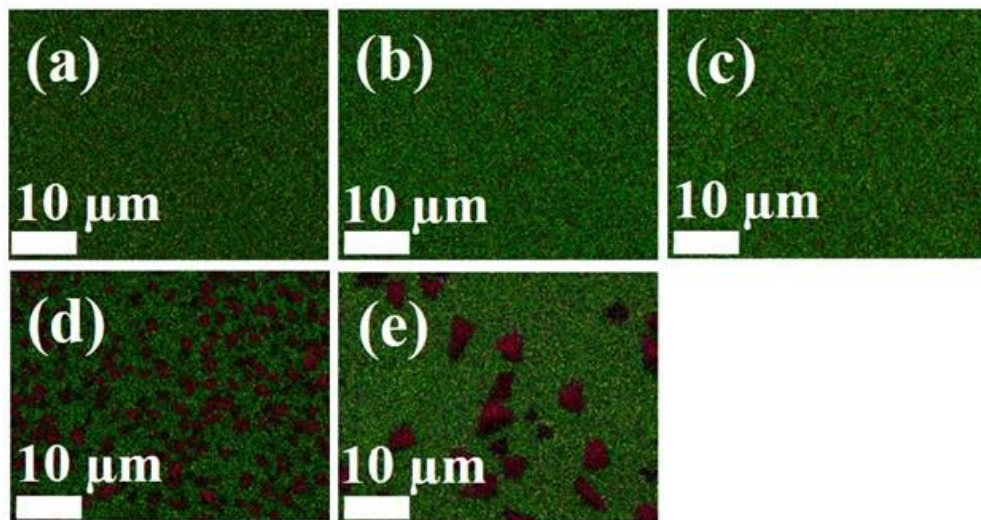


Figure 36 EDS elemental mapping images of Ni-W/diamond composite films fabricated at current density of 0.15 A/cm^2 , diamond concentration of 10 g/L , temperature of 75°C , pH 8.9, and different size of diamond particles, (a) $0.2 \text{ }\mu\text{m}$, (b) $0.3 \text{ }\mu\text{m}$, (c) $0.9 \text{ }\mu\text{m}$, (d) $3 \text{ }\mu\text{m}$, (e) $6 \text{ }\mu\text{m}$.

CHULALONGKORN UNIVERSITY

The diamond content and incorporation are reported to be at the maximum value for samples fabricated with $3 \text{ }\mu\text{m}$ sized diamond particles. The apparent difference in size of the co-deposited diamond particles can also be seen in the Element mapping images for the NWD samples fabricated with various sizes of diamond particles.

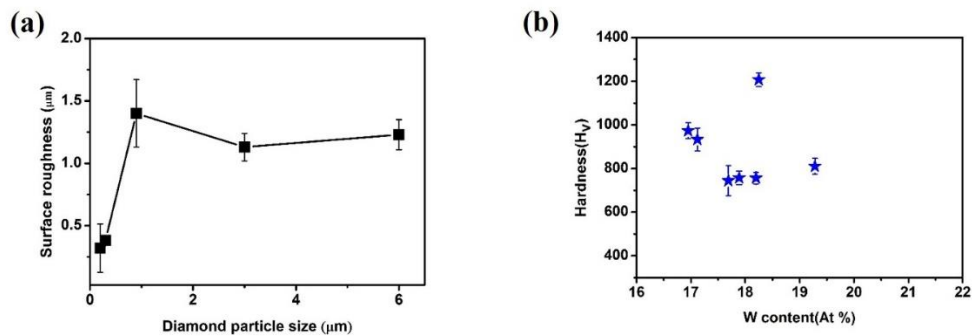


Figure 37 (a) Surface roughness values for Ni-W/diamond composite deposits at different size of diamond particles fabricated at 10g/L of diamond concentration, current density of 0.15 A/cm^2 , temperature of 75°C and pH 8.9 (b) The effect of the tungsten content on the hardness of the Ni-W/diamond composite deposits fabricated at current densities ranging from $0.05\text{-}0.2 \text{ A/cm}^2$, diamond concentration ranging from 1-10 g/L, 75°C temperature and pH 8.9.

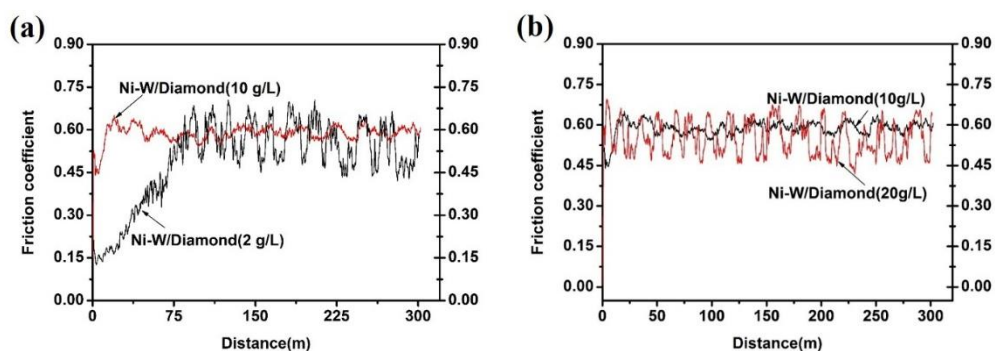


Figure 38 The wear properties of Ni-W/diamond composite coatings fabricated at temperature of 75°C and pH 8.9 (a) The friction co-efficient of the Ni-W/diamond (10 g/L and 2 g/L) composite coatings (b) The friction co-efficient of the Ni-W/diamond (10 g/L and 20 g/L) composite coatings.

The surface roughness of the deposits varies within the range of 1 micron for most of the samples (Figure 37 (a)). The value of surface roughness remains fairly constant for samples with diamond particles of size 0.9-6 microns. The effect of the W content in the deposits has been shown in Figure 37 (b). The samples exhibit high hardness

even with considerably lower values of W content in the deposits. This suggests the lesser influence of the W particles towards enhancing the hardness of the deposits as compared to the diamond particles. The friction co-efficient range and variation during the wear test of the 2 g/L samples (Figure 38 (a)) and of 20 g/L sample (Figure 38 (b)) was reported to be higher than the sample with 10 g/L diamond concentration.

4.1.5 Conclusion

- (1) The diamond content in the deposits increases upon increasing the diamond concentration in the plating bath upto 10 g/L and current density upto 0.15 A/cm². The maximum diamond content in the deposits was reported at 32 vol. %.
- (2) The W content of the deposits reports a relative decline as the diamond content increases.
- (3) The hardness of the deposits is found to depend more on the diamond content of the deposits as compared to the W content. The deposits with high diamond content report a high value of hardness despite having lower values of W content in them. The maximum value of hardness reported was 1207 Hv.
- (4) The samples with high diamond content are relatively smoother and report a lower value of surface roughness. Moreover, the surface roughness varies

the least for the sample fabricated at 10 g/L diamond concentration in the plating bath.

- (5) The wear resistance is also improved upon increase in the diamond content in the deposits and the wear rate is the least for the sample fabricated at 10 g/L diamond concentration in the plating bath. The values of friction coefficient is also lower for the samples fabricated with 10 g/L diamond concentration in the plating bath as compared to the samples with a lower plating bath concentration (2 g/L), higher diamond concentration in the bath (20 g/L) or the Ni-W alloy samples fabricated without diamond.

4.2 Effect of diamond particles on the microstructure and composition of pulse plated multilayer Ni-W/diamond composite coatings

Malay Kumar Das¹, Jiaqian Qin², Priya Karn^{3,4}

¹ International graduate program of Nano-science and technology, Chulalongkorn University, Bangkok 10330 Thailand

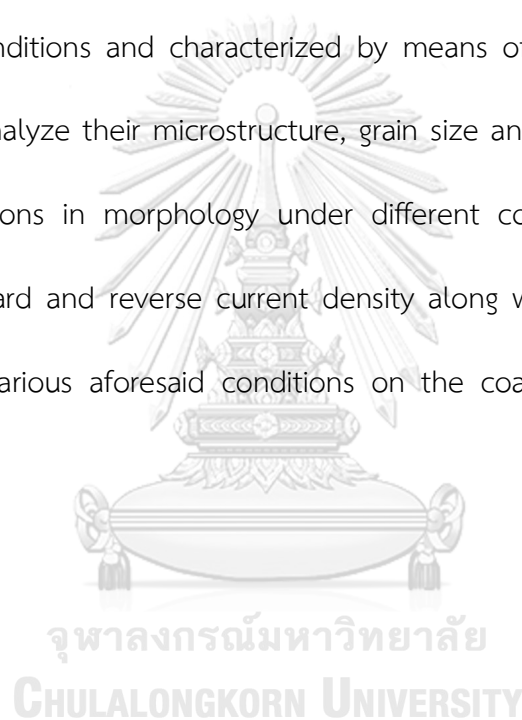
² Metallurgy and materials science research institute, Chulalongkorn University, Bangkok 10330, Thailand

³ Institute of Engineering- Tribhuvan University Purwanchal campus, Dharan, Nepal

⁴ PM Education and Research Center of Excellence, Nepal

Abstract

The research encompasses the fabrication of multilayer Ni-W-diamond composite deposits by pulse current electrodeposition. The mean surface diameter of the diamond used for the research was 0.9 microns. The composites were fabricated under various conditions and characterized by means of SEM, EDS and XRD to investigate and analyze their microstructure, grain size and elemental distribution along with variations in morphology under different conditions. The effect of variations in forward and reverse current density along with duty cycle and the combination of various aforesaid conditions on the coatings were studied and analyzed.



4.2.1 Introduction

Nanocrystalline Ni-W alloys and composites have a wide arrays of applications such as fabricating the alloys in some sort of barrier/capping layers for ultra large scale integration applications in copper metallization and also potential applications in Microelectromechanical systems and also various allied applications in mold inserts, magnetic heads and relays, bearings, resistors, electrodes accelerating hydrogen

evolution from alkaline solutions, environmentally safe substitute for hard chromium plating in the aerospace industry, etc.[59]. Hard-chrome plating has been used as a surface finishing technique in various engineering industries because it has good advantages such as high hardness, corrosion resistance, wear resistance, aesthetic qualities and durability. However, Hard-chrome plating solutions are toxic, carcinogenic and hazardous to human health [60, 118] to substitute chromium; the new alternate surface finishing method must maintain hard-chrome's advantages. One very important and sustainable prospect is to substitute Hard-Chrome plating with metal alloys/composites plating which is certainly better than plating metals with alloys as alloys and composite plating directly on a suitable substrate tends to enhance the abrasion resistance and resistance to surface erosion phenomena while on the other hand acts as a highly viable and suitable substitute to hard chrome plating[118]. In various industrial applications (for example boilers) it has been documented that the surface of the equipment and components involved in the running of the plant are highly to prone to mechanical stress, corrosion and damage by wear. This in turn leads to plant closures and subsequent loss in revenue and operations in related industries like mining, mineral processing etc. Hence it becomes imperative to work upon strategies to enhance the surface properties rather than bulk properties [62, 63, 80] in a wide scope of engineering materials and components used in industries. It is also an interesting prospect to try and introduce various composites

Ni-W/diamond composite coatings were electrodeposited by means of pulse plating on a 2*2 carbon steel substrate. The operating conditions were modified to obtain a multilayer electrodeposited coating of varying properties, thickness, composition and attributes constituting the aforesaid composites. Diamond composite incorporation into the Nickel-Tungsten alloy matrix could significantly enhance the mechanical properties of the Ni-W base coated matrix in terms of hardness[119], wear resistance, corrosion resistance, abrasion resistance, increased durability, thermal resistance and also the overall roughness of the coatings. However, the major issue that needs to be fixed before embarking on the fabrication of multilayer coatings is to ensure the uniform distribution of diamond particles on the coated matrix. Various contemporary researchers have employed the means of pulse plating to fabricate ni-w and other alloys and composites[120]. Employing suitable pulse parameters is quite crucial to obtain desirable deposits. Fabrication of Multilayer coatings also enhance the versatility of the deposits in terms of varying layers of different surface roughness, friction and wear resistance along with hardness. The influence on the microstructure of a multilayer coating is also profound and very important in terms of enhancement of film structure and quality.

4.2.2 Experimental Details

Ni-W-diamond composites were fabricated by means of electrodeposition from an ammonia-citrate bath (200 ml). The bath composition was nickel sulphate 15.8 g/L, sodium tungstate 46.20 g/L, tri-sodium citrate 147 g/L, ammonium chloride 26.7 g/L and sodium bromide 15.8 g/L respectively. The operating temperature was 75 °C the pH, stirring speed and the deposition time was kept constant at 8.9, 200 RPM and 2 hours, respectively.

4.2.2.1 Preparation of Steel

The substrate was subjected to pre-treatment before deposition by means of washing it with soap solution, keeping it immersed in 10% NaOH solution and 14% HCL. Prior to insertion of the electrodes in the plating bath, the substrate was activated by 14% HCL. Except the deposition area the other undesirable parts of the substrate were covered with polymer tape.

4.2.2.2 Pulse Parameters

Table 4 Pulse Parameters for the Experiments

Sample	Diamond	Forward	Forward	Reverse	Reverse	Duration
	Concentration	Current	Duration	Current	Duration	of Each
	(g/L)	Density	(ms)	Density	(ms)	Layer
		A/cm ²		A/cm ²		(minutes)

A	5	0.2	20	0.3	3	-
B	5	0.2	20	0.15	2	-
C	5	0.2	20	0	3	-
D	5	0.2	20	0	0	-
A_ND	0	0.2	20	0.3	3	-
AB_0.1	5	A=0.2	A=20	A=0.3	A=3	A=0.1
		B=0.2	B=20	B=0.15	B=3	B=0.1
AC_0.1	5	A=0.2	A=20	A=0.3	A=3	A=0.1
		C=0.2	C=20	C=0	C=3	C=0.1
AD_0.1	5	A=0.2	A=20	A=0.3	A=3	A=0.1
		D=0.2	D=2	D=0	D=0	D=0.1
AC_1	5	A=0.2	A=20	A=0.3	A=3	A=1
		C=0.2	C=20	C=0	C=3	C=1
AC_2	5	A=0.2	A=20	A=0.3	A=3	A=2
		C=0.2	C=20	C=0	C=3	C=2

4.2.2.3 Estimation of crystalline size by XRD

X-Ray Diffraction technique was employed to analyze crystalline size of the coatings. Brooker D8 advance X-ray diffractometer operated at Cu K α radiation (nickel filtered) at a rating of 40 kV, 20 mA. The scan rate was 0.02° per step and the measuring

time 0.5 second/step. Scherrer's equation[121] was employed for the calculation of the grain size of the electrodeposited crystals

$$D = \frac{0.9 \lambda}{\beta \cos \theta}$$

Where, D is the crystalline size, λ is the incident radiation (1.5418 Å), β is the corrected peak width at half maximum intensity and θ is the angular position.

4.2.2.4 Scanning Electron microscope (SEM) and Energy Dispersive X-Ray Spectroscopy (EDS) Analysis

The samples were characterized in terms of morphology and microstructure by JEOL JSM-6400 SEM with EDS capability embedded into it. The coated deposits were viewed at 15KV with 2000, 3000 and 5000X magnifications. The deposit surface was subjected to EDAX/EDS analysis (relative's ratios) at 20KV for the elemental analysis and chemical composition of the deposits.

4.2.3 Results and Discussions

4.2.3.1 Effect of the Pulse plating on the Grain size

Upon analyzing the grain size, a progressive reduction in grain size is observed from A to D. For the Multilayer AD has the optimal size of 7 nm whereas grain size is subsequently enlarged in case of AB and AC with each alternating layer deposited for 0.1 minutes respectively. The incorporation of diamond composites into the alloy

matrix/grains increases the grain size from 18 to 23 nm. Therefore, the incorporation of diamond particles into the coating matrix is subsequently established. It is clear that the diamond particles have been embedded into the coating matrix by means of a chemical bonding with the base alloy matrix and not merely by means of physical adhesion or mechanical cohesion. This is a relevant result to further study the means to enhance the level of incorporation of diamond particles and the distribution of diamond particles in the coatings.

Table 5 Grain size of the coatings

Sample	Grain size(nm)
A_ND	18
A	23
B	19
C	4
D	5
AB_0.1	16
AC_0.1	8
AD_0.1	7

4.2.3.2 SEM and EDS Analysis

Comparative analysis for Figure 39 and 40 reveals the morphological differences between the samples with and without diamond addition. This reveals the importance and the indispensability of diamond composites addition in the Nickel-Tungsten. There is a marked difference in the microstructure for samples with and without diamond addition. Figure 39 depicts a uniform film structure and distribution of diamond particles. Moreover, there are no cracks and pit formations in the samples containing diamond composites encapsulated into the matrix. Unlike the former the samples without diamond have a lot of quasi circular formations for almost all magnifications. There seems to be a lot of pit formations in all of the images without diamond. There is a clear evidence of numerous cracks and fissures on the microstructure for Figure 40 (b). The coating is discontinuous with evidence of internal strain which causes cracks and lack of continuity and uniformity in the film thereby severely affecting the microstructure and in turn the properties associated with them. The coatings with diamond reveal uniform crystalline formations also with no sharp grain boundaries unlike the samples without diamond which has highly discontinuous formations on the surface with no uniformity in terms of deposition and film quality. The comparison between the morphologies of Figure 39 and 40 clearly established the need for use of diamond composites in Ni-W alloy matrix in order to enhance the properties of the

coatings. This is a very relevant and substantial result in terms of our justifications for the use of the diamond particles as composites in the coating matrix.

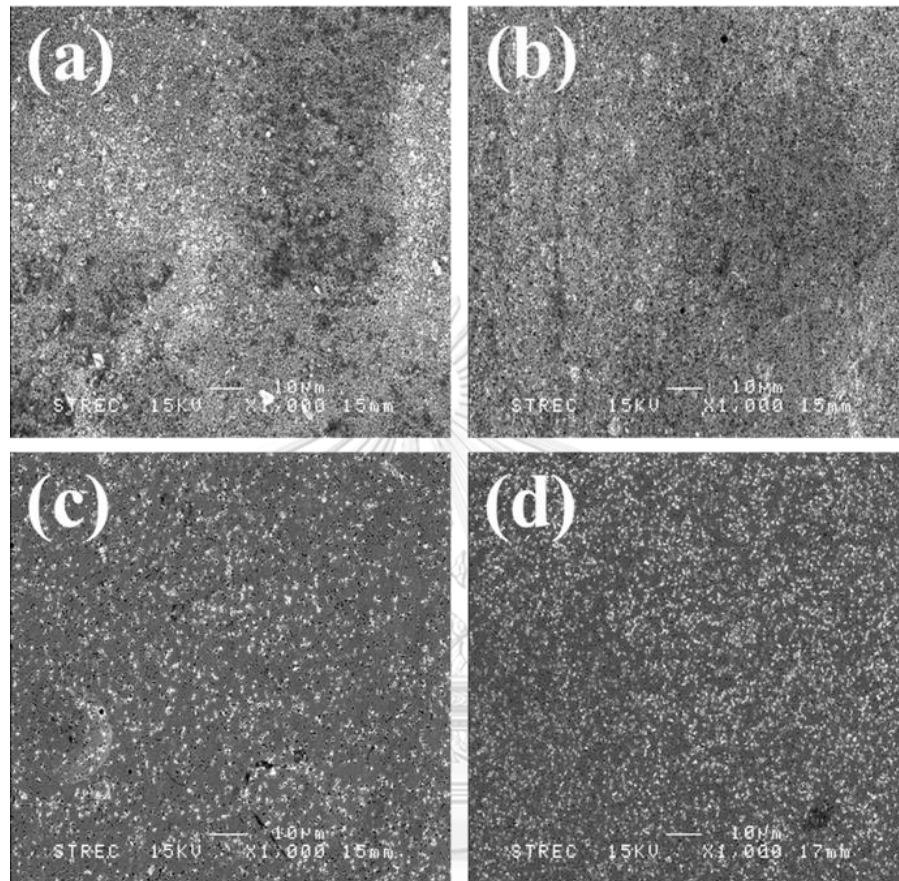


Figure 39 SEM Images of (a) A monolayer layer (b) B monolayer (c) C monolayer (d) D monolayer

Figure 40 depicts the SEM images for the Multilayer coating AB_0.1, AC_0.1 and AD_0.1. The image 3 (b) exhibits stark differences in terms of distribution of diamond particles, cracks and irregularity in crystal structure. The pairs AB_0.1 and AD_0.1 are similar and have a uniform crystal structure. The important results that is evident from Figure 41 is that the while fabrication of multilayer AC layer is not desirable in terms

of morphology and microstructure. Therefore, either AB or AD should be used a template layer for fabrication of multilayer Ni-W-Diamond.

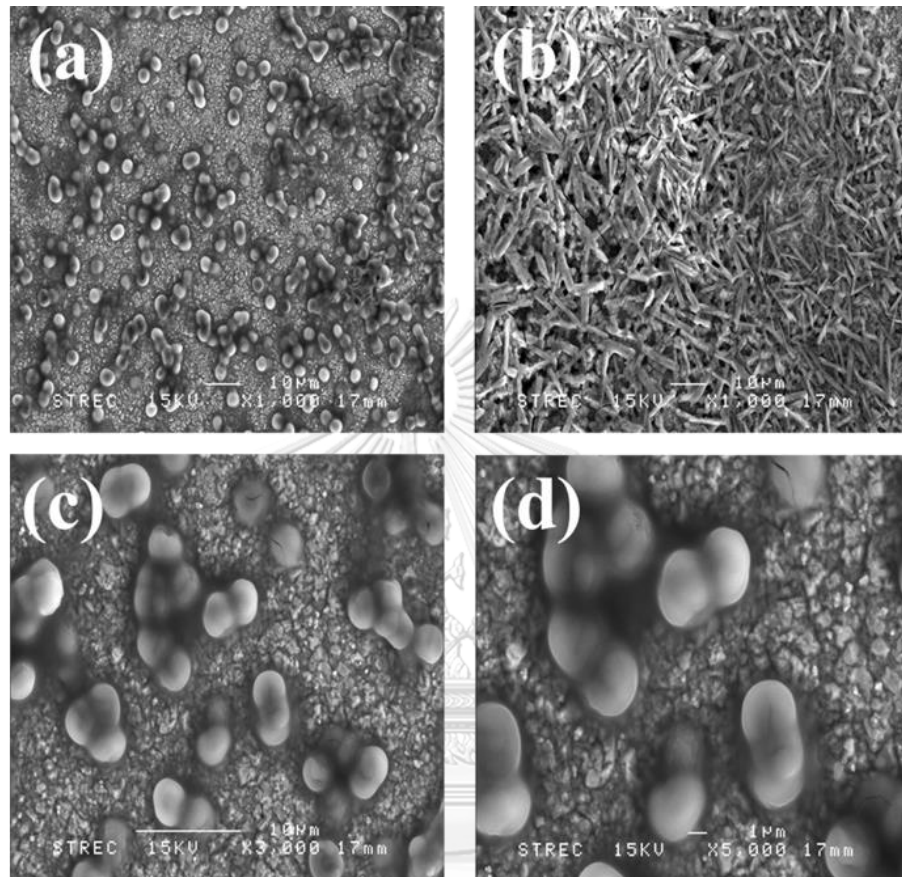


Figure 40 SEM Images for A layer without diamond (a) for 1000X (b) for 2000X (c) for 3000X (d) for 5000X

The diamond content in the coatings of AC_0.1 also appears to be considerably lesser than both AB_0.1 and AD_0.1. However, upon close analysis it is revealed that the surface contamination is greater in case of AB_0.1 as compared to AD_0.1, an idea which is corroborated by the presence of a large number of white spots which are most likely to be oxygen and carbon contaminants encapsulated into the coating

during the deposition process. The SEM analysis acts as an important tool to identify and ascertain the optimal and suitable conditions for the Ni-W-diamond coatings.

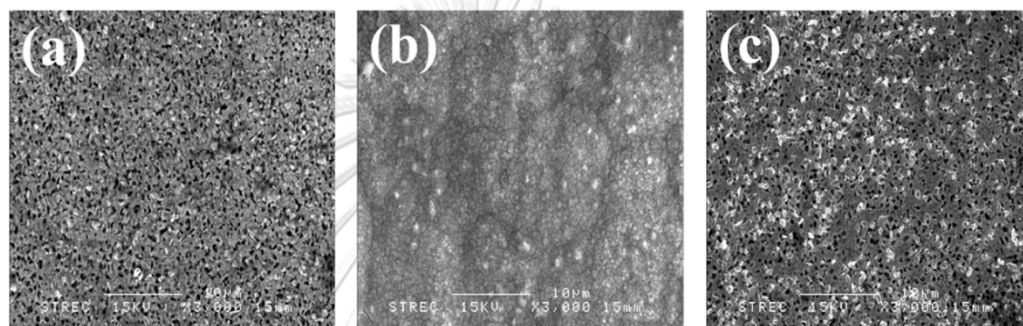


Figure 41 SEM Images for (a) AB_0.1 (b) AC_0.1 (c) AD_0.1

4.2.3.3 EDS analysis

Table 6 Elemental composition of Ni and W in the deposits as reported by the EDS results

Sample	Ni (At %)	W (At %)
A_ND	95.42	4.58
A	99.06	0.94
B	97.62	2.38
C	78.58	21.42
D	85.56	14.44

AB_0.1	92.97	7.03
AC_0.1	82.87	17.13
AD_0.1	75.75	24.25

The EDS results suggest enhanced Tungsten content in the AD_0.1 layer. This is possibly because D is the direct current which allows for an enhanced duty cycle and thereby an enhanced plating rate leading to a higher co-deposition of tungsten. However, the Tungsten Content decreases drastically when diamond is added to the A layer. This is due to the encapsulation of diamond particles into the coating matrix. The carbon content results in the EDS analysis might also contain carbon contaminants on the coated surface which is why the diamond content by weight in the coatings needs to be investigated by dissolving the coating and the entire substrate in iron and in turn measuring the difference in weight to give the diamond content.

4.2.3.4 Relationship between Grain Size and Tungsten content

Table 7 shows a clear relationship between grain size and tungsten content wherein the smaller grain size facilitates an increased concentration of tungsten in most cases. Upon analysis of AD_0.1, A_0.1, C and D it's clear that a smaller grain size enables more co-deposition of tungsten in the coated matrix thereby enhancing the tungsten content in the deposits. However, the nature of the current that causes the deposition is also an important factor to determine the tungsten content in the coating which is

evident from the fact that the samples AD_0.1 which has D layer as direct current deposited layer has the highest tungsten content among all the coated layers. However, the tungsten content probably follows a limiting value of grain size beyond which tends to violate the aforesaid trend which is why a very reduced tungsten content is observed in case of single layers A, B, C and D and also in case of A_ND layer without diamond. The substantial reduction in grain size for the A single layer without diamond and with diamond can also be credited to the fact that diamond encapsulation into the base matrix tends to reduce the tungsten content. The SEM images as in Figure 39 and 40 along with the relative data of tungsten content reduction and grain size increment can be used as arguments to prove that diamond has been embedded into the coatings uniformly by means of a chemical bonding and not mere physical adhesion or mechanical cohesion.

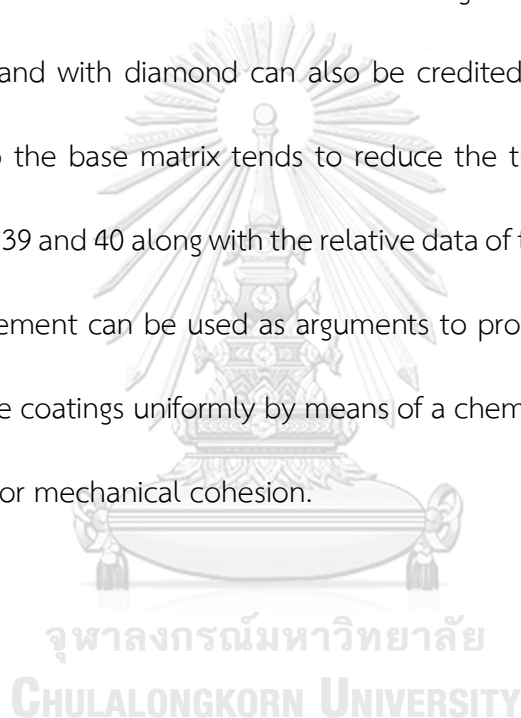


Table 7 Grain Size and Tungsten Content comparison for various conditions

Layer Conditions	Grain Size(nm)	W (At %)
A_ND	18	4.58
A	23.1	0.94
B	19.1	2.38
C	4.1	21.42

D	5.1	14.44
AB_0.1	16.5	7.03
AC_0.1	8.4	17.13
AD_0.1	7	24.25

4.2.4 Conclusion

The following conclusions can be drawn from the above-mentioned results:

- AD_0.1 has an optimal grain size of 7 nm and the most suitable SEM morphology in terms of uniform distribution of diamond particles, film quality, finer grain size and less pronounced grain boundaries as compared to AB and AC 0.1 min multilayer deposits. There are also almost nil cracks as per SEM morphology for AD_0.1 and AB_0.1 unlike AC_0.1
- The incorporation of diamond is meagre, and the distribution also not uniform in the case of AC_0.1. AC_0.1 layer also doesn't have the most suitable grain size, or the tungsten content as compared to AD_0.1 layer.
- The tungsten content is the maximum in case of AD_0.1 layer and it is the most desirable in terms of both SEM morphology and grain size. However, the actual values of diamond content in the deposits along with various other mechanical properties namely hardness, wear and

corrosion resistance need to be figured out before attributing it as the most suitable condition for multilayer

- Smaller grain size and suitable layer conditions facilitate larger deposition rate of tungsten in the coatings and an overall increased tungsten content as per EDS results
- Lack of NiC_x phase in the AD_0.1 multilayer deposits also suggests that it more desirable as per experiment conditions and requirements. However, further characterization is essential to hold credence and finality to the conformation of AD_0.1 to the required standards of properties and microstructure.

4.3 Influence of Co^{2+} ions on the microstructure and mechanical properties of Ni-W/diamond nano-composite coatings

Malay Kumar Das^{a,b}, Xinyu Zhang^{c*}, Yuttanat Boonyongmaneerat^b, Jiaqian Qin^{b*}, Riping Liu^c

^aInternational Graduate Program of Nanoscience & Technology, Chulalongkorn University, Bangkok 10330, Thailand

^bSurface Coatings Technology for Metals and Materials Research Unit, Metallurgy and Materials Science Research Institute, Chulalongkorn University, Bangkok 10330, Thailand

^cState Key Laboratory of Metastable Materials Science and Technology, Yanshan University, Qinhuangdao 066000, P.R. China

Journal of Nanoscience and Nanotechnology: Accepted manuscript

Abstract

The Co^{2+} ions were introduced in the Ni-W/diamond plating bath in varying quantities before the electrodeposition process of the Ni-W/diamond coatings. The effect of the Co content in the deposits was analyzed in terms of various mechanical properties and microstructure. The morphology and the composition of the deposits were investigated by means of SEM and EDS, respectively. The addition of small quantities

of Co^{2+} ions in the plating bath tends to enhance the hardness and wear performance of the Ni-W/diamond deposits. Upon increasing the amount of CoSO_4 beyond 0.2 g/L in the plating bath both the hardness and the wear resistance of the deposits decrease sharply. The Co content in the deposits also increases progressively upon increasing the amount of CoSO_4 in the plating bath.

Keywords: Composite coatings, electrodeposition, hardness, wear resistance

*E-mail address: jiaqian.q@chula.ac.th (J.Q), xyzhang@ysu.edu.cn (X.Z), tel: +66 2218

4243, fax: +66 2611 7586

4.3.1 Introduction



Metal alloy composites exhibit advanced surface and mechanical properties which have been established by the means of various classical as well as recent research findings. The emergence of nanoscale materials in the recent times has successfully led to the fabrication of various nanomaterials including nano-crystalline deposits, nano-scale multilayer deposits and nano-composites. The above-mentioned deposits find applications in a wide array of appliances and industries. This includes improved

performance of functional coatings, applications in printed circuit boards, memory storage systems and also enhanced micro hardness in devices such as micro-electrical-mechanical systems (MEMS)[122]. The pioneering work for the development of composite coatings by electrodeposition was carried out in 1950's and 1960's [123]. Further research in this field during the next two decades was more dedicated towards enhancement of the mechanical, corrosion and tribological properties of the electrodeposited composite coatings developed in the previous two decades.

The introduction of various ceramics (Diamond, SiC, WC, TiO and Al₂O₃) as reinforcing particles into electrodeposited nickel based alloy matrix has been able to bring about significant enhancements in the mechanical properties of the deposits such as hardness, wear resistance and corrosion resistance[2, 3, 7, 56-58, 124]. Diamond is known to possess a high hardness, excellent oxidation resistance and chemical stability along with good anti wear and corrosion performance[13, 125]. The above-mentioned properties of diamond have been used to reinforce nickel based alloy deposits by various contemporary researchers [2, 7, 13, 21, 110, 125]. Ni-W/diamond (NWD) composite coating is one such diamond reinforced Ni-W alloy coating which is known to be a super hard material with enhanced anti-wear and anti-corrosion performance. The higher diamond content in the NWD composite deposits have been known to enhance the hardness and wear resistance of the deposits[7].

Various additives have been introduced in electrodeposited Ni based alloy and composite coatings to enhance the properties of the deposits. Pramod Kumar U et al. studied the effect of salicylaldehyde additives on the microstructure and corrosion resistance of Ni-W nanocrystalline alloy coatings[126]. Their results exhibit that the deposits fabricated with salicylaldehyde additives were more uniform and smoother in texture as compared to the Ni-W deposits fabricated without the presence of aforesaid additive. The thickness of the deposits was also found to increase as the additive concentration was increased up to 100 ppm in the plating bath. Das et al. studied the effect of saccharin sodium on the microstructure and hardness of electrodeposited Ni-W coatings and exhibited that the saccharin sodium additives enhance the hardness and W content of the Ni-W coatings[127]. Golonka et al. studied the effect of MgO addition to Ni-W/Al₂O₃ composite coatings. The researchers observed that the addition of magnesium oxide controlled the microstructure of Al₂O₃ polycrystals, thereby limiting abnormal grain growth. However, in case of the Ni-Al₂O₃ composites a pinning effect emanating from the nano-nickel particles mostly caused the reduction of alumina grain size.

Ni-Co electrodeposited coatings serve as a viable alternative for conventional Ni deposits because of high hardness, strength and wear resistant properties. Li et al. investigated the effect of Co concentration (in the electrolytic solution) on the surface morphology and micro hardness of Ni-Co alloys. They reported that addition of Co in an appropriate amount (up to 4 g/L) in the plating bath could result in a finer structure

of Ni-Co alloys and also enhance the hardness of the Ni-Co electrodeposits. However, further increase in the Co concentration to 5 g/L (beyond the optimal 4g/L) in the plating bath resulted in the decline of the hardness of the deposits as per the inverse Hall-Petch relationship [128]. The introduction of cobalt ions in the Ni based plating bath tends to reduce the need of addition of organic grain refiners (saccharin, SDS etc.) during the electrodeposition process. The organic grain refiners are responsible for the Sulphur and carbon impurities in the electrolytic solution. Therefore, Co as an additive plays an important role in improving the microstructure of Ni based alloy deposits and decreasing the need for addition of organic grain refiners, in turn leading to a reduction in the level of impurities in the plating bath during the process of fabricating Ni- based nano-crystalline deposits [128, 129]. However, for NWD composite coatings no significant literature is available on the use of Co (Co^{2+}) as an additive during the fabrication of NWD composite deposits. Therefore, this paper aims to investigate the effect of the Co cation additive on the electrodeposited NWD composite deposits.

In the present study, varying amounts of CoSO_4 additives were added to the NWD plating bath and its effect on the NWD deposits was investigated. The effect of Co^{2+} ions on the microstructure and mechanical properties of the NWD deposits was analyzed.

4.3.2 Experiment details

The NWD samples were co-electrodeposited in a 200 ml plating bath. The bath composition and the experimental conditions for the samples have been mentioned in Table 8.

Table 8 Plating bath composition and deposition conditions for the NWD composite coatings with varying amounts of CoSO_4 .

Chemicals) g/L(Deposition parameters	
Nickel sulphate	18	Temperature	75 °C
Sodium tungstate	53	Current density	0.15 A/cm ²
Tri-sodium citrate	168	pH	8.9
Ammonium chloride	31	Electrode distance	35 mm
Sodium bromide	18	Stirring speed	200RPM
Cobalt sulphate	0-1.5	Deposition time	2 hours
Diamond)3 μm(10		

Carbon steel substrates were pre-treated with 10% NaOH and 14% HCl solution before being immersed into the plating bath for the deposition process. The material for the anode was a platinum mesh. The samples were coated for a fixed area of 2×2 cm². The uncoated parts of the substrate were insulated from the electrolyte by means of a plastic tape.

X-Ray diffraction was used as a means to characterize phase and the structure of the samples. The samples were analyzed at a scan rate of 0.02° and the measuring time was 0.5 second/step. Scherer's equation [110] was used as a means to analyze the grain size of the deposits.

SEM/EDX integrated analysis system (Horiba Limited) was used to investigate the surface and the structure of the coatings, cross-section and also the element (Ni, W, Co, etc.) content in the co-deposited coatings. A Vickers diamond indenter equipped hardness testing equipment (Mitutoyo hardness tester) was used to determine the hardness of the NWD coatings under a normal load of 0.1 kgf (0.98 N). Seven different indentations were made on the coating surface and the average value was calculated to determine the hardness. The wear test was performed with a zirconia ball (Zirconia ball hardness~ 1300) on disc tribometer under a normal load of 20 N for a linear sliding distance of 300 m.

The roughness and the wear volume loss of the sample was calculated by Taylor Hobson surface profilometer. The scan rate was fixed at $1500 \mu\text{m}/\text{second}$ and the X-spacing at 5 microns for the wear track scanning and the calculation of roughness of the deposit. The Y-spacing was fixed at 25 microns while scanning the wear track. The wear volume loss was calculated by 3-d scanning of 4 different sections of the wear track to calculate the average volume loss per unit area of the track and then the net

volume loss was calculated by multiplying the unit volume loss of the sample with the total area of the wear track. The wear rate was calculated by the following formula:

$$K_i = \frac{V_i}{FS} \quad (1)$$

Where, K_i is the specific wear rate coefficient, V_i is the wear volume, F is the normal load applied during the wear test and S is the sliding distance.

The Archard equation is expressed as:

$$Q = K NL/H \quad (2)$$

Here, Q is the wear volume loss, K is the wear co-efficient, L is the applied normal Load, N is the sliding distance and H is the hardness of the deposit.

4.3.3 Results and Discussion

4.3.3.1 Effect of the cobalt concentration on the NWD deposits

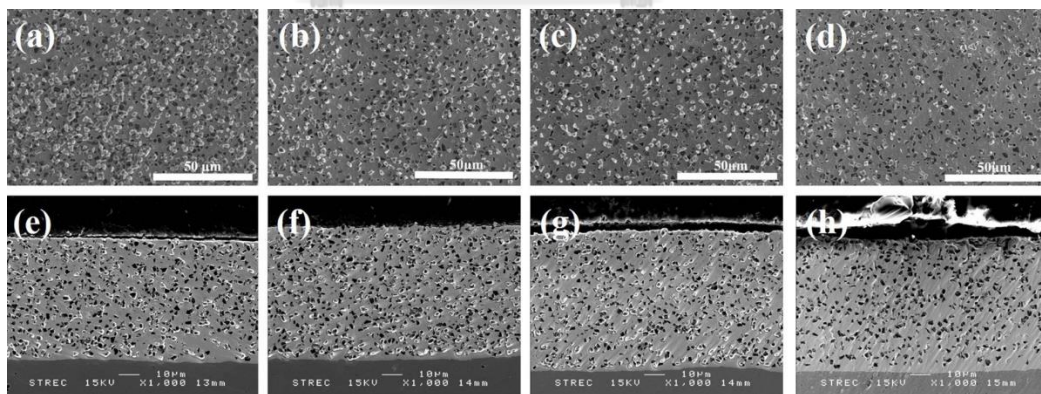


Figure 42 (a-d) SEM micrographs for the Ni-W/diamond composite coating samples fabricated with varying amounts of CoSO_4 additive (a) 0 g/L (b) 0.1 g/L (c) 0.5 g/L (d) 1.5 g/L at 75° C (e-h) cross-sectional SEM micrographs for the Ni-W/diamond composite coating samples fabricated with varying amounts of CoSO_4 additive (e) 0 g/L (f) 0.1 g/L (g) 0.5 g/L and (h) 1.5 g/L.

Figure 42 (a-d) shows the SEM micrographs of NWD composite deposits fabricated with 0 g/L, 0.1 g/L, 0.5 g/L and 1.5 g/L of CoSO_4 in the plating bath, respectively. The element mapping image for the diamond particles has been inserted in Figure 42 (a, b and c). These particles in the inserted image correspond to the diamond particles that have been co-deposited into the Ni-W matrix in the Figure 42. The diamond particles appear to be uniformly incorporated and distributed on the base Ni-W matrix for all the NWD samples fabricated with varying amounts of CoSO_4 . Addition of CoSO_4 additive to the plating bath does not significantly alter the distribution of the diamond particles on the base Ni-W matrix. However, the diamond particles incorporation in the base matrix appears to be slightly diminished as the amount of CoSO_4 is increased in the NWD plating bath from 0 to 1.5 g/L. Figure 42 (e-h) shows the cross-sectional SEM micrograph for the NWD samples fabricated with 0 g/L, 0.1 g/L, 0.5 g/L and 1.5 g/L of CoSO_4 in the plating bath, respectively. The diamond particles also appear to be uniformly distributed throughout the matrix in the cross-sectional SEM micrograph. The coating thickness has been estimated by calculating the average of 12 random points on the cross-section of the NWD deposits. The thickness of the deposits varies between 58-62.8 μm . The deposition rates of the deposits were 28.5 $\mu\text{m/hr}$, 30.4 $\mu\text{m/hr}$, 30.94 $\mu\text{m/hr}$, 31.43 $\mu\text{m/hr}$, 29.98 $\mu\text{m/hr}$ and 29.66 $\mu\text{m/hr}$ for the samples fabricated with 0 g/L, 0.1 g/L, 0.2 g/L, 0.5 g/L, 1 g/L and 1.5 g/L of CoSO_4 added to the

NWD plating bath, respectively. The effect of CoSO_4 addition on the deposition rate of the NWD deposits has been shown in Figure 43. The deposition rates vary marginally for various quantities of CoSO_4 in the plating bath. The NWD sample fabricated without CoSO_4 exhibits the lowest deposition rate in all the samples. However, the deposition rate and consequently the thickness of the deposits exhibit marginal variation as the CoSO_4 amount is increased in the NWD plating bath.

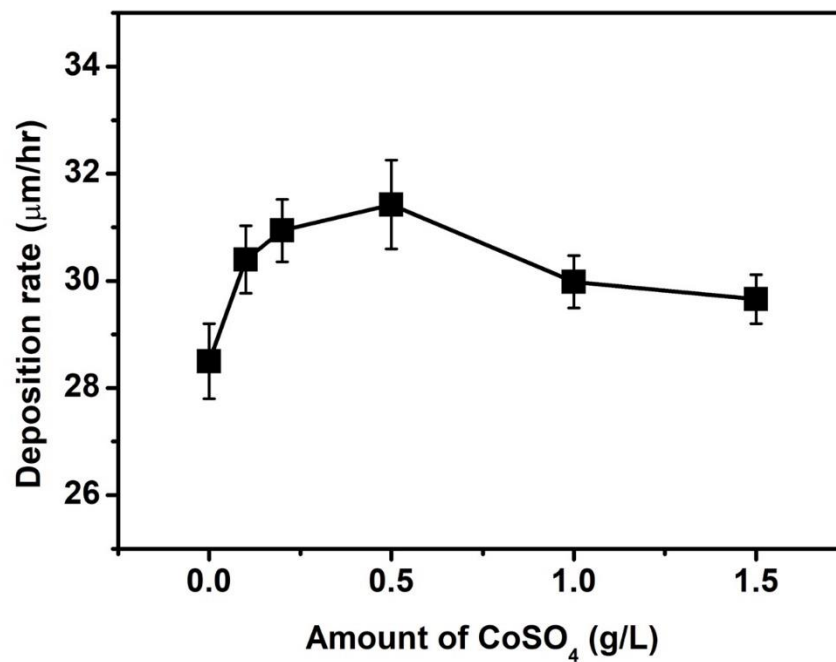


Figure 43 Effect of CoSO_4 on the deposition rate of the Ni-W/diamond samples.

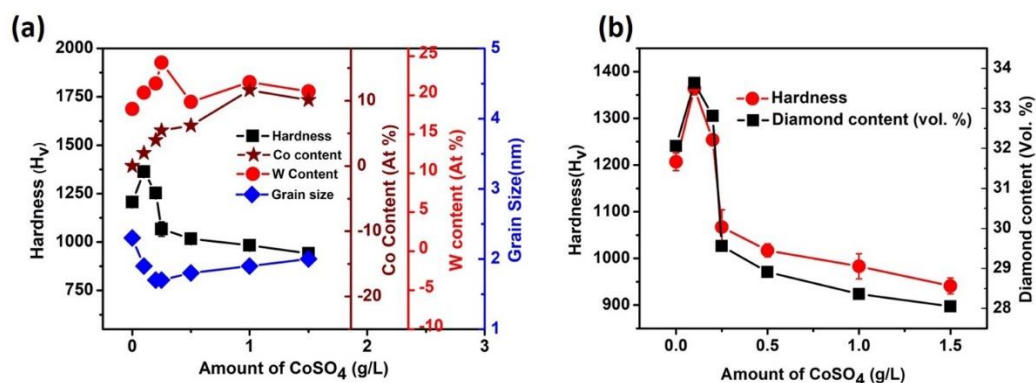


Figure 44 Effect of CoSO₄ on the hardness, Co content, W content and grain size of the Ni-W/diamond samples.

Figure 44 (a) shows the effect of the addition of CoSO₄ in the NWD plating bath on the hardness, Co content, W content and the grain size of the deposits. The samples report hardness values of 1207 ± 19 , 1364 ± 12 , 1254 ± 12 , 1067 ± 37 , 1017 ± 14 , 983 ± 27 , 941 ± 17 for 0 g/L, 0.1 g/L, 0.2 g/L, 0.25 g/L, 0.5 g/L, 1 g/L and 1.5 g/L of CoSO₄ in the NWD plating bath, respectively. The W content of the NWD varies between ~18-24 at. %. The diamond content of the deposits was reported to be ~32.06 %, 33.63%, 32.81 %, 29.56 %, 28.91 %, 28.36 % and 28.05 % for the NWD samples fabricated with 0 g/L, 0.1 g/L, 0.2 g/L, 0.25 g/L, 0.5 g/L, 1 g/L, and 1.5 g/L of CoSO₄ in the NWD plating bath, respectively. It is observed that the diamond content in the NWD deposits exhibits a progressive decline as the amount of CoSO₄ is increased beyond 0.2 g/L in the NWD plating bath. The correlation of the diamond content with the hardness for the varying amounts of CoSO₄ in the plating bath has been reported in Figure 44 (b). The samples with a higher value of hardness report a higher diamond content. Diamond co-deposition is decreased as the amount of Co²⁺ is increased in the plating

bath. The decline of W, diamond content and the simultaneous increase of Co content in the deposits suggest that the Co^{2+} tend to be deposited into the base matrix as a Ni-W-Co alloy instead of being additives in the Ni-W base matrix as the amount of Co^{2+} is increased in the plating bath. The hardness of the deposits shows a very close correlation with the diamond content underlining the role of the co-deposited diamond particles towards enhancing the hardness of the deposits. The Co content in the deposits also increases as the amount of CoSO_4 is increased in the plating bath (Figure 44). The Co content in the deposits varies between ~2-12 at. % for the different amounts of CoSO_4 added to the NWD plating bath. The increase of Co content in the deposits is because of the increase in the Co^{2+} cation concentration in the plating bath [127, 130]. The hardness is reported to be highest for the NWD sample fabricated with 0.1 g/L CoSO_4 . However, as the amount of CoSO_4 in the plating bath is increased beyond 0.2 g/L the hardness value exhibits a continuous decline. The decline in the value of hardness is small for 0.2 g/L of CoSO_4 in the NWD plating bath and it tends to get steeper upon increasing the CoSO_4 content in the plating bath beyond 0.2 g/L. The lowest value of hardness is reported for the sample with 1.5 g/L of CoSO_4 and there is a significant difference in the hardness of the sample fabricated with 0.1 and 1.5 g/L of CoSO_4 in the NWD plating bath, respectively. It is therefore, evident that the addition of small amounts of CoSO_4 in the NWD plating bath tends to cause a progressive enhancement in the value of hardness of the deposits and as the amount of CoSO_4 is increased (beyond 0.2 g/L), the hardness drops significantly. Therefore, the introduction

of small quantities of Co^{2+} cation in the NWD plating bath causes an enhancement in the micro hardness of the NWD deposits. The addition of small quantities of Co^{2+} ions in the plating bath also tends to decrease the deviation from the mean value of the hardness of the coatings which is evident by the lower error margins in the values of the hardness for the NWD samples with 0.1 and 0.2 g/L CoSO_4 , respectively. The value of hardness tends to decrease as the diamond content in the deposits decreases in the NWD samples. The grain size of the coatings varied in the range of 1.7-2.3 nm.

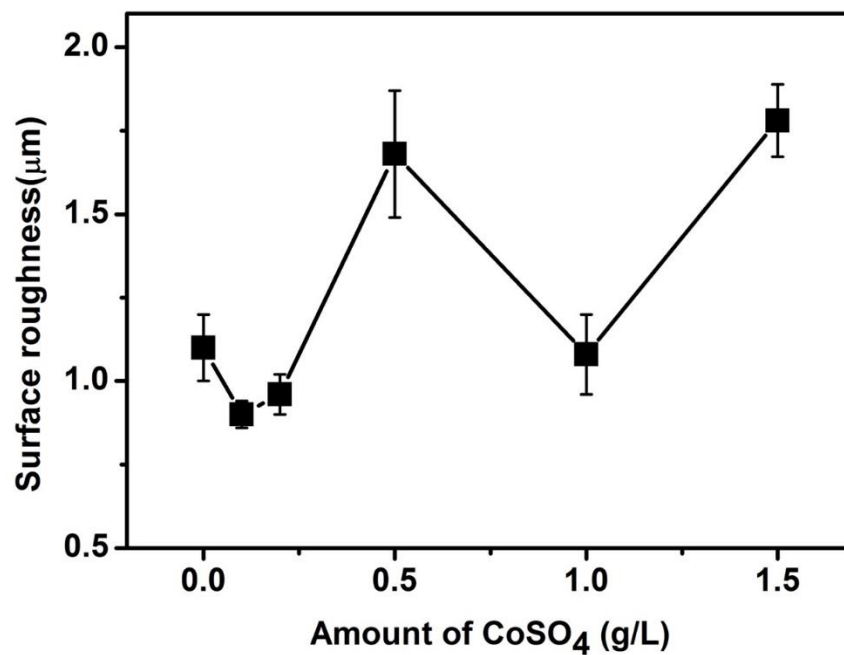


Figure 45 Effect of CoSO_4 on the surface roughness of the Ni-W/diamond samples.

Figure 45 shows the effect of CoSO_4 addition on the surface roughness of the fabricated deposits. The roughness of the deposits varies between 1.1 to 1.8 microns.

The samples tend to get rougher with an increase in the amount of CoSO_4 beyond 0.2 g/L in the plating bath. Ni is the most abundantly used wear resistant electrodeposit after hard chrome coatings [131]. NWD composite coatings have also been found to exhibit excellent anti-wear properties [2, 110]. Therefore, the wear performance of NWD composite coatings with varying amount of Co^{2+} cation additive was analyzed to investigate the effect of Co^{2+} additive on the wear performance of NWD deposits.

4.3.3.2 Wear results

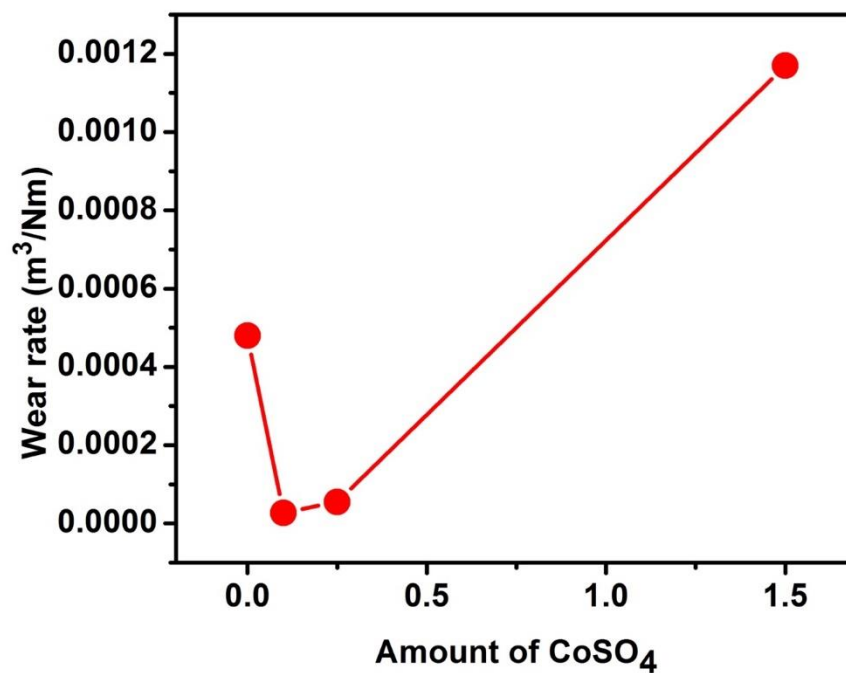


Figure 46 Effect of CoSO_4 on the wear rate of the Ni-W/diamond samples.

Figure 46 shows comparison between the wear rate of the Ni-W alloy as well as NWD composite deposits fabricated with different amount of CoSO_4 in the NWD plating

bath. The friction co-efficient data of the samples for the samples with 0, 0.1 and 1.5 g/L of CoSO_4 in the plating bath has been reported in Figure 47. The tests were performed at a load of 20 N, a linear speed of 9.42 cm/s for a total sliding distance of 300m. The volume of the coating material removed during the wear test was 0.286 mm^3 , 0.0164 mm^3 , 0.033 mm^3 and 0.702 mm^3 for the NWD samples fabricated with 0 g/L, 0.1 g/L, 0.2 g/L and 1.5 g/L of CoSO_4 , respectively. The wear rate was reported to be $48 \times 10^{-5} \text{ mm}^3/\text{Nm}$, $2.7 \times 10^{-5} \text{ mm}^3/\text{Nm}$, 5.5×10^{-5} and $117.02 \times 10^{-5} \text{ mm}^3/\text{Nm}$ for the NWD samples fabricated with 0 g/L, 0.1 g/L, 0.2 g/L and 1.5 g/L of CoSO_4 , respectively. The wear rate for the NWD deposits with 0.1 g/L CoSO_4 declines sharply (by a factor of ~ 17.8) as CO^{2+} cations are introduced in the NWD plating bath are co-deposited on the base Ni-W matrix to fabricate NWD composite deposits. The increase of Co content in the deposits (Figure 44 (a)) results in the wear rate to decline (Figure 48). This suggests that as the amount of Co^{2+} is increased in the plating bath the Co^{2+} tend to be deposited into the base matrix as a Ni-W-Co alloy instead of being as independent additives in the Ni-W base matrix. The wear rate increases slightly as 0.2 g/L of CoSO_4 is added into the NWD plating bath. However, the wear rate exhibits a significant increase in value (by a factor of ~ 21) when the amount of CoSO_4 is increased to 1.5 g/L in the NWD plating bath. The sharp decrease in wear rate for NWD composite deposits (with 0.1 and 0.2 g/L of CoSO_4 additives) establishes the role of the co-deposited diamond particles and Co^{2+} additives towards enhancing the anti-wear performance of the base Ni-W matrix. It is shown in Figure 46 that the wear rate of

the NWD deposits increases upon increasing the amount of CoSO_4 (beyond 0.2 g/L) in the plating bath. Consequently, the wear resistance of the NWD deposits decreases upon increasing the amount of CoSO_4 in the plating bath. The anti-wear performance of the NWD deposits is slightly enhanced upon addition of small quantity of CoSO_4 in the NWD plating bath. The anti-wear performance for NWD samples fabricated with 0.1 g/L of CoSO_4 is significantly better than that of NWD sample without Co^{2+} additive. However, the sample with 1.5 g/L of CoSO_4 exhibits a relatively lesser degree of anti-wear performance as compared to NWD samples with no Co^{2+} additives. The samples reporting a low wear rate (Figure 46) also report a lower value of surface roughness (Figure 45) and lower values of friction co-efficient (Figure 47) [132]. The smoother samples as a result tend to be more resistant to wear as compared to samples with a high value of surface roughness.

4.3.3.3 Wear and Friction co-efficient correlation

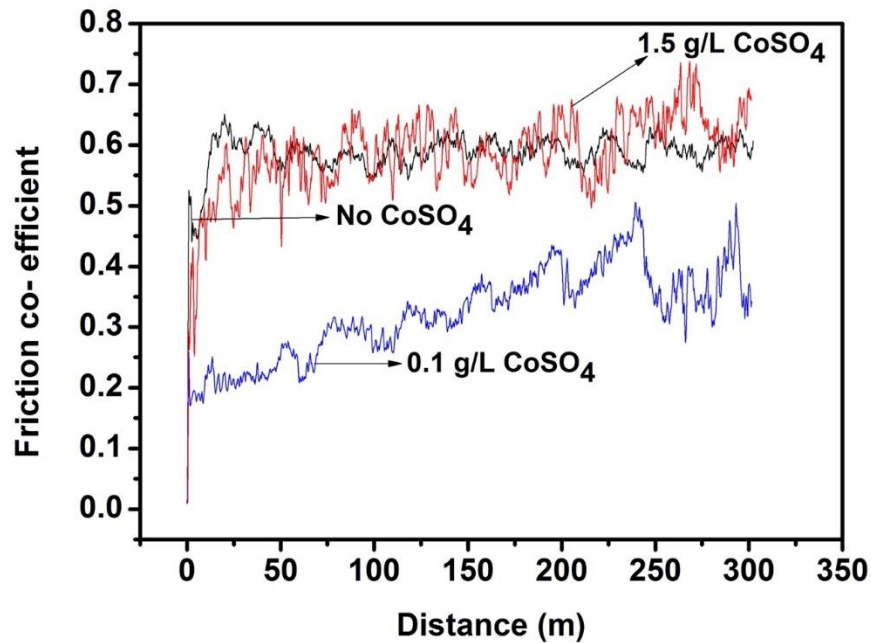


Figure 47 Effect of CoSO₄ on wear friction co-efficient of the Ni-W/diamond samples.

Figure 47 shows that the values of the friction co-efficient is also relatively lower for the NWD samples with 0.1 g/L of CoSO₄ as compared to NWD samples fabricated with 0 g/L and 1.5 g/L of CoSO₄, respectively (Figure 47). The improvement of wear resistance (Figure 46) also corresponds to an increase in the hardness (Figure 44) of the NWD deposits fabricated with 0.1 and 0.2 g/L CoSO₄, respectively. This phenomenon can be explained using the Archard's equation[133] which states that the volume of the debris removed during the wear is proportional to the work done by the friction forces on the sample subjected to wear test. It is clear from Archard equation that the

volume of the debris removed during the wear test of the sample is inversely proportional to the micro hardness of the deposit. Therefore, the samples reporting a higher value of hardness would tend to have a lower volumetric loss of material during the wear test and in turn an enhanced resistance to wear as compared to the other samples with lower values of hardness.

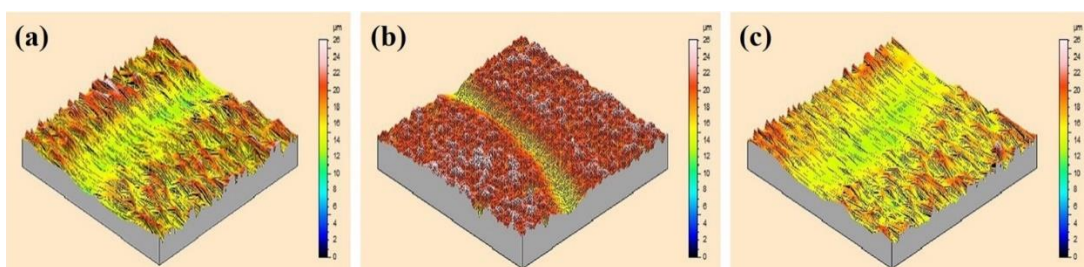


Figure 48 Section of the Wear track profile of NWD coatings fabricated with (a) 0 g/L CoSO₄ (b) 0.1 g/L CoSO₄ (c) 1.5 g/L CoSO₄ as reported by the surface profilometer.

Figure 48 shows the wear track profile for a section of the wear track as obtained by the surface profilometer. The mean depth of the wear track was estimated by the surface profilometer. The sample fabricated with 0 g/L, 0.25 g/L and 1.5 g/L CoSO₄ in the plating bath reported wear track depths of 6.1 μm, 4.13 μm and 4.83 μm, respectively. The coating thickness was calculated in the range of 58-62.6 μm. Therefore, the zirconia ball was able to penetrate through roughly 10% of the deposit thickness during the wear. The track profile for the NWD sample fabricated with 0 g/L CoSO₄ (Figure 48 (a)) and 1.5 g/L CoSO₄ (Figure 48 (c)) exhibits a wider track which corresponds to a higher volume of material lost by the wear effect of the zirconia ball

on the sample as compared to the sample fabricated with 0.1 g/L CoSO_4 (Figure 48 (b)). The wear track width for the NWD sample fabricated with 0.1 g/L of CoSO_4 (Figure 48 (b)) in the plating bath appears to be significantly narrower as compared to the wear track width of the other NWD samples fabricated with 0 g/L CoSO_4 (Figure 48 (a)) and 1.5 g/L CoSO_4 (Figure 48 (c)), respectively. The narrower track for the NWD sample fabricated with 0.1 g/L CoSO_4 is due to a higher degree of resistance to wear offered by the coating material to the wear effect of the zirconia ball. This also corresponds with the wear volume loss of the NWD sample fabricated with 0.1 g/L CoSO_4 (0.0164 mm^3) which is several times lower than the wear volume loss for the NWD samples fabricated with no CoSO_4 (0.286 mm^3) or with 1.5 g/L CoSO_4 (0.702 mm^3). This establishes the role of Co^{2+} additives in the enhancement of the wear performance of the NWD deposits when they are added to the NWD plating bath in small quantities.

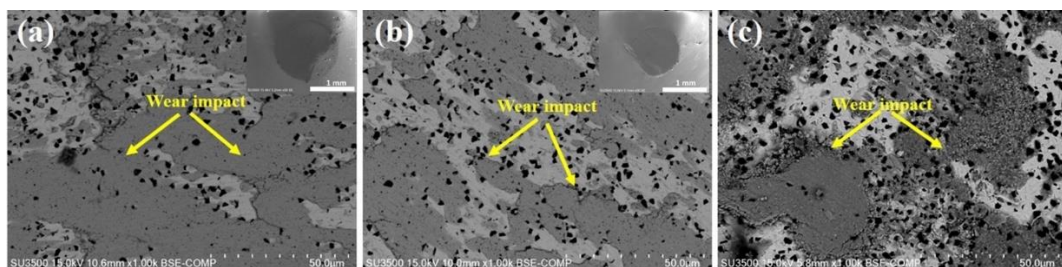
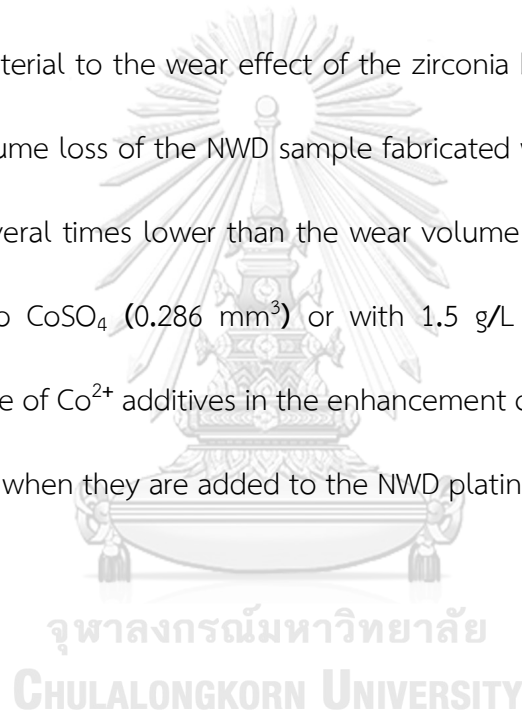


Figure 49 SEM (BSE mode) micrograph of worn surface of Ni-W/diamond composite coatings fabricated with (a) 0 g/L CoSO_4 (b) 0.1 g/L CoSO_4 and (c) 1.5 g/L CoSO_4 .

Figure 49 shows the SEM micrograph for the worn surface of the NWD composite coatings fabricated with 0, 0.1 and 1.5 g/L of CoSO_4 additives, respectively. The inserted image in Figure 49 (a, b) shows the SEM micrograph of the zirconia ball. The arrow marks in the images represent the impact on the sample due to the wear by the zirconia ball during the wear test. The wear nodules for the sample fabricated with 0.1 g/L of CoSO_4 (Figure 49 (b)) in the plating bath appears to be less abundant as compared to the nodules as seen for the other NWD samples fabricated with 0 g/L CoSO_4 (Figure 49 (a)) and 1.5 g/L CoSO_4 (Figure 49 (c)), respectively. The nodules signify the impact on the deposits due to wearing of the sample by the zirconia ball. The smeared appearance of the wear track in Figure 49 (c) indicates that more material of the deposits has been worn out and there is significant plastic deformation for the NWD samples fabricated with 1.5 g/L of CoSO_4 as compared to the other samples. The worn morphology of the NWD sample fabricated with 0.1 g/L of CoSO_4 also exhibits a smoother surface than the worn surface of NWD samples fabricated with 0 g/L CoSO_4 and 1.5 g/L CoSO_4 . The worn surface also exhibits that the wear loss and plastic deformation of the NWD sample fabricated with 0.1 g/L CoSO_4 is significantly lesser than the other NWD samples. The worn morphology of the NWD deposits suggests that the wear mechanism is dominated by adhesive wear along with abrasive wear[110]. The EDS analysis for the various sections of the wear track reveals that various amounts of Zirconia is present in the wear track for the different samples. The samples with 0 g/L and 0.1 g/L of CoSO_4 report 8.82 at. % and 7.15 at. % of Zirconia

on the surface of the wear track. However, the samples fabricated with 0.25 g/L and 1.5 g/L of CoSO_4 report 3.30 at. % and 1.95 at. % of Zirconia on the wear track. The SEM micrograph inserted for the ball in Figure 49 (a) clearly shows a higher amount of debris from the deposit on the surface of the zirconia ball as compared to the SEM micrograph for the ball inserted in Figure 49 (b). The EDS analysis of the zirconia ball for 0 g/L CoSO_4 shows 48 at. % of the debris (C, Co, Ni and W) on the surface of the zirconia ball and 31 at. % of the debris is reported for the sample fabricated with 0.25 g/L of CoSO_4 . The EDS for the wear track, zirconia ball and zirconia SEM data suggests that the wear mechanism is adhesive for the NWD samples with 0 and 0.1 g/L CoSO_4 (Figure 49 (a, b)) as the presence of zirconia on the wear track (8.82 at. % and 7.15 at. %, respectively) and the amount of debris on the zirconia ball (48 at. % and 31 at. %, respectively) is comparatively higher for the above mentioned samples and also the hardness of the zirconia ball ($\sim 1300 \text{ H}_v$) is comparable to the hardness of the samples which is 1207 ± 19 and 1364 ± 12 for the samples fabricated with 0 and 0.1 g/L CoSO_4 in the NWD plating bath[134]. The wear track for both the aforesaid samples doesn't have any sharp cuts, edges, scratches or a high degree of plastic deformation and the wear impact appears to be typical of an adhesive wear on the samples. However, for the NWD sample fabricated with 1.5 g/L CoSO_4 (Figure 49 (c)) the wear mechanism appears to be abrasive because the hardness of the sample ($941 \pm 17 \text{ H}_v$) is much lower than the hardness of the zirconia ball used during the wear test[135]. This can also be observed by the presence of sharp edges, scratches and with

significant plastic deformation on the surface of the deposits caused by the abrasion during the wear test. The SEM micrographs in Figure 49 corroborate with the friction co-efficient (Figure 46) and the wear rate data (Figure 47) as the NWD sample with 0.1 g/L CoSO_4 exhibits a smoother wear track (Figure 49 (b) also reports a lower value of friction coefficient and the least wear rate (in turn the best wear performance) as compared to the other NWD samples fabricated with 0 g/L and 1.5 g/L CoSO_4 additive, respectively.

4.4 Conclusion

- (1) The NWD samples with 0.1 g/L CoSO_4 additive report the highest value of hardness ($1364 \pm 12 \text{ Hv}$). Upon increasing the concentration of CoSO_4 in the bath from 0.1 g/L to 1.5 g/L the value of the hardness drops to $941 \pm 17 \text{ Hv}$. The Co content of the deposits also increased progressively as the CoSO_4 concentration in the plating bath is increased. The deposition rates and the coating thickness of the NWD deposits vary marginally as varying amounts of CoSO_4 is introduced in the NWD plating bath.
- (2) The NWD samples tend to get rougher as the CoSO_4 concentration is increased in the plating bath.
- (3) The wear volume loss for the NWD sample fabricated with 0.1 g/L CoSO_4 is significantly lesser than the other NWD samples fabricated with different amounts of CoSO_4 .

(4) The results also establish that the wear resistance of the NWD deposits (without Co^{2+} ions) is lesser than that of the NWD deposits fabricated with small quantities of Co^{2+} (0.1 and 0.2 g/L CoSO_4 , respectively) additive in the NWD plating bath. The wear rate of the NWD samples increases drastically as the concentration of CoSO_4 is increased in the NWD plating bath.



CHAPTER V

CONCLUSIONS AND FUTURE PRESPECTIVE

5.1 Conclusions

The Ni-W alloys and composite coatings as designed and fabricated during the course of the research threw up several significant findings which can be further exploited in various other systems for the overall clarity of basic metal forming and protective coatings in general and enhancement of structure and mechanical properties of such binary alloys and composite coatings systems in particular. The various portions can be concluded as below:

- (a) The study on the effect of operating conditions and surfactants on the electrodeposition of Ni-W alloys highlighted the significant effect that the current density and various organic as well as inorganic surfactants have on the morphology, hardness and various other surface properties of the deposits such as crack density and the grain size. The use of SDS and NaBr tends to enhance the hardness and the W content of the deposits when used in optimal quantities (0.1 g/L and 25 g/L, respectively). Moreover, the effect of NaBr is more pronounced in terms of refinement of the grain structure, enhancement of the W content in the deposits and reduction of the crack density while nominally affecting hardness of the deposits.

(b) Synthesis of Ni-W/diamond composite deposits was the most significant step during the course of entire research. Operating conditions (current density, concentration of diamond particles in the plating bath) and composite particles attributes (diamond particle size) were reasonably varied to arrive at an optimal conclusion of a set of conditions which yielded the best result in terms of hardness, surface morphology, diamond particle distribution and the reasonable and significant incorporation of diamond particles into the base Ni-W alloy matrix. The progressive and increased encapsulation of diamond particles tended to report an enhancement of the surface hardness of the base matrix which was significantly higher than the known hardness of the base Ni-W matrix. Moreover, a decline in the W content of the deposits was also observed as the diamond concentration in the plating bath and the diamond content in the deposits reported an increase in values. This result highlights the sole and significant impact of the diamond particles in enhancing the hardness of the base Ni-W matrix. The surface also tended to get smoother as the diamond content in the deposits was increased successively, while the coatings reported an enhanced anti-wear performance with an increase in the level of diamond incorporation into the base matrix. Also, the friction coefficient decreased as the diamond content of the coatings were enhanced highlighting a very significant phenomena where the surface are hard and smooth enough for a counter material to scratch against it and remove the surface due to wear

impact of the counter material against the surface of the deposits, thereby rendering the significantly resistant against wear damage. Upon fabrication of pulse plated multilayer Ni-W/diamond nanocomposite coatings using a multitude of variations in the pulse parameters (forward current, reverse current, layer duration, forward/reverse current duration) it was revealed that the multilayer coating with alternating layers fabricated by direct current reports the optimal grain size, relative reduction in crack density and a significant enhancement in the W content, diamond particle distribution and incorporation of the deposits is reported.

(c) Ni-W/diamond coating were also fabricated with a varying amount of CoSO_4 additive to investigate the impact of Co^{2+} additives on the the coatings. It is observed that the addition of cobalt sulphate contributes towards enhancing the hardness and wear resistance of the deposits only when miniamal amount of cobalt sulphate is introduced into the deposits (upto 0.1 g/L). The increase in the amount of cobalt sulphate in the plating bath also directly enhances the cobalt content of the deposits as fabricated which in turn directly translates into the fact that successive increase in the cobalt content in the plating bath tends to directly alter the composition of the NWD deposits as fabricated without any cobalt sulphate additive in the plating bath and beyond a particular concentration in the plating bath, the Co^{2+} ceases to be a composite

additive and perhaps interferes in the Ni-W alloy matrix and thereby, altering the composition of the base matrix.



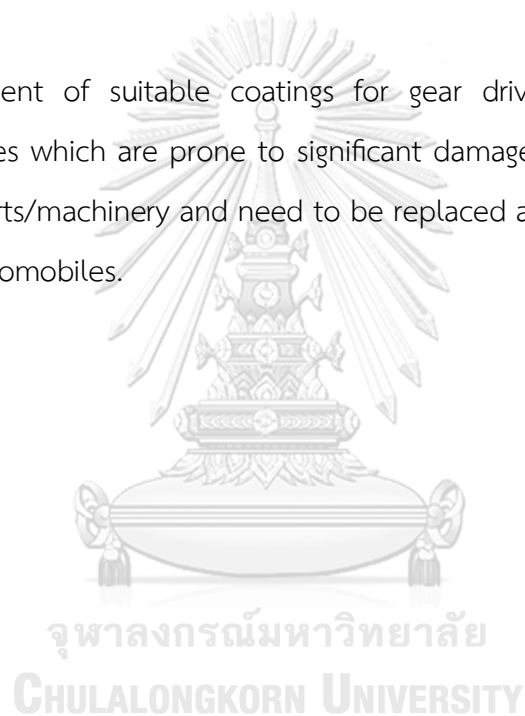
5.2 Future Perspective

The study of the various modifications both at the operational level and the experimental levels during the fabrication of binary metal deposits and composite coatings is a very encompassing field which needs significant further research and analysis to develop a relationship between various metal alloy and composite systems. The super-hard, wear resistant diamond composite deposits can also find several varied applications in industry and civic society. Moreover, there is a pressing need to reduce the net cost of fabrication of such deposits by investigating and optimizing various other binary and ternary alloy system (Ni-P, Ni-P-Co, Ni-Al-Fe, Ni-Fe as few examples) as base matrix for super hard composite particle co-deposition. Cost reduction is one such significant factor that if not addressed properly can lead to detrimental impact in the development of this technology to its prime. Moreover, the coatings can be redesigned with a different base alloy system and a mixture of diamond particles of various size so as to enable a variety of applications and also to ensure a matrix that can encapsulate higher volume % of composite particles to the tune of 80 volume % as. The few applications that can be targeted further can be:

- (a) Development of a water-resistant coating system with similar mechanical as well as morphological attributes as Ni-W/diamond composite coatings. This can lead to significant benefits in the automobile industry. In the power plant industries as the car bodies are usually prone to damage by rainfall and corrosion damage while in the power plant industries also there is a significant loss incurred by means of corrosion of the inner walls of boilers and heat exchangers due to the intermittent moisture present in water vapours or the water that flows through them. Coating the inner surface of such boilers and heat exchangers by the above-mentioned coating can contribute towards

significantly reducing the damage to these vital industrial equipments that drive the economy of various countries

- (b) Development of heat-resistant nanocomposite insulating coatings which can possibly be used in industrial parts prone to fire hazard, short-circuiting due to over-heating of the underlying materials
- (c) Development of suitable coatings for gear driving and driven tooth of automobiles which are prone to significant damage and loss due to wear of moving parts/machinery and need to be replaced adding to the maintenance cost of automobiles.



REFERENCES

1. Ogihara, H., M. Safuan, and T. Saji, *Effect of electrodeposition conditions on hardness of Ni-B/diamond composite films*. Surface and Coatings Technology, 2012. **212**: p. 180-184.
2. Zhang, X., et al., *Co-electrodeposition of hard Ni-W/diamond nanocomposite coatings*. Scientific reports, 2016. **6**: p. 22285.
3. Boonyongmaneerat, Y., et al., *Effects of WC addition on structure and hardness of electrodeposited Ni-W*. Surface and Coatings Technology, 2009. **203**(23): p. 3590-3594.
4. Boonyongmaneerat, Y., et al., *Pulse co-electrodeposition and characterization of NiW-WC composite coatings*. journal of alloys and compounds, 2010. **506**(1): p. 151-154.
5. Lee, E. and J. Choi, *A study on the mechanism of formation of electrocodeposited Ni-diamond coatings*. Surface and coatings technology, 2001. **148**(2-3): p. 234-240.
6. Lee, E. and I. Moon, *Electrolytic codeposition of diamond particles with nickel and cobalt metals*. Plating and surface finishing, 2002. **89**(12): p. 55-59.
7. Zhang, X., et al., *Preparation and hardness of pulse electrodeposited Ni-W-diamond composite coatings*. Surface and Coatings Technology, 2015. **276**: p. 228-232.
8. Qin, J., et al., *The high concentration and uniform distribution of diamond particles in Ni-diamond composite coatings by sediment co-deposition*. Surface and Interface Analysis, 2015. **47**(3): p. 331-339.
9. Donten, M., H. Cesiulis, and Z. Stojek, *Electrodeposition and properties of Ni_{1-x}W_x, Fe_{1-x}W_x and Fe_{1-x}Ni_xW_x amorphous alloys. A comparative study*. Electrochimica Acta, 2000. **45**(20): p. 3389-3396.
10. Sofer, Y., Y. Yarnitzky, and S. Dirnfeld, *Evaluation and uses of composite Ni-Co matrix coatings with diamonds on steel applied by electrodeposition*. Surface and coatings technology, 1990. **42**(3): p. 227-236.

11. Hui, W.-h., et al., *A study of wear resistance of a new brush-plated alloy Ni-Fe-W*. *Wear*, 1996. **192**(1-2): p. 165-169.
12. Wang, H., S. Yao, and S. Matsumura, *Preparation, characterization and the study of the thermal strain in Ni-W gradient deposits with nanostructure*. *Surface and Coatings Technology*, 2002. **157**(2-3): p. 166-170.
13. Shrestha, N.K., T. Takebe, and T. Saji, *Effect of particle size on the co-deposition of diamond with nickel in presence of a redox-active surfactant and mechanical property of the coatings*. *Diamond and Related Materials*, 2006. **15**(10): p. 1570-1575.
14. Wang, L., et al., *Effects of bivalent Co ion on the co-deposition of nickel and nano-diamond particles*. *Surface and Coatings Technology*, 2005. **191**(1): p. 1-6.
15. Jappes, J.W., B. Ramamoorthy, and P.K. Nair, *Novel approaches on the study of wear performance of electroless Ni-P/diamond composite deposits*. *Journal of materials processing technology*, 2009. **209**(2): p. 1004-1010.
16. Shi, Y., et al., *Preparation of electroplated Ni-P-ultrafine diamond, Ni-P-carbon nanotubes composite coatings and their corrosion properties*. *Journal of materials science*, 2004. **39**(18): p. 5809-5815.
17. Reddy, V., B. Ramamoorthy, and P.K. Nair, *A study on the wear resistance of electroless Ni-P/Diamond composite coatings*. *Wear*, 2000. **239**(1): p. 111-116.
18. Ogihara, H., et al., *Electrodeposition of super hard Ni-B/diamond composite coatings*. *Chemistry Letters*, 2011. **40**(10): p. 1072-1073.
19. Lee, W.-H., S.-C. Tang, and K.-C. Chung, *Effects of direct current and pulse-plating on the co-deposition of nickel and nanometer diamond powder*. *Surface and Coatings Technology*, 1999. **120**: p. 607-611.
20. Hou, K.-H., H.-H. Sheu, and M.-D. Ger, *Preparation and wear resistance of electrodeposited Ni-W/diamond composite coatings*. *Applied Surface Science*, 2014. **308**: p. 372-379.
21. Wang, H.-T., et al., *The effect of heat treatment on the microstructure and mechanical properties of electrodeposited nanocrystalline Ni-W/diamond composite coatings*. *Surface and Coatings Technology*, 2014. **259**: p. 268-273.

22. Burkat, G., et al., *Preparation of composite electrochemical nickel–diamond and iron–diamond coatings in the presence of detonation synthesis nanodiamonds*. *Diamond and related materials*, 2005. **14**(11-12): p. 1761-1764.
23. Huang, W., Y. Zhao, and X. Wang, *Preparing a high-particle-content Ni/diamond composite coating with strong abrasive ability*. *Surface and Coatings Technology*, 2013. **235**: p. 489-494.
24. Kim, S.-J., et al., *Experiment-based statistical prediction on diamond tool wear in micro grooving Ni P alloys*. *Diamond and Related Materials*, 2014. **41**: p. 6-13.
25. Xu, H., et al., *Synthesis and properties of electroless Ni–P–Nanometer Diamond composite coatings*. *Surface and coatings technology*, 2005. **191**(2-3): p. 161-165.
26. Suzuki, T. and T. Konno, *Improvement in tool life of electroplated diamond tools by Ni-based carbon nanotube composite coatings*. *Precision Engineering*, 2014. **38**(3): p. 659-665.
27. Wang, L., et al., *Effects of nano-diamond particles on the structure and tribological property of Ni-matrix nanocomposite coatings*. *Materials Science and Engineering: A*, 2005. **390**(1-2): p. 313-318.
28. Arieta, F. and D. Gawne, *The wettability and durability of chromium plating*. *Surface and Coatings Technology*, 1995. **73**(1-2): p. 105-110.
29. Mishra, A.C., A.K. Thakur, and V. Srinivas, *Effect of deposition parameters on microstructure of electrodeposited nickel thin films*. *Journal of Materials Science*, 2009. **44**(13): p. 3520-3527.
30. Kwon, S., et al., *Characterization of intermediate Cr-C layer fabricated by electrodeposition in hexavalent and trivalent chromium baths*. *Surface and Coatings Technology*, 2004. **183**(2-3): p. 151-156.
31. Capel, H., P. Shipway, and S. Harris, *Sliding wear behaviour of electrodeposited cobalt–tungsten and cobalt–tungsten–iron alloys*. *Wear*, 2003. **255**(7-12): p. 917-923.
32. Schuh, C., T. Nieh, and H. Iwasaki, *The effect of solid solution W additions on the mechanical properties of nanocrystalline Ni*. *Acta Materialia*, 2003. **51**(2): p. 431-443.

33. Iwasaki, H., K. Higashi, and T. Nieh, *Tensile deformation and microstructure of a nanocrystalline Ni-W alloy produced by electrodeposition*. Scripta Materialia, 2004. **50**(3): p. 395-399.
34. Yang, F.Z., et al., *Electrodeposition, structure and corrosion resistance of nanocrystalline Ni-W alloy*. Chinese Journal of Chemistry, 2004. **22**(3): p. 228-231.
35. Ordine, A., et al., *Electrochemical study on Ni-P electrodeposition*. Electrochimica acta, 2006. **51**(8-9): p. 1480-1486.
36. Sriraman, K., S.G.S. Raman, and S. Seshadri, *Synthesis and evaluation of hardness and sliding wear resistance of electrodeposited nanocrystalline Ni-W alloys*. Materials Science and Engineering: A, 2006. **418**(1-2): p. 303-311.
37. Wang, L., et al., *Corrosion resistance and lubricated sliding wear behaviour of novel Ni-P graded alloys as an alternative to hard Cr deposits*. Applied Surface Science, 2006. **252**(20): p. 7361-7372.
38. Sriraman, K., S.G.S. Raman, and S. Seshadri, *Corrosion behaviour of electrodeposited nanocrystalline Ni-W and Ni-Fe-W alloys*. Materials Science and Engineering: A, 2007. **460**: p. 39-45.
39. Krstajić, N., et al., *Electrodeposition of Ni-Mo alloy coatings and their characterization as cathodes for hydrogen evolution in sodium hydroxide solution*. International Journal of Hydrogen Energy, 2008. **33**(14): p. 3676-3687.
40. Królikowski, A., et al., *Effects of compositional and structural features on corrosion behavior of nickel-tungsten alloys*. Journal of Solid State Electrochemistry, 2009. **13**(2): p. 263-275.
41. Su, C.-w., et al., *Electrodeposition of Ni, Fe and Ni-Fe alloys on a 316 stainless steel surface in a fluoroborate bath*. Electrochimica Acta, 2009. **54**(26): p. 6257-6263.
42. Hou, K.-H., et al., *The heat treatment effect on the structure and mechanical properties of electrodeposited nano grain size Ni-W alloy coatings*. Thin Solid Films, 2010. **518**(24): p. 7535-7540.

43. Jones, A., et al., *Nanocrystalline Ni-W alloy coating for engineering applications*. *Plat. Surf. Finish*, 2010. **97**(4): p. 52.
44. Rupert, T.J. and C.A. Schuh, *Sliding wear of nanocrystalline Ni-W: Structural evolution and the apparent breakdown of Archard scaling*. *Acta Materialia*, 2010. **58**(12): p. 4137-4148.
45. Wang, H., et al., *Electrodepositing amorphous Ni-W alloys for MEMS*. *Microelectronic Engineering*, 2010. **87**(10): p. 1901-1906.
46. Arganaraz, M.Q., et al., *Ni-W coatings electrodeposited on carbon steel: chemical composition, mechanical properties and corrosion resistance*. *Electrochimica Acta*, 2011. **56**(17): p. 5898-5903.
47. Chang, L., et al., *Study on microstructure and properties of electrodeposited Ni-W alloy coating with glycolic acid system*. *Journal of Alloys and Compounds*, 2011. **509**(5): p. 1501-1504.
48. Chianpairot, A., et al., *Corrosion of nanocrystalline Ni-W alloys in alkaline and acidic 3.5 wt.% NaCl solutions*. *Corrosion Science*, 2011. **53**(3): p. 1066-1071.
49. Kumar, K.A., G.P. Kalaighan, and V. Muralidharan, *Pulse electrodeposition and characterization of nano Ni-W alloy deposits*. *Applied Surface Science*, 2012. **259**: p. 231-237.
50. Beltowska-Lehman, E., et al., *Electrodeposition of nanocrystalline Ni-W coatings strengthened by ultrafine alumina particles*. *Surface and Coatings Technology*, 2012. **211**: p. 62-66.
51. Wang, Y., et al., *The heat treatment effect on microstructure and dynamic mechanical properties of electroformed nanocrystalline Ni-W alloy*. *Materials Science and Engineering: A*, 2012. **547**: p. 104-109.
52. Sunwang, N., P. Wangyao, and Y. Boonyongmaneerat, *The effects of heat treatments on hardness and wear resistance in Ni-W alloy coatings*. *Surface and Coatings Technology*, 2011. **206**(6): p. 1096-1101.
53. Arganaraz, M.Q., et al., *The chemistry and structure of nickel-tungsten coatings obtained by pulse galvanostatic electrodeposition*. *Electrochimica Acta*, 2012. **72**: p. 87-93.

54. Detor, A.J. and C.A. Schuh, *Tailoring and patterning the grain size of nanocrystalline alloys*. Acta Materialia, 2007. **55**(1): p. 371-379.
55. Nielsen, C.B., P. Leisner, and A. Horsewell, *On texture formation of chromium electrodeposits*. Journal of Applied Electrochemistry, 1998. **28**(2): p. 141-150.
56. Aruna, S., V.W. Grips, and K. Rajam, *Ni-based electrodeposited composite coating exhibiting improved microhardness, corrosion and wear resistance properties*. Journal of Alloys and compounds, 2009. **468**(1-2): p. 546-552.
57. Tsubota, T., et al., *Composite electroplating of Ni and surface-modified diamond particles with silane coupling regent*. Diamond and related materials, 2005. **14**(3-7): p. 608-612.
58. Hou, K., et al., *The wear behaviour of electro-codeposited Ni-SiC composites*. Wear, 2002. **253**(9-10): p. 994-1003.
59. Eliaz, N., T. Sridhar, and E. Gileadi, *Synthesis and characterization of nickel tungsten alloys by electrodeposition*. Electrochimica Acta, 2005. **50**(14): p. 2893-2904.
60. Nagai, T., K. Hodouchi, and H. Matsubara, *Relationship between film composition and microhardness of electrodeposited Ni-W-B films prepared using a citrate-glycinate bath*. Surface and Coatings Technology, 2014. **253**: p. 109-114.
61. Shang, Y.-L., et al., *Electrorheological property of M-doped (M= Na, Zr) nano-sized TiO₂ particle materials, influence of surface composition and microstructure*. Colloids and Surfaces A: Physicochemical and Engineering Aspects, 2008. **325**(3): p. 160-165.
62. An, Y.-L., et al., *Interfacial structure and mechanical properties of surface iron-nickel alloying layer in pure iron fabricated by surface mechanical attrition alloy treatment*. Materials & Design, 2013. **46**: p. 627-633.
63. Krauss, G., *Advanced surface modification of steels*. Journal of Heat Treating, 1992. **9**(2): p. 81-89.
64. Sudagar, J., et al., *The performance of surfactant on the surface characteristics of electroless nickel coating on magnesium alloy*. Progress in Organic coatings, 2012. **74**(4): p. 788-793.

65. Monteiro, O.R., S. Murugesan, and V. Khabashesku, *Electroplated Ni-B films and Ni-B metal matrix diamond nanocomposite coatings*. Surface and Coatings Technology, 2015. **272**: p. 291-297.
66. Wu, B.Y., *Synthesis and characterization of nanocrystalline alloys in the binary Ni-Co system*. 2004, Massachusetts Institute of Technology.
67. Shakoor, R.A., et al., *Synthesis and properties of electrodeposited Ni-B-CeO₂ composite coatings*. Materials & Design, 2014. **59**(0): p. 421-429.
68. Correa, E., et al., *Nickel-boron plating on magnesium and AZ91D alloy by a chromium-free electroless process*. Surface & Coatings Technology, 2012. **206**(13): p. 3088-3093.
69. Delaunois, F. and P. Lienard, *Heat treatments for electroless nickel-boron plating on aluminium alloys*. Surface and Coatings Technology, 2002. **160**(2-3): p. 239-248.
70. Delaunois, F., et al., *Autocatalytic electroless nickel-boron plating on light alloys*. Surface and Coatings Technology, 2000. **124**(2-3): p. 201-209.
71. Liu, Z., et al., *Electroless preparation and characterization of Ni-B nanoparticles supported on multi-walled carbon nanotubes and their catalytic activity towards hydrogenation of styrene*. Materials Research Bulletin, 2012. **47**(2): p. 338-343.
72. Orinakova, R., et al., *Electrodeposition of composite Ni-B coatings in a stirred heterogeneous system*. Journal of Solid State Electrochemistry, 2011. **15**(6): p. 1159-1168.
73. Weng, Y.-C. and T.-C. Chou, *Electrodeposited nickel-boron thin-film ethanol sensor*. Journal of The Electrochemical Society, 2006. **153**(6): p. H127-H132.
74. Ebrahimi, F. and Z. Ahmed, *The effect of current density on properties of electrodeposited nanocrystalline nickel*. Journal of Applied Electrochemistry, 2003. **33**(8): p. 733-739.
75. Hassani, S., K. Raeissi, and M.A. Golozar, *Effects of saccharin on the electrodeposition of Ni-Co nanocrystalline coatings*. Journal of Applied Electrochemistry, 2008. **38**(5): p. 689-694.

76. Natter, H. and R. Hempelmann, *Nanocrystalline Copper by Pulsed Electrodeposition: The Effects of Organic Additives, Bath Temperature, and pH*. The Journal of Physical Chemistry, 1996. **100**(50): p. 19525-19532.
77. Cziráki, Á., et al., *Microstructure and growth of electrodeposited nanocrystalline nickel foils*. Journal of Materials Science, 1994. **29**(18): p. 4771-4777.
78. Wang, L., et al., *A comparative study on the tribological behavior of nanocrystalline nickel and cobalt coatings correlated with grain size and phase structure*. Materials Chemistry and Physics, 2006. **99**(1): p. 96-103.
79. Wang, L., et al., *Grain size effect in corrosion behavior of electrodeposited nanocrystalline Ni coatings in alkaline solution*. Scripta Materialia, 2006. **55**(7): p. 657-660.
80. Shang, Y.-L., et al., *Electrorheological property of M-doped (M=Na, Zr) nano-sized TiO₂ particle materials, influence of surface composition and microstructure*. Colloids and Surfaces A: Physicochemical and Engineering Aspects, 2008. **325**(3): p. 160-165.
81. Wu, Y., et al., *Influence of boric acid on the electrodepositing process and structures of Ni-W alloy coating*. Surface and Coatings Technology, 2003. **173**(2): p. 259-264.
82. Hamid, Z.A., *Mechanism of electroless deposition of Ni-W-P alloys by adding surfactants*. Surface and Interface Analysis, 2003. **35**(6): p. 496-501.
83. Le, Z., et al., *Solution synthesis of the unsupported Ni-W sulfide hydrotreating catalysts*. Catalysis Today, 2008. **130**(1): p. 24-31.
84. Mohajeri, S., A. Dolati, and S. Rezagholibeiki, *Electrodeposition of Ni/WC nano composite in sulfate solution*. Materials Chemistry and Physics, 2011. **129**(3): p. 746-750.
85. Chen, L., et al., *Effect of surfactant on the electrodeposition and wear resistance of Ni-Al₂O₃ composite coatings*. Materials Science and Engineering: A, 2006. **434**(1): p. 319-325.
86. Ger, M.-D., *Electrochemical deposition of nickel/SiC composites in the presence of surfactants*. Materials Chemistry and Physics, 2004. **87**(1): p. 67-74.

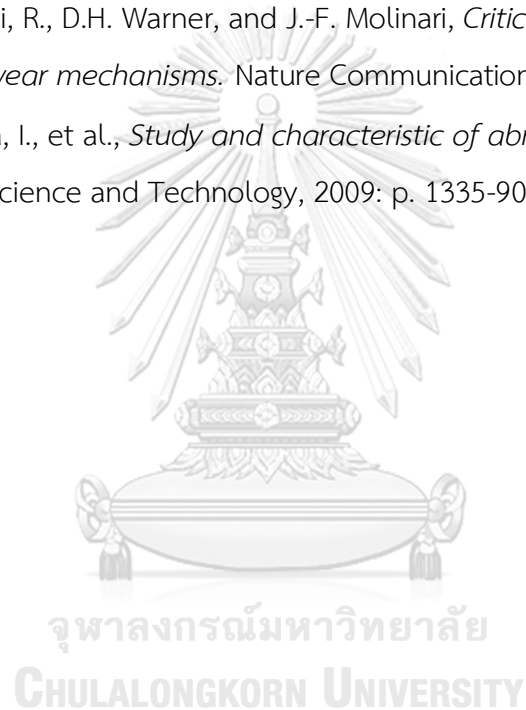
87. Shrestha, N.K., M. Masuko, and T. Saji, *Composite plating of Ni/SiC using azo-cationic surfactants and wear resistance of coatings*. *Wear*, 2003. **254**(5): p. 555-564.
88. Guo, C., et al., *Effects of surfactants on electrodeposition of nickel-carbon nanotubes composite coatings*. *Surface and Coatings Technology*, 2008. **202**(14): p. 3385-3390.
89. Feng, Q., et al., *Investigation on the corrosion and oxidation resistance of Ni-Al₂O₃ nano-composite coatings prepared by sediment co-deposition*. *Surface and Coatings Technology*, 2008. **202**(17): p. 4137-4144.
90. Rudnik, E., et al., *Electrodeposition of nickel/SiC composites in the presence of cetyltrimethylammonium bromide*. *Applied Surface Science*, 2010. **256**(24): p. 7414-7420.
91. Sahoo, P.K., et al., *Synthesis of tungsten nanoparticles by solvothermal decomposition of tungsten hexacarbonyl*. *International Journal of Refractory Metals & Hard Materials*, 2009. **27**(4): p. 784-791.
92. Subramania, A., A.R. Sathiya Priya, and V.S. Muralidharan, *Electrocatalytic cobalt-molybdenum alloy deposits*. *International Journal of Hydrogen Energy*, 2007. **32**(14): p. 2843-2847.
93. Yamasaki, T., et al., *Formation of amorphous electrodeposited Ni-W alloys and their nanocrystallization*. *Nanostructured Materials*, 1998. **10**(3): p. 375-388.
94. Zemanová, M., et al., *Pulse current electrodeposition and corrosion properties of Ni-W alloy coatings*. *Journal of Applied Electrochemistry*, 2011. **41**(9): p. 1077-1085.
95. Fan, G.J., et al., *A model for the inverse Hall-Petch relation of nanocrystalline materials*. *Materials Science and Engineering: A*, 2005. **409**(1): p. 243-248.
96. Meyers, M.A., A. Mishra, and D.J. Benson, *Mechanical properties of nanocrystalline materials*. *Progress in Materials Science*, 2006. **51**(4): p. 427-556.
97. Takeuchi, S., *THE MECHANISM OF THE INVERSE HALL-PETCH RELATION OF NANOCRYSTALS*. *Scripta Materialia*, 2001. **44**: p. 1483-1487.

98. Song, H.W., S.R. Guo, and Z.Q. Hu, *A coherent polycrystal model for the inverse Hall-Petch relation in nanocrystalline materials*. Nanostructured Materials, 1999. **11**(2): p. 203-210.
99. Ogihara, H., et al., *Electrodeposition of Super Hard Ni-B/Diamond Composite Coatings*. Chemistry Letters, 2011. **40**(10): p. 1072-1073.
100. Qin, J., et al., *The high concentration and uniform distribution of diamond particles in Ni-diamond composite coatings by sediment co-deposition*. Surface and Interface Analysis, 2015. **47**(3): p. 331-339.
101. Arieta, F.G. and D.T. Gawne, *The wettability and durability of chromium plating*. Surface and Coatings Technology, 1995. **73**(1-2): p. 105-110.
102. Donten, M., H. Cesiulis, and Z. Stojek, *Electrodeposition and properties of Ni-W, Fe-W and Fe-Ni-W amorphous alloys. A comparative study*. Electrochimica Acta, 2000. **45**(20): p. 3389-3396.
103. Kwon, S.C., et al., *Characterization of intermediate Cr-C layer fabricated by electrodeposition in hexavalent and trivalent chromium baths*. Surface and Coatings Technology, 2004. **183**(2-3): p. 151-156.
104. Wu, Y., et al., *Effects of 2-butyne-1,4-diol on structures and morphologies of electroplating Ni-W alloy*. Surface and Coatings Technology, 2003. **162**(2-3): p. 269-275.
105. Sriraman, K.R., S. Ganesh Sundara Raman, and S.K. Seshadri, *Synthesis and evaluation of hardness and sliding wear resistance of electrodeposited nanocrystalline Ni-W alloys*. Materials Science and Engineering: A, 2006. **418**(1-2): p. 303-311.
106. Schuh, C.A., T.G. Nieh, and H. Iwasaki, *The effect of solid solution W additions on the mechanical properties of nanocrystalline Ni*. Acta Materialia, 2003. **51**(2): p. 431-443.
107. Panagopoulos, C.N., G.D. Plainakis, and D.A. Lagaris, *Nanocrystalline Ni-W coatings on copper*. Mater. Sci. Eng. B, 2011. **176**(6): p. 477-479.
108. Aruna, S.T., V.K. William Grips, and K.S. Rajam, *Ni-based electrodeposited composite coating exhibiting improved microhardness, corrosion and wear*

- resistance properties*. Journal of Alloys and Compounds, 2009. **468**(1–2): p. 546-552.
109. Hou, K.H., et al., *The wear behaviour of electro-codeposited Ni–SiC composites*. Wear, 2002. **253**(9–10): p. 994-1003.
110. Hou, K.-H., et al., *Preparation and wear resistance of electrodeposited Ni–W/diamond composite coatings*. Applied Surface Science, 2014. **308**: p. 372-379.
111. Guglielmi, N., *Kinetics of the deposition of inert particles from electrolytic baths*. Journal of the Electrochemical Society, 1972. **119**(8): p. 1009-1012.
112. Robin, A., J.C.P. de Santana, and A.F. Sartori, *Co-electrodeposition and characterization of Cu–Si₃N₄ composite coatings*. Surface and Coatings Technology, 2011. **205**(19): p. 4596-4601.
113. Yao, Y.W., S.W. Yao, and L. Zhang, *Preparation, mechanical properties and wear resistance of Ni-W/SiC nanocomposite coatings*. Materials Science and Technology, 2008. **24**(2): p. 237-240.
114. Younes, O., et al., *Electroplating of amorphous thin films of tungsten/nickel alloys*. Langmuir, 2001. **17**(26): p. 8270-8275.
115. Chou, M.-C., et al., *The Ni–P–SiC composite produced by electro-codeposition*. Materials Chemistry and Physics, 2005. **92**(1): p. 146-151.
116. Medeliene, V. and A. Kosenko, *Structural and functional properties of electrodeposited copper metal matrix composite coating with inclusions of WC*. Mater. Sci, 2008. **14**(1): p. 29-33.
117. Riyadh, A., A. Khair El Rafezi, and Y. Al-Douri, *Evaluate the effects of various surface roughness on the tribological characteristics under dry and lubricated conditions for Al-Si alloy*. J. Surf. Eng. Mater. Adv. Tech., 2012. **2012**.
118. Xiaohe, W. and X.B.-s.H. Zhen-feng, *Progress in developing electrodeposition for substitute hard chromium*. New Technology and New Process, 2009.
119. Yuan Xuetao, W.Y., Sun Dongbai, Yu Hongying, *Influence of pulse parameters on the microstructure and microhardness of nickel electrodeposits*. Surface & Coatings Technology, 2008. **202**: p. 1895-1903.

120. El-Sherik, A.M., U. Erb, and J. Page, *Microstructural evolution in pulse plated nickel electrodeposits*. Surface and Coatings Technology, 1997. **88**(1–3): p. 70-78.
121. B.D.Cullity, S.R.S., S.Stock,, *ElementsofX-rayDiffraction Fraction*. 2001, LONDON: Addison-Wesley.
122. Low, C.T.J., R.G.A. Wills, and F.C. Walsh, *Electrodeposition of composite coatings containing nanoparticles in a metal deposit*. Surface and Coatings Technology, 2006. **201**(1–2): p. 371-383.
123. Williams, R. and P. Martin, *Electrodeposited composite coatings*. Electroplat. and Met. Finish, 1966. **19**(3): p. 92-96.
124. Das, M.K., et al., *Effect of electrodeposition conditions on structure and mechanical properties of Ni-W/diamond composite coatings*. Surface and Coatings Technology, 2017. **309**: p. 337-343.
125. Lin, C.R. and C.T. Kuo, *High adhesion and quality diamond films on steel substrate*. Diamond and Related Materials, 1998. **7**(6): p. 903-907.
126. Pramod Kumar, U., C.J. Kennady, and Q. Zhou, *Effect of salicylaldehyde on microstructure and corrosion resistance of electrodeposited nanocrystalline Ni-W alloy coatings*. Surface and Coatings Technology, 2015. **283**: p. 148-155.
127. Kumar Das, M., et al., *Effect of Saccharin Sodium on the Microstructure and Hardness of Electrodeposited Ni-W Coatings*. Key Engineering Materials, 2015. **659**: p. 535-539.
128. Li, Y., et al., *Effects of saccharin and cobalt concentration in electrolytic solution on microhardness of nanocrystalline Ni-Co alloys*. Surface and Coatings Technology, 2008. **202**(20): p. 4952-4956.
129. Li, Y., et al., *Effects of peak current density on the mechanical properties of nanocrystalline Ni-Co alloys produced by pulse electrodeposition*. Applied Surface Science, 2008. **254**(21): p. 6865-6869.
130. ZAMANI, M., A. AMADEH, and S.L. BAGHAL, *Effect of Co content on electrodeposition mechanism and mechanical properties of electrodeposited Ni-Co alloy*. Transactions of Nonferrous Metals Society of China, 2016. **26**(2): p. 484-491.

131. Inwood, B.C. and A.E. Garwood, *Electroplated coatings for wear resistance*. Tribology International, 1978. **11**(2): p. 113-119.
132. Riyadh, A., A. Khair el Rafezi, and Y. Al-Douri, *Evaluate the effects of various surface roughness on the tribological characteristics under dry and lubricated conditions for Al-Si alloy*. Journal of Surface Engineered Materials and Advanced Technology, 2012. **2012**.
133. Archard, J., *Contact and rubbing of flat surfaces*. Journal of applied physics, 1953. **24**(8): p. 981-988.
134. Aghababaei, R., D.H. Warner, and J.-F. Molinari, *Critical length scale controls adhesive wear mechanisms*. Nature Communications, 2016. **7**: p. 11816.
135. Kovaříková, I., et al., *Study and characteristic of abrasive wear mechanisms*. Materials Science and Technology, 2009: p. 1335-9053.





จุฬาลงกรณ์มหาวิทยาลัย
CHULALONGKORN UNIVERSITY

VITA

NAME MALAY KUMAR DAS

DATE OF BIRTH 23 Mar 1990

PLACE OF BIRTH PATNA, INDIA

INSTITUTIONS ATTENDED 2009-2013 B. Tech (Chemical Engineering) CMJ University, India

2013- Doctor of Philosophy In NanoScience and Technlogy
CHULALONGKORN UNIVERSTY, Thailand

HOME ADDRESS ROOM 1406, 14 FLOOR MMRI BUILDING, SOI CHULA 12
WANG MAI PATHUMWAN BANGKOK 10330 THAILAND

PUBLICATION

1. M.K. Das, Xinyu Zhang, Jiaqian Qin*, Yuttanant Boonyongmaneerat, Riping Liu, Influence of Co²⁺ ions on the microstructure and mechanical properties of Ni-W/diamond nano-composite coatings, Journal of Nanoscience and Technology (Accepted Article)
2. Malay Kumar Das, Rongxia Li, Jiaqian Qin*, Xinyu Zhang*, Kumkumlata Das, Adisak Thueploy, Sarintorn Limpanart, Yuttanat Boonyongmaneerat, Mingzhen Ma, Riping Liu, Effect of electrodeposition conditions on structure and mechanical properties of Ni-W/diamond composite coatings, Surface and Coatings Technology 309 (2017) 337-343.
(DOI: <http://dx.doi.org/10.1016/j.surfcoat.2016.11.074>)
3. Xinyu Zhang, Jiaqian Qin*, Malay Kumar Das, Ruru Hao, Hua Zhong, Adisak Thueploy, Sarintorn Limpanart,

Yuttanant Boonyongmaneerat, Mingzhen Ma, Riping Liu, Co-electrodeposition of hard Ni-W/diamond nanocomposite coatings, Scientific Reports, 6 (2016) 22285 (doi: <http://10.1038/srep22285>)

4. Malay Kumar Das, Jiaqian Qin*, Xinyu Zhang*, Rongxia Li, Adisak Thueploy, Sarintorn Limpanart, Yuttanat Boonyongmaneerat, Mingzhen Ma, Riping Liu, Effect of Sodium Dodecyl Sulphate and Sodium Bromide Additives on Ni-W Nanocoatings, Journal of Nanoscience and Nanotechnology 17 (2017) 1217-1224 (DOI: <https://doi.org/10.1166/jnn.2017.12665>)

5. Xinyu Zhang, Jiaqian Qin*, Thanyanant Perasinjareon, Wichitra Aeksen, Malay Kumar Das, Ruru Hao, Bing Zhang, Panyawat Wangyao, Yuttanant Boonyongmaneerat, Sarintorn Limpanart, Mingzhen Ma, Riping Liu, Preparation and hardness of pulse electrodeposited Ni-W-diamond composite coatings, Surface and Coatings Technology 276 (2015) 228–232. (DOI: <http://dx.doi.org/10.1016/j.surfcoat.2015.06.073>)

6. Malay Kumar Das, Ruru Hao, Ekachai Srikaen, Adisak Thueploy, Sarintorn Limpanart, Yuttanat Boonyongmaneerat, Jiaqian Qin*, Effect of saccharin sodium on the microstructure and hardness of electrodeposited Ni-W coatings, Key Engineering Materials, 659 (2015) 535-539. (DOI: [10.4028/www.scientific.net/KEM.659.535](http://www.scientific.net/KEM.659.535))

7. Jiaqian Qin*, Xinyu Zhang, Yannan Xue, Malay Kumar Das, Adisak Thueploy, Sarintorn Limpanart, Yuttanant Boonyongmaneerat, Mingzhen Ma, Riping Liu, The high concentration and uniform distribution of diamond particles in Ni-diamond composite coatings by sediment co-deposition, *Surface and Interface Analysis* 47 (2015) 331-339. (DOI: 10.1002/sia.5712)

8. Malay Kumar Das, Jiaqian Qin, Priya Karn, Effect of diamond particles on the microstructure and composition of pulse plated multilayer Ni-W/diamond composite coatings, 2018, Accepted for Presentation in Joint International Conference of Metallurgical and Materials Science Engineering. (Accepted for Publication in IOP Conference Series: Materials Science and Engineering)

AWARD RECEIVED

1. 100 Anniversary of Chulalongkorn University Fund for Doctoral Studies

2. Chulalongkorn University Overseas Academic Presentation Scholarship

3. Chulalongkorn University Overseas research Scholarship

4. Best paper award at Joint Conference on Metallurgical and Materials Engineering, New Zealand 2018